University of Southampton

Photoisomerising effects in Chiral Liquid Crystal Systems

Anna Marie Remnant

Doctor of Philosophy

Southampton Liquid Crystal Institute
Department of Physics and Astronomy
University of Southampton

August 2002

UNIVERSITY OF SOUTHAMPTON

ABSTRACT

FACULTY OF SCIENCE

PHYSICS AND ASTRONOMY

Doctor of Philosophy

Photoisomerising Effects in Chiral Liquid Crystal Systems

By Anna Marie Remnant

Photoisomerising liquid crystals are added to smectic and chiral nematic systems. The consequences of dye addition to the phase sequence and switching properties of the host material are described. The effect of ultra violet illumination, causing a shape changing photoisomerisation of the dye molecules, on these mixtures is explored.

The photoisomerisation of the azobenzene molecules, used as dyes, is to change the straight trans isomer that is very compatible with the liquid crystalline phase to the bent cis isomer that is less compatible. This conversion is caused by illumination by ultra violet, the reverse isomerisation can be caused thermally or by illumination by infra red wavelengths.

Organosiloxane liquid crystals produce stable ferroelectric smectic C* liquid crystalline phases that have a tilt angle close to 45° and a high spontaneous polarisation. The effect of monomesogenic and bimesogenic dye addition was to add a smectic A phase to the sequence, which showed a large electroclinic, effect and aided the alignment of the ferroelectric phase. The bimesogenic dye acted as a template for the monomesogenic host molecules, inducing an anticlinic antiferroelectric arrangement.

The effect of ultra violet illumination was to reversibly reduce the phase transition temperatures, the spontaneous polarisation and the tilt angle of the mixtures indicating a reduction in the order of the system.

Azobenzene dyes were added to chiral nematic bimesogens mixtures with a high flexoelectric coefficient. The effect of ultra violet was to reduce the phase transition temperatures and the helical pitch. The response time and tilt angle were unchanged. The results indicate a reduction in the order parameter but no measurable change of the flexoelectric constants.

The photoisomerising effects of a mixture with a large divergence in the tilt and pitch close to the chiral nematic – smectic A transition was also investigated. Similar results were obtained indicating a reduction in the order parameter but no measurable change in the flexoelectric coefficient.

For all the systems studied the effect of photoisomerisation of the dye molecules caused a reversible reduction in the order of the mixture.

Contents

Acknowledgements

To Harry Coles for guidance and encouragement

To Adrian, Byron, Dave, Ian, Lucy, Lyn, Matthew, Reuben, Ron and Ross
for keeping in touch

To Francis, Rachel, Kate, Chrissy and Zoë
for much Guiding fun

To Bronje, Cecile, Dean, Chris, Marcus, Steve, Piers, Matt, Jon and Steve
Andrew, Yong-Il, Martin and Mike
for interesting discussions and fun nights out

Funding from the EPSRC

Chapter 1

Introduction

Chapter 1 Introduction

Thermotropic liquid crystalline materials form a range of phases that appear at temperatures between the solid and liquid phases, rather than a direct transition from the solid to the liquid. Often called mesophases, these phases are literally intermediate in character between the solid and liquid states. Calamitic thermotropic liquid crystals composed of rigid rod like molecules are discussed in this thesis. The order of the liquid crystalline materials can be positional or orientational and small changes in the molecular composition or shape can cause significant changes in the order which are readily observed by electro-optic measurements.

Liquid crystals provide a wealth of novel properties to be investigated by new chemical synthesis, physical measurements and theoretical insight. For example, what is the effect of molecular composition and shape on the phases expressed? What happens as the molecules switch in electric or magnetic fields? How do the molecules interact with each other? What is the difference between the bulk liquid crystal and the structure present in thin cells? There is also much to be learnt about the molecular order of the phases and the changes that occur as one phase transforms into another.

The nematic phase is the simplest and least ordered of the liquid crystalline phases, and if present, is the first to appear on cooling from the isotropic liquid. The molecules are ordered so that their long molecular axes are "on average"co-aligned. The average direction of alignment, shown in figure 1.1 is called the director. If the molecules making up the phase include a chiral component it is found that the director rotates helically in space as shown in figure 1.2. Although the director changes periodically there are no physical layers of molecules. Suitably aligned it is possible to demonstrate flexoelectric switching in such materials. We have discovered new flexoelectric chiral nematics which will be investigated in this thesis.

The smectic A phase has a layered molecular packing with a two dimensional liquid like ordering, within the layers, as shown in figure 1.3. The molecules are

oriented, on average, parallel to the layer normal. The achiral smectic C phase is the same as the smectic A phase, except that the director makes an angle to the layer normal, figure 1.4. In the chiral, smectic C* phase, the angle changes helically from one layer to the next as shown in figure 1.5. Novel chiral liquid crystalline materials with smectic C* phases, with ferroelectric and antiferroelectric switching, and a smectic A* phase, with electroclinic switching, have been investigated herein.

To measure the electro-optic properties of the smectic C* liquid crystals they are enclosed in a thin (~10μm) glass cell coated with an alignment layer that promotes alignment of the molecules parallel to the cell surface. The surface anchoring is great enough to unwind the helix and this arrangement is called a surface stabilised ferroelectric liquid cell.[1] This orientation has an optic axis, corresponding to the long molecular axis that is parallel to the cell surfaces. Coupling of the polarisation of the molecules and an applied electric field produces a rotation of this optic axis as shown in figure 1.6.into two stable states. For the antiferroelectric phase there are three npossible states. Herein the spontaneous polarisation, tilt angle and response time are measured for new ferroelectric and antiferroelectric liquid crystals.

The chiral smectic A* phase also exhibits a form of electro-optic switching[2] called electroclinic switching first observed as a pretransitional effect close to the smectic A* – smectic C* phase transition. As we will show such switching can penetrate far into the smectic A* phase. The amplitude of this switching is smaller than that in the ferroelectric phase but it is linear with the applied electric field giving possible greyscale applications.

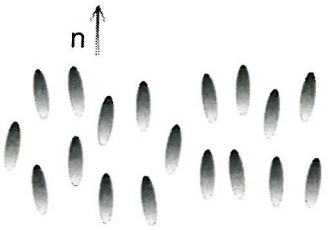

Figure 1.1 The nematic liquid crystal phase showing the average director n and the lack of positional order.

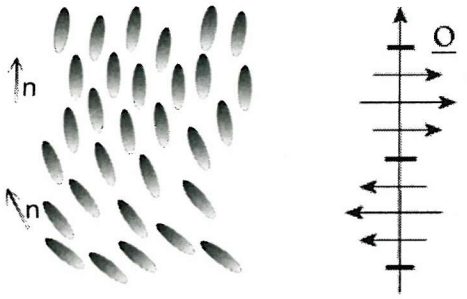

Figure 1.2 The twisted nematic liquid crystal phase, N*, showing how the director n and the optic axis o change in space while there is no physical layering of the molecules. (Note n rotates around o.)

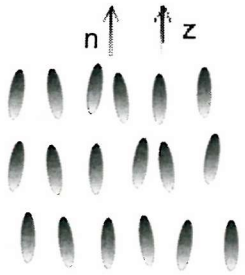

Figure 1.3 The smectic A liquid crystal phase with the average director n perpendicular to the layers.

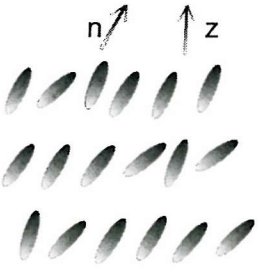

Figure 1.4 The smectic C liquid crystal phase with the average director n at an angle to the layer normal z.

Figure 1.5 The chiral smectic C*phase showing the director n precessing around z from layer to layer.

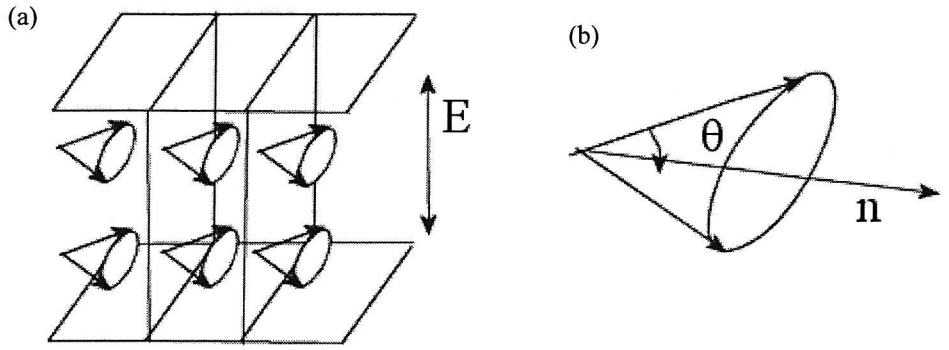

Figure 1.6 (a) Schematic diagram of the surface stabilised ferroelectric liquid crystal device (b) the tilt angle, θ, is the angle between the layer normal, n, and the molecular axis.

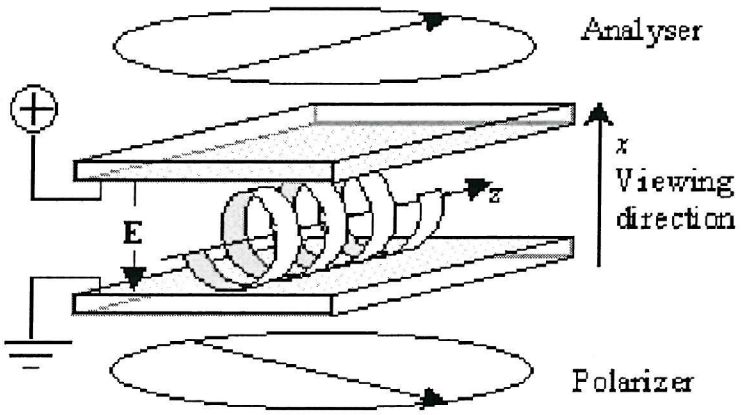

Figure 1.7 Schematic arrangement of the uniformly lying helix texture, with chiral nematic helix and hence the optic axis parallel to the cell surfaces.

The flexoelectric switching of chiral nematic liquid crystals can also be observed in planar aligned glass cells. The uniformly lying helix texture can be produced by shearing the cell while a small field is applied across it. As shown in figure 1.7 the optic axis is then perpendicular to the viewing direction. This optic axis can be rotated by coupling of the flexoelectric polarisation with an applied electric field.

Dye guest host systems will be investigated herein by incorporating dye molecules into complimentary host structures to produce good miscibility and high dye

concentrations. The effect of dyes with different compositions and conformations will then be investigated. Photoisomerising dyes will be used, that change from a linear to a bent conformation upon illumination by ultra violet light. The effect on the macroscopic properties of a mixture when the shape of the dye is changed will then be investigated.

Photochromic molecules have properties that are altered upon illumination by specific wavelengths. If a steric or shape change occurs this effect will be called photoisomerisation. In the azobenzene materials investigated in this thesis the effect of ultra violet illumination on the azo linkage is to change it from the cis to the trans isomer. This causes a change from a straight conformation to a bent conformation as shown in figure 1.8. This change is reversed either thermally or by illumination by infra-red illumination.[3] Liquid crystalline systems are ideal vehicles for observation of the effects of these shape changes since small changes of their degree of order markedly affect their observable macroscopic electro-optic properties.

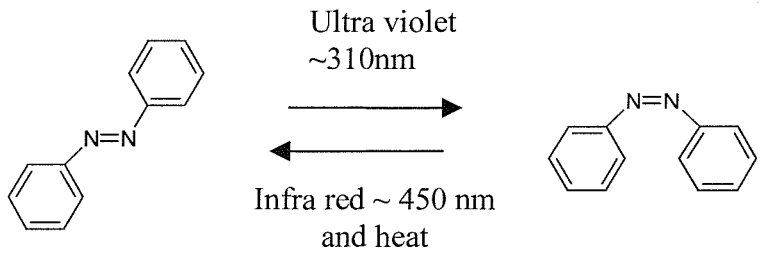

Figure 1.8 The straight trans isomer converts to the bent cis isomer under ultra violet illumination and is returned by heat and infra red illumination

Although azobenzene mesogens can be synthesised that have limited liquid crystalline phases, these molecules will be used as dyes in hosts with a more stable phase over which measurements can be made. Photoisomerising effects will be investigated in ferroelectric and antiferroelectric smectic C* phases, electroclinic smectic A* phases and flexoelectric chiral nematic phases. The purpose of this work is to investigate how the microscopic shape changes of even small dye

concentrations will cause a macroscopic change on the properties of the host material.

The next chapter gives a short explanation of the phases studied, ferroelectric and antiferroelectric switching in smectic C* phases, electroclinic switching in chiral smectic A phases and flexoelectric switching in chiral nematic phases. It also includes a discussion of the order parameter in these phases and some of the work carried out on photoisomerising liquid crystal systems. Chapter three details the experimental procedures used to collect the data presented in the following chapters.

Chapters four and five will compare the addition of a monomesogenic and a bimesogenic photoisomerising nitroazo dyes, respectively, to a ferroelectric organosiloxane host. Organosiloxane materials will be investigated because they produce rugged, fast switching ferroelectric smectic C* phases. Each mesogen is made up of two parts. A liquid crystalline mesogen attached by a hydro-carbon chain to siloxane core unit. The siloxane units are thought to microseparate[4] from the mesogens thereby producing rugged smectic phases. The chiral nature of the mesogen produces ferroelectric phases. Both dyes will have the same siloxane unit as the host material to encourage good miscibility. The monomesogenic dye has a single nitro azo mesogen attached to the siloxane core, while the bimesogenic has one at either end. The miscibility of the dye and host and the mesophase characteristics of the resulting mixtures will be investigated.

Chapters six and seven will examine the effect of "photoisomerising" illumination, on the two orgaosiloxane systems, with ultra violet light. The effect of ultra violet illumination on the transition temperatures, spontaneous polarisation and tilt angles will give an indication of any change in the order parameter of the mesophase.

Chapters eight and nine will describe flexoelectric chiral nematic materials. The bimesogenic host molecules[5,6,7] have been designed to combine a pear and banana shape asymmetry and show a large flexoelectric coefficient. In chapter nine the mixtures of 8OCB and a chiral agent will be used that have a smaller flexoelectric coefficient but because a smectic A phase is present below the chiral nematic phase

there is more of a variation of the properties with temperature. The changes in phase transition temperatures and helical pitch and response times for both flexoelectric mixtures with ultra violet illumination will be investigated to evaluate any changes in the order parameter or flexoelectric coefficient.

The concluding chapter ten will discuss the new experimental data presented here concerning the dye guest host properties of new smectic and chiral nematic mixtures. The miscibility of dye and host molecules with a similar structure will be investigated. The consequences of the addition of dye on the phase characteristics and switching properties of the host will be detailed. The effect of ultra violet illumination on the photoisomerising dye molecules and consequently on the mixtures as a whole will be investigated.

References for Chapter 1

[1] Clark, N.A., Lagerwall, S.T., Appl. Phy. Lett., **36(11)**, 899, (1980)

[2] Garoff, S., Meyer, R.B., Phys.Rev.Lett, **38**, 848-851, (1977)

[3] Photochromism, Ed. G.H.Brown, Wiley Interscience (1971)

[4] Coles, H.J., Owen, H., Newton, J., Hodge, P., Liquid Crystals, **15(5)**, 739-744, (1993)

[5] Musgrave, B., Lehmann,P., Coles,H.J., Liquid Crystals, **26(8)**, 1235-1249, (1999)

[6] Musgrave, B., Lehmann, P., Coles, H.J., Mol.Crys.Liq.Cryst, **238**, 309-316(1999)

[7] H.J.Coles, M.J.Coles, S.Perkins, B.Musgrave, D.Coates, E.U. Patent EP 99119114, (1999)

Chapter 2

Background Theory and Considerations

Chapter 2 Background Theory and Considerations

2.1 Introduction

The liquid crystalline phases and switching behaviour to be examined in this thesis will be explained in this chapter. The electrical and optical measurements will be explained in principle in this chapter and practical considerations will be described in chapter 3. The effect of the order in a liquid crystal system on its physical properties will be discussed. In this thesis the order will be changed experimentally by incorporating a photoisomerising azo dye. The shape of these dyes can be changed by illumination with ultra violet light, converting a straight molecular configuration to a bent form.

The materials that are to be investigated in this thesis exhibit liquid crystalline phases. For liquid crystalline materials a range of phases appear at temperatures between the solid and liquid phases, rather than there being a direct transition from solid to liquid. Often called mesophases these phases are literally, intermediate in character between the solid and liquid states. Liquid crystalline phases were first proposed by Freidrich Reinitzer[1] in 1888 when two different melting points were observed in a derivative of cholesterol.

The molecules of a liquid possess no long range positional or orientational order. This random arrangement cancels out any microscopic anisotropy of the molecules producing a macroscopically isotropic medium. In contrast, the molecules of a solid are constrained in a three-dimensional lattice and can be macroscopically anisotropic. Liquid crystals form a range of mesophases with varying order intermediate between that of a solid and of a liquid. This can be positional or orientational order or a combination of the two. Positional order in one dimension is shown in the layered structure of smectic liquid crystals. Nematic liquid crystals show orientational order of the constituent molecules.

2.2 Liquid Crystalline Phases

Two main groups of liquid crystalline phases appear as the temperature of a material is varied. The nematic phase, denoted N, has the lowest order and, if

present, will appear at higher temperatures than the smectic phases. The nematic liquid crystals have no long-range positional order of their constituent molecules. However, the average direction of the molecules tends to be parallel to a common director $\underline{n}$ giving orientational order. The nematic material is uniaxially anisotropic along this director. For achiral molecules and racemic mixtures the form of nematic shown in figure 2.1 occurs.

If the nematic material contains a chiral component it is found that the director rotates helically in space as shown in figure 2.2. This chiral nematic phase can also be called cholesteric as it was originally observed in derivatives of cholesterol and is denoted N*. Although the director changes periodically there are no physical layers of molecules. A more detailed description of the chiral nematic phase and flexoelectric switching will be given in section 2.7.

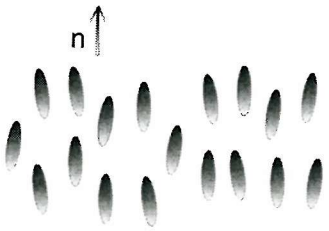

Figure 2.1 The nematic liquid crystal phase showing the average director $\underline{n}$ and the lack of positional order.

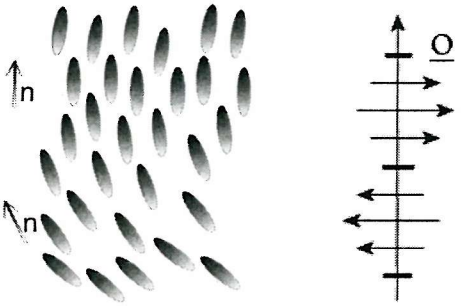

Figure 2.2 The twisted nematic liquid crystal phase, N*, showing how the director $\underline{n}$ and the optic axis $\underline{o}$ changes in space while there is no physical layering of the molecules.

Smectic liquid crystals, however, form layered structures. The most common phases, with the lowest symmetry, are smectic A and smectic C. In these structures the molecules are randomly arranged within the layers, each layer being analogous to a two dimensional liquid. The direction of the molecules in the smectic A phase tends towards that of the layer normal as shown in figure 2.3. The layer spacing is

consistent with the length of the molecules and the material is optically uniaxial in either direction parallel to the layer normal.

In the smectic C phase the direction of the molecules tends to be tilted away from the layer normal as shown in figure 2.4 and consequently the layer spacing is less than the molecular length. If a chiral molecule is present in the mesophase the direction of tilt precesses from layer to layer as shown in figure 2.5. The switching in chiral smectic phases will be discussed further in sections 2.4, 2.5 and 2.6.

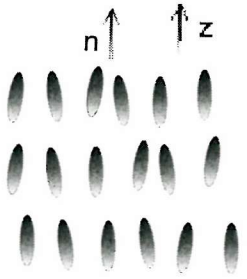

Figure 2.3 The smectic A liquid crystal phase with the average director n perpendicular to the layers.

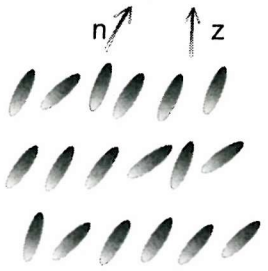

Figure 2.4 The smectic C liquid crystal phase with the average director n at an angle to the layer normal z.

Figure 2.5 The chiral smectic C* phase showing the director n precessing from layer to layer

There exist many more smectic phases with increasing order within the layer plane. For example in the smectic B, smectic I and smectic F phases there is hexagonal packing of the molecules in each layer, without any correlation between the layers. A

more detail description of the higher order smectic phases can be found in the book by Gray and Goodby.[2] The phases discussed above can be identified by their microscopic textures, which are described more fully in section 3.3.

Much of the work for display applications has concentrated on twisted nematic structures with chiral aditives. In this thesis investigations of electro-optic effects in chiral nematic, smectic C* and smectic A* liquid crystals are investigated. An explanation of the theoretical characteristics of these phases is given in the next sections.

2.3 Order of liquid crystalline phases

So far the order of liquid crystalline phases has been discussed qualitatively in terms of the positional and orientational order present in the mesophase. A more quantitative order parameter can be defined, that has a maximum possible value of one in a perfectly ordered example of the phase and a minimum value of zero at temperatures above the transition to the isotropic phase.

The nematic phase can be modelled as a collection of simple rods.[3] For example the Maier-Saupe[4] theory is a molecular field approximation for which two symmetrical properties can be defined. There must be cylindrical symmetry about the director $\underline{n}$ and the directions $\underline{n}$ and $-\underline{n}$ are fully equivalent. The order parameter can be defined as a function of the angle, θ, of the molecular axes from the director. The function used in equation 2.1 is the statistical average of the second Legendre polynomial and is equal to one for a perfectly ordered nematic and to zero for randomly arranged rods.

$$S = \frac{1}{2}\left\langle 3\cos^2\theta - 1 \right\rangle \qquad \text{equation 2.1}$$

The order parameter can be directly related to experimentally determinable properties of a nematic material[3]. For example the diamagnetic anisotropy, the optical anisotropy and from nuclear magnetic resonance measurements. The elastic constants, to be discussed further with respect to the flexoelectric chiral nematic switching are proportional to the square of the order parameter[5].

As the nematic phase changes to the smectic A phase the orientational order of the molecules is unchanged. However the positional order is increased as the layers are formed. The nematic to smectic A transition may theoretically be first or second order. If the transition is second order pretransitional effects will occur in the nematic phase just above the transition[6]. There is often a marked pretransitional effect in the elastic properties as the twist and bend elastic deformations present in the nematic phase do not exist in the smectic phase.

The phase transition from the smectic A to smectic C* phase involves a change in the tilt of the molecules from the layer normal. The Landau theory[7] of phase transitions for ferroelectric materials has the tilt angle as the primary order parameter. Minimisation of the free energy written as a function of the order parameter gives a relationship between the tilt angle, θ, and the temperature, T, equation 2.2 where T_c is the smectic A to smectic C* transition temperature and K_θ is a constant. The mean field approximation predicts that the constant β has a value of 0.5 and it has been found experimentally to range from 0.35 to 0.5[8]. This relationship is analogous with the Bose condensation of superfluid helium.

$$\theta = K_\theta (T_C - T)^\beta \qquad \text{equation 2.2}$$

The magnitude of the spontaneous polarisation in a ferroelectric smectic C* phase depends on the tilt angle[9]. As the tilt angle goes to zero the polarisation goes to zero. If the tilt angle is changed from positive to negative the sign of the polarisation is reserved so the polarisation can be described as an odd function of the tilt. For many materials, especially at low tilts this relationship is linear and the polarisation follows the same law as the tilt, equation 2.3.

$$P = K_P (T_C - T)^\beta \qquad \text{equation 2.3}$$

The change from a ferroelectric smectic C* phase to the isotropic phase is often first order causing a discontinuous change in the tilt angle and spontaneous polarisation at the phase transition.

2.4 The Ferroelectric Smectic C* phase

The ferroelectric properties of materials with a smectic C* phase will be investigated in this thesis. They are of particular interest for display applications because of their fast switching times and bi-stable switching[10,11,12,13]. For a dielectric material the relationship between the applied electric field and the electric polarisation is linear, but for a ferroelectric material hysteresis occurs as shown in figure 2.6. From this it can be seen that a ferroelectric material has a threshold voltage, before which it will not switch, and will have an electric dipole moment in the absence of an external electric field. However this cannot usually be observed macroscopically because of an accumulation of charge on the surface from the atmosphere. Ferroelectric materials can be identified from their hysteresis loops or from the presence of a single current pulse, as the dipoles re-orient, in an alternating current passed through the material illustrated in figure 2.7.

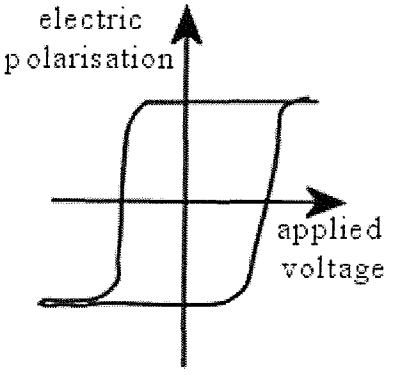

Figure 2.6 Hysteresis of the electric polarisation of a ferroelectric material with the applied voltage.

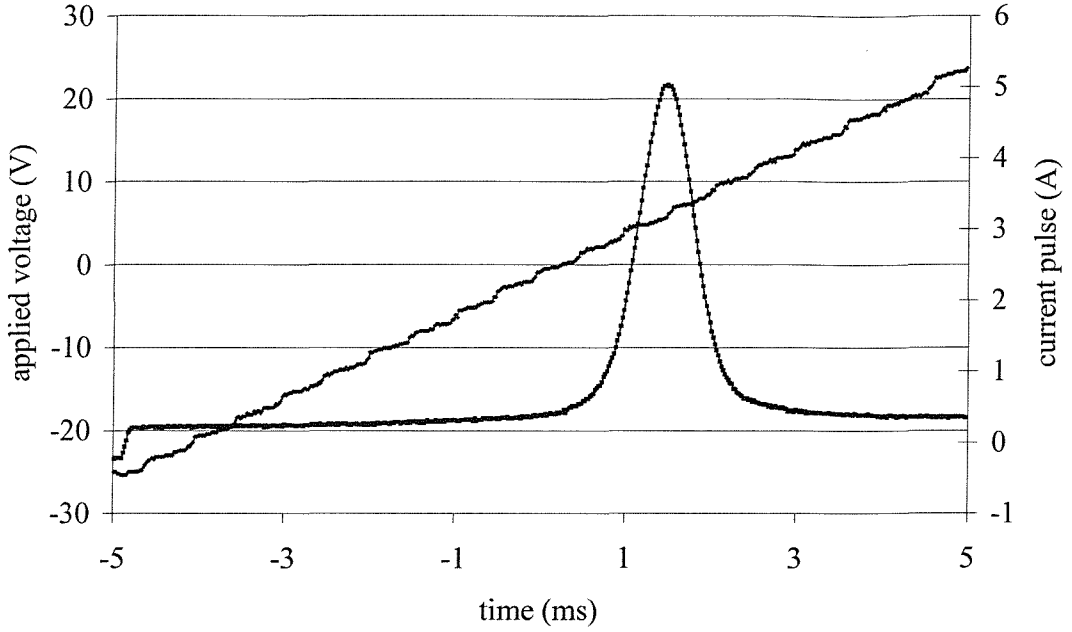

Figure 2.7 Example of a single current pulse for the ferroelectric material Br11-Si3

Symmetry can be used to identify the liquid crystalline phases that may exhibit ferroelectricity, and those that are incapable of producing a macroscopic polarisation. Von Neuman's principle states that the physical properties of a material, for example the polarisation, will include the symmetry characteristics of that material. The smectic C* phase is the least ordered mesophase capable of exhibiting ferroelectricity. The smectic I* and smectic F* phases, which possess hexagonal ordering within the smectic layers, can also be ferroelectric[14]. From the prediction by Meyer[10] in 1975 the material DOBAMBC was shown to exhibit ferroelectricity in the smectic C* phase

It can be shown that the achiral smectic C phase cannot generate a spontaneous polarisation because it posses too much symmetry. The symmetry of this phase consists of a centre of inversion; a mirror plane normal to the layers and a two fold rotation axis perpendicular to both the layer normal and the director. The chirality of the molecules in the smectic C* phase reduces this symmetry to just the two fold rotation axis as shown in figure 2.8 and there is the potential for a spontaneous polarisation parallel to this axis. To maximise this polarisation the liquid crystal molecules should have a large dipole moment perpendicular to the long molecular axis.

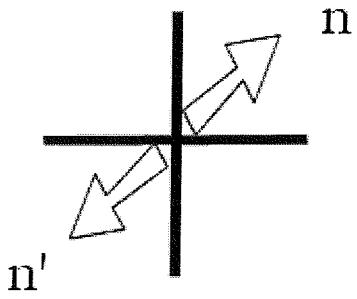

Centre of Inversion $x \rightarrow -x,\ y \rightarrow -y,\ z \rightarrow -z$

$\underline{n} = \underline{n}'$ for achiral Smectic C $\quad \underline{n} \neq \underline{n}'$ for chiral Smectic C*

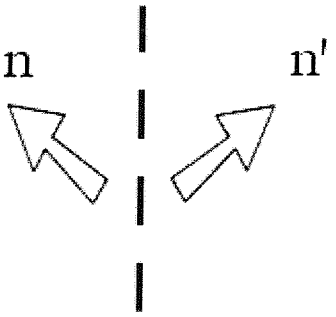

Mirror plane

$\underline{n} = \underline{n}'$ for achiral Smectic C $\quad \underline{n} \neq \underline{n}'$ for chiral Smectic C*

Two fold Rotation Axis

$\underline{n} = \underline{n}'$ for achiral Smectic C and for Chiral Smectic C*

Figure 2.8 For an achiral material the three symmetry operations leave the medium unchanged. For a chiral material only the two fold rotation leaves the material unchanged.

In the bulk smectic C* phase the spontaneous polarisation rotates from layer to layer with the director and is cancelled out over a macroscopic distance. This twisted phase should properly be called helielectric. However, as suggested by Clark and Lagerwall[12], if a sufficiently thin sample is prepared the surface interactions are enough to unwind the helix producing a surface stabilised ferroelectric liquid crystal (SSFLC) device.

A schematic diagram, figure 2.9a, of the SSFLC device shows the bookshelf geometry with the smectic layers perpendicular to the cell surfaces. The anisotropy of the rod shaped molecules produces an optic axis parallel to the long axis of the molecule. The tilt angle, θ, is defined as the angle between this optic axis and the layer normal, figure 2.9b. If an electric field is applied, the molecules will switch through twice the tilt angle. To minimise the energy of the switch and maintain the optimum layer thickness the molecules rotate 180° around a cone within the layer. This switching is called Goldstone switching and causes a change from positive to negative spontaneous polarisation.

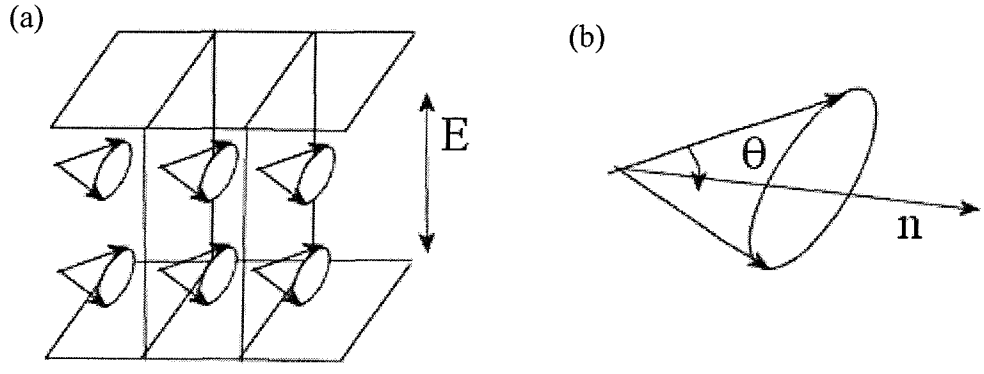

Figure 2.9 (a) Schematic diagram of the surface stabilised ferroelectric liquid crystal device (b) the tilt angle, θ, is the angle between the layer normal, n, and the molecular axis.

The smectic C* phase often cools directly from the smectic A phase. Rather than breaking and reforming, the smectic layers can retain their spacing and tilt into chevrons[15] as shown in figure 2.10. This chevron structure produces characteristic

zigzag defects. However this has never been observed in the organosiloxane materials studied in this thesis so a perfect bookshelf geometry is assumed.

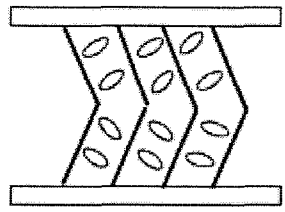

Figure 2.10 Schematic diagram of the chevron structure of a surface stabilised ferroelectric cell cooled from the smectic A phase.

A well aligned surface stabilised ferroelectric liquid crystal device acts as a uniform anisotropic material with a characteristic birefringence. The transmitted intensity through crossed polarisers for incident light of intensity, I_0, and wavelength, λ, depends on the tilt angle, θ, the birefringence, Δn, and the cell thickness, d as shown in equation 2.4.

$$I = I_0 \sin^2(4\theta)\sin^2\left(\frac{\pi\Delta nd}{\lambda}\right) \quad \text{equation 2.4}$$

The maximum transmission occurs when both terms are equal to one. The cell thickness and birefringence can be chosen to produce a peak in the visible spectrum. The first term is maximised when the angle is equal to 22.5° so many materials have been synthesised with tilt angles close to this value. Materials with a tilt angle close to 45°, for example the organosiloxane materials studied in this thesis, can be used in displays with just one polariser[16].

The characteristic response time of a material to an applied electric field can be defined in more than one way and measured via more than one physical property. The electrical and optical response times used in this thesis are explained in section 3.7. All the definitions of the response time have a similar dependence on the physical properties of the material. For a ferroelectric smectic C* material the response time, τ, is dependent on the viscosity, γ, the spontaneous polarisation, P, and the applied

electric field, E, as shown in equation 2.5[17]. The viscosity is exponentially proportional to the temperature, T, via an activation energy. E_A, in an Arrhenius type law, equation 2.6.

$$\tau = \frac{\gamma}{PE} \qquad \text{equation 2.5}$$

$$\gamma = \gamma_0 e^{\frac{E_A}{RT}} \qquad \text{equation 2.6}$$

Ferroelectric materials could be more useful than nematic materials for display applications because the coupling of the polarisation with an applied field results in a faster switching time and bistability. However it can be difficult to produce a grey scale in the SSFLC geometry.

2.5 Antiferroelectric Smectic C* phase

Some liquid crystals with a smectic C* phase exhibit an antiferroelectric phase either instead of or in addition to a ferroelectric phase. The antiferroelectric phase has three stable states which produce a DC threshold in the apparently ferroelectric switching. Chandani et al[18] were the first to recognise that tristable switching and a DC threshold were both caused by an antiferroelectric state. In the unperturbed, zero field antiferroelectric state the molecules in the smectic layers form a helicoidal pattern as in a ferroelectric phase. However the orientation of the dipole in each adjacent layer has the opposite sense as shown in figure 2.11. This is an exaggerated depiction as the pitch is much larger than the layer spacing[19], $p/d \approx 10^3$. In the surface stabilised situation the helix is unwound and the dipoles in adjacent layers cancel producing zero polarisation as shown in figure 2.12b. As an alternating current is applied the antiferroelectric structure is switched to the two extreme ferroelectric structures, as shown in figure 2.12. This produces a double hysteresis loop with a DC threshold as shown in figure 2.13 and a double pulse in the current passed through a cell, figure 2.14.

Antiferroelectric materials have applications in display devices. The double hysteresis loop and the use of a positive and negative driving voltage gives rise to a large

viewing angle[19]. A contrast ratio of up to 30[20] is possible and fast response times of 50μs. However the presence of a pretransitional effect below the threshold voltage

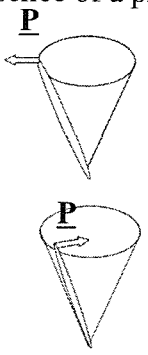

may decrease the contrast ratio.

Figure 2.11 Schematic diagram of the helicoidal antiferroelectric structure. The tilt precesses from layer to layer while the orientation of the dipole reverses from layer to

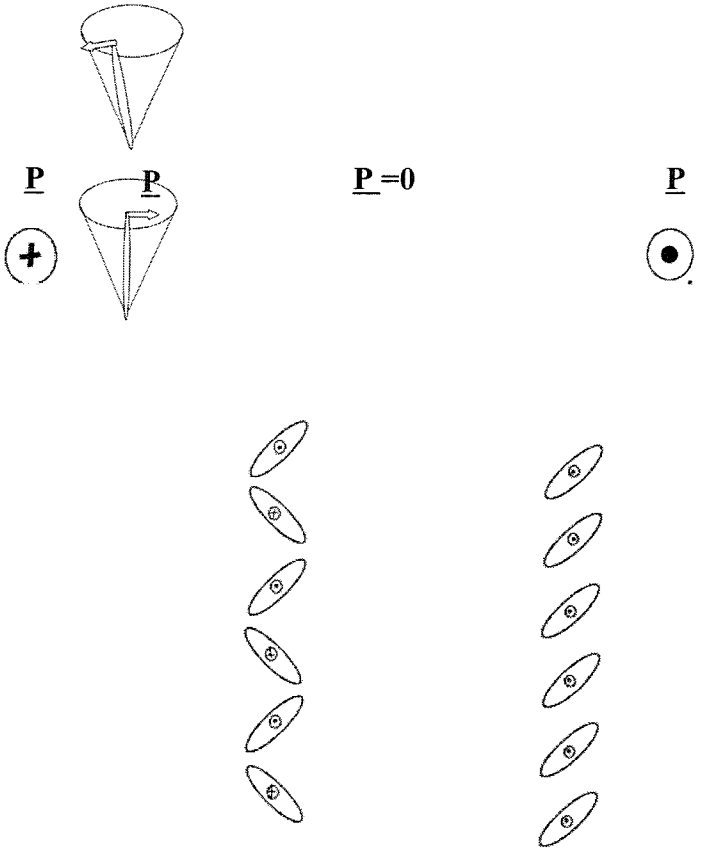

layer.

(a) E+ (b) E=0 (c) E-

Figure 2.12 (a) ferroelectric state for positive electric field (b) zero field antiferroelectric state (c) ferroelectric state for negative electric field

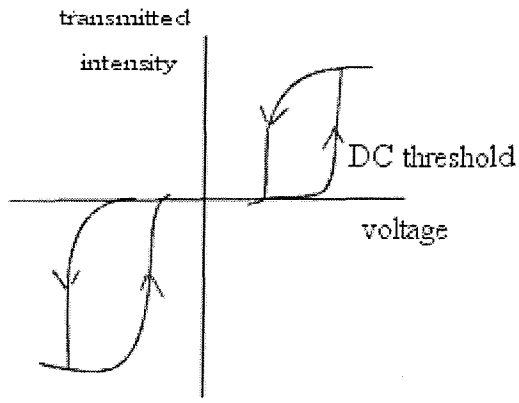

Figure 2.13 Hysteresis loop for transmitted intensity against voltage showing the DC threshold

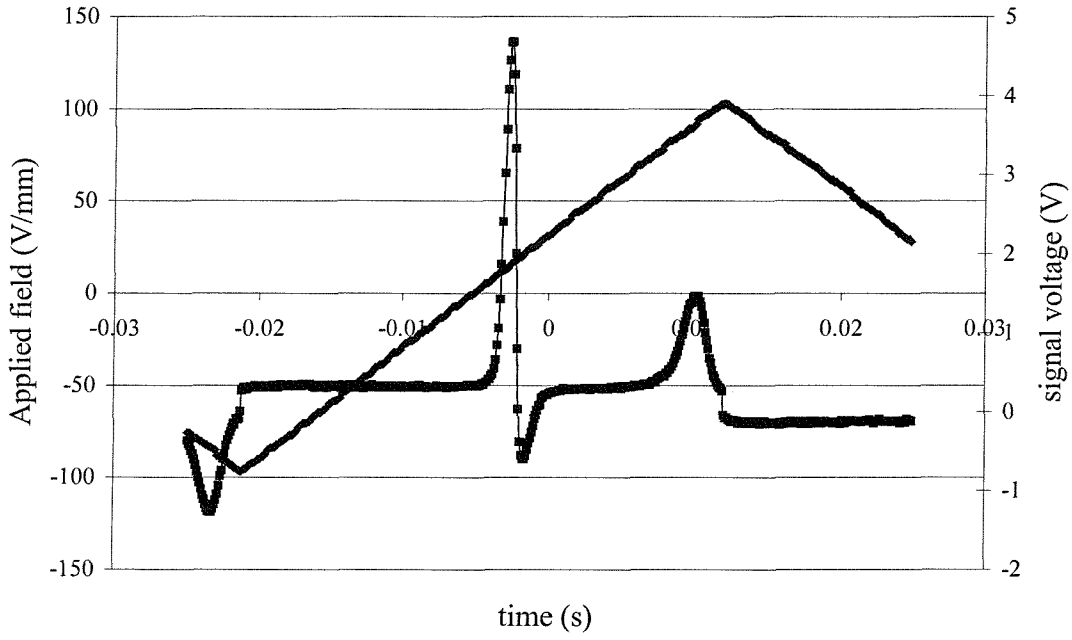

Figure 2.14 Double current pulse peak in response to a triangular wave

Other subphases of the smectic C* phase have been detected by differential scanning calorimetry. The relationship between the direction of tilt in these phases is more complex than for the ferroelectric and antiferroelectric. The phase designated smectic

C^*_γ has been shown by conoscopy and by observations of its switching properties to be ferrielectric.

2.6 Electroclinic Smectic A phase

The chiral smectic A* phase also exhibits a form of electro-optic switching. This is called electroclinic switching and occurs predominantly at temperatures close to the smectic A* to smectic C* transition. It can also penetrate into the smectic C* phase, and was originally investigated as a pretransitional effect by Garoff and Meyer in 1977[21]. The electroclinic switching is dielectric in origin and an induced polarisation grows linearly with the applied field. There is a reduction in symmetry[22] of the chiral smectic A phase from the achiral version analogous to that which causes a spontaneous polarisation in the smectic C* phase. Because of this reduced symmetry, the application of an electric field perpendicular to the layer normal produces a tilt that is linear with the field.

Whereas in the Goldstone mode the optic axis moves around a cone, in electroclinic switching there is a simple change of tilt. This is traditionally called soft mode in spectroscopy, and takes place at higher frequencies than Goldstone switching. Other materials that exhibit linear electro-optic effects include antiferroelectric liquid crystals at voltages below the transition to the ferroelectric state[22], the deformed helix mode in short pitch ferroelectrics[23] and the flexoelectric effect in chiral nematics.

As the field is applied perpendicular to the optic axis, the induced tilt of this optic axis is also linear with the applied field. It can be shown that a small tilt angle, θ, of the optic axis is related, equation 2.5, to the applied electric field, E, by the electroclinic coefficient, e_c. Where μ is the dipole moment per unit volume per unit tilt and α is a constant and T is the temperature and T_c is the smectic A-smectic C* transition temperature. And the response time, τ, is independent of the applied field but dependent on the viscosity, γ, and the temperature as shown by equation 2.6.

$$\theta = e_c E \qquad \theta = \frac{\mu}{\alpha(T - T_c)} E \quad \text{equation 2.5}$$

$$\tau = \frac{\gamma}{\alpha(T - T_c)}$$ equation 2.6

The switching could be useful in applications because it is very fast and thresholdless and produces a grey scale. However the change of the tilt angle with temperature narrows its possible operating range.

2.7 Flexoelectric Chiral Nematic phase

Flexoelectric coupling can occur between an applied electric field and the molecular dipoles of nematic, chiral nematic and smectic phases. For the purpose of this thesis we will describe the flexoelectric effect in the chiral nematic phase. There is a linear coupling of an electric field with the splay and bend deformations resulting in the modulation of the optic axis. Meyer compared this coupling in strongly asymmetric nematic molecules to piezoelectricity in crystals[24]. A flexoelectric-optic effect was first observed in chiral nematic material by Patel and Meyer[25] in 1987 and reported more fully by the Chalmers group[26] in 1994.

First the chiral nematic phase will be explained in more detail. The director, n, changes helically with a characteristic pitch as shown in figure 2.15. An aligned chiral nematic has a uniaxial optic axis parallel to the helix axis. The dependence of the pitch upon temperature is not well understood. For many materials the pitch increases as the temperature is reduced, the strongest variation in pitch occurring in materials with a smectic A phase[8,6] below the chiral nematic phase.

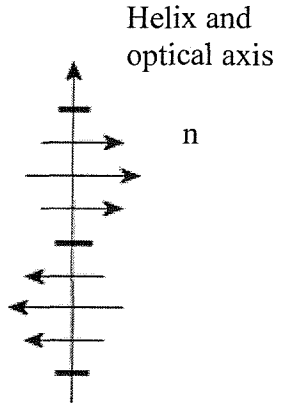

$n_x = \cos\theta, \quad n_y = \sin\theta, \quad n_z = 0$

$\theta = \frac{2\pi}{p} z$ equation 2.7

Figure 2.15 Schematic diagram of the helix of a chiral nematic

The application of an electric, magnetic or shear field can cause three major deformations of the chiral nematic liquid crystal. Elastic deformations of the three main geometries, splay, twist and bend, dielectric coupling between the field and the dielectric anisotropy and flexoelectric coupling in the splay and bend modes.

The splay, twist and bend elastic deformations are shown schematically in figure 2.16. Any deformation of a nematic can be reduced to a combination of these three deformations. In reality the distance over which significant variations occurs is of the order of 1μm compared to the molecular dimension of 20 Å so a continuum theory that disregards molecular detail can be used to describe the deformations.[27]

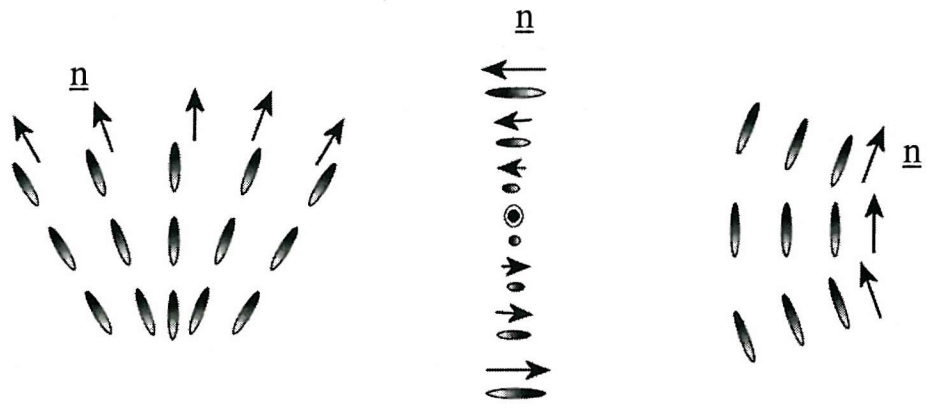

Figure 2.16 (a) splay (b) twist (c) bend deformations of a chiral nematic

The free energy of a nematic can be expressed as the sum of the elastic energy of the splay, twist and bend distortions as described by equation 2.8[28]. Where K_1, K_2 and K_3 are the splay, twist and bend elastic constants and $\underline{n}$ is the director.

$$F_e = \frac{1}{2}K_1(\nabla.\underline{n})^2 + \frac{1}{2}K_2(\underline{n}.(\nabla\times\underline{n}))^2 + \frac{1}{2}K_3(\underline{n}(\nabla\times\underline{n})) \qquad \text{equation 2.8}$$

A molecule with a significant dielectric anisotropy will couple with an applied electric field. The dielectric anisotropy, $\Delta\varepsilon$, is equal to the difference between the dielectric

constant parallel to and perpendicular from the molecular axis. The dielectric coupling is proportional to the square of the electric field, equation 2.9, and for materials with a positive dielectric anisotropy causes the molecules to line up with the applied electric field.

$$F_d = -\frac{\Delta\varepsilon}{8\pi}(\underline{n}.\underline{E})^2 \quad \text{equation 2.9}$$

An undisturbed chiral nematic is twisted. If the molecules have a large shape asymmetry and a molecular dipole, the application of an electric field will add a bend and splay deformation due the flexoelectric coupling. The effect of an electric field applied perpendicular to the helix axis is to induce a flexoelectric deformation that rotates the optic axis away from the helix axis. The director is rotated around an axis parallel to the applied electric field by an angle, θ, as shown in figure 2.17. A cut through the material at that angle shows an alternating bend and splay configuration shown in figure 2.18.

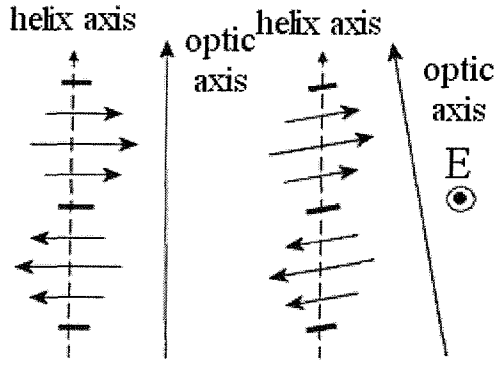

Figure 2.17 Rotation of the optic axis around an axis parallel to the applied electric field

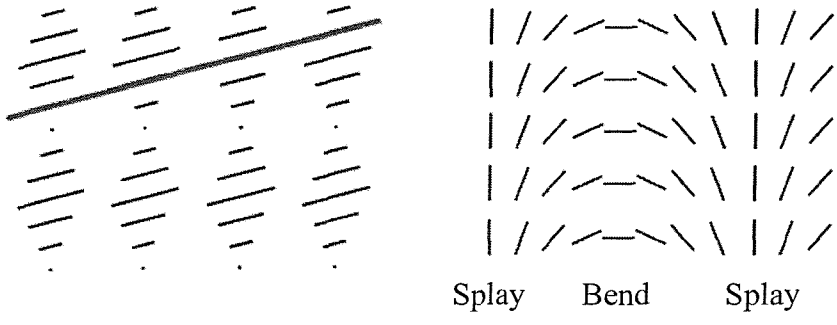

Figure 2.18 The slice (shown in red) taken at an angle parallel to the director shows alternate splay and bend deformations

The free energy of the flexoelectric distortions depends upon the splay and bend flexoelectric coefficients, e_s and e_b and is linear with the applied field as shown equation 2.10.

$$F_f = -\underline{E}\left(e_s \underline{n}.\nabla.\underline{n} + e_b \underline{n} \times \nabla \times \underline{n}\right) \quad \text{equation 2.10}$$

The presence of molecule with either a pear or banana shape will enhance the splay and bend deformations[24] respectively as shown in figure 2.19.

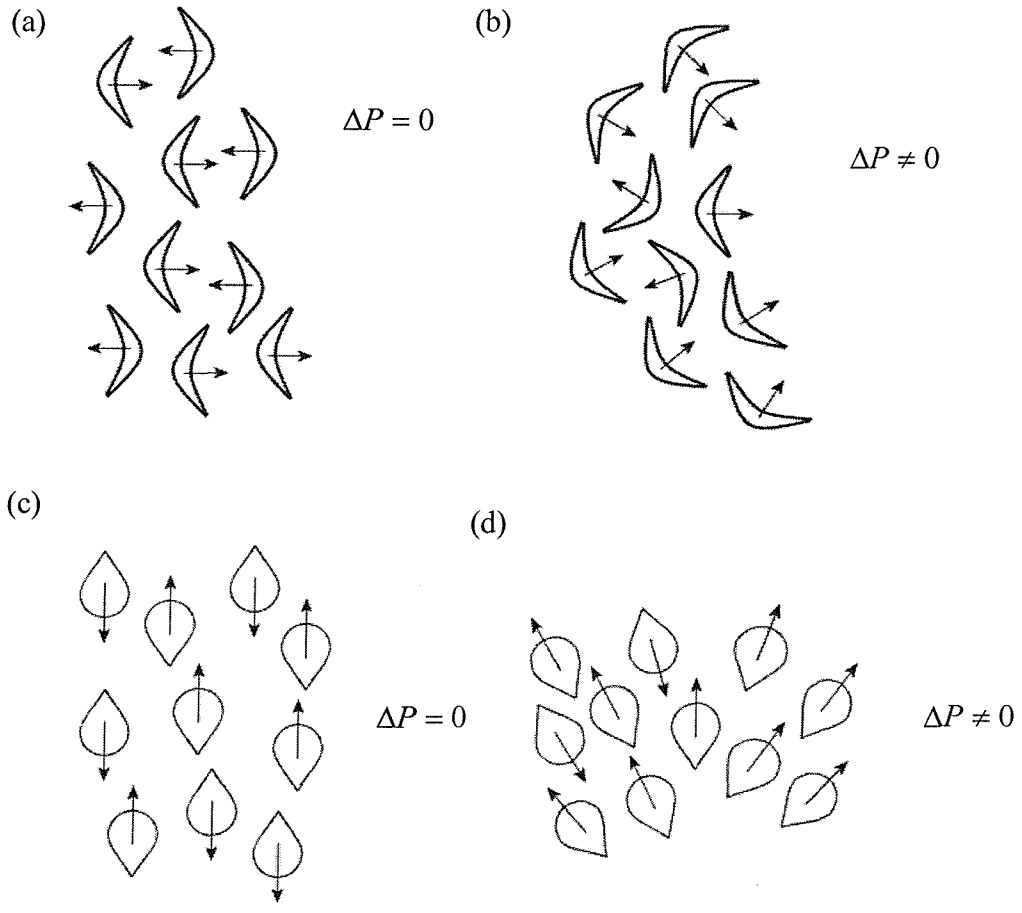

Figure 2.19 (a) undisturbed banana shaped molecules (b) banana shaped molecules with a bent configuration and a net polarisation (c) undisturbed pear shaped molecules (d) pear shaped molecules with a splay configuration and a net polarisation

The sum of the free energies for the elastic deformations, the dielectric coupling and the flexoelectric coupling must be taken into account. The flexoelectric coupling is linear with the applied field, while the dielectric coupling is quadratic with field. Hence, the flexoelectric effect is dominant for low applied fields and the dielectric term can be ignored while describing the tilt angle. If the splay and bend elastic constants K_1 and K_3 are taken to be equal and the dielectric term ignored, minimising the free energy and assuming that the tilt angle is small gives the tilt angle, θ, of the optic axis. The average terms, $\bar{e}$, for the splay and twist flexoelectric coefficients and, K, for the splay and twist elastic coefficients have been introduced.

$$\tan\theta = \frac{\bar{e}pE}{2\pi K} \quad \text{equation 2.11}$$

$$K = \frac{K_1 + K_3}{2} \qquad \bar{e} = \frac{e_s + e_b}{2}$$

For small angles this tilt angle is proportional to the applied electric field. Despite being a small angle approximation it has been fitted successfully to angles up to 32°[26]. To maximise the tilt angle a flexoelectric material must have a large ratio of flexoelectric to elastic coefficients and a large pitch. The maximum pitch is constrained by the occurrence of a visible fingerprint texture. For a material with a constant pitch the angle is independent of temperature as both the flexoelectric coefficient and the elastic constant scale with the square of the order parameter.

At high fields the dielectric effect becomes more significant and the relationship between the tilt angle and the applied electric field can become non linear. As the field increases the dielectric coupling becomes dominant and at a threshold voltage the twisted conformation is converted to the homeotropic texture with all the molecules parallel. This critical voltage depends upon the twist elastic constant, the pitch and the dielectric anisotropy as given by equation 2.11.

$$E_C = \frac{\pi^2}{p}\left(\frac{4\pi K_2}{\Delta\varepsilon}\right)^{\frac{1}{2}}$$ equation 2.11

The response time, τ, is related to the viscosity,γ, as shown in equation 2.12. The response time is potentially very fast. To minimise the response time a material must have a short pitch, a low viscosity and a large elastic constant. As for the ferroelectric materials the viscosity has an Arrhenius temperature dependence as shown in equation 2.13.

$$\tau = \frac{\gamma p^2}{4\pi^2 K}$$ equation 2.12

$$\gamma = \gamma_0 e^{\frac{E_A}{RT}}$$ equation 2.13

To measure the flexoelectric coupling in a chiral nematic material it must be in the uniformly lying helix texture. A cell with ITO electrodes provides an electric field across the cell and planar alignment. When cooled from the isotropic to the chiral nematic phase a material with a positive dielectric anisotropy will form a natural texture of a Grandjean or standing helix. This is shown schematically and as viewed perpendicular to the cell surface in figure 2.20 (a) with the optic axis perpendicular to the cell surface. When a small field is applied the helices start to tilt and a grid and stripe pattern may be observed, figure 2.20 (b). There may be a direct transition to the focal conic texture if this structure is not stable or the focal conic texture may appear without an increase in the voltage as this structure breaks down. The focal conic texture has random areas of helix as shown in figure 2.20 (c). If the focal conic texture is sheared, by application of a small pressure to the cell for example, the helices will align perpendicular to the cell surfaces producing the uniformly lying helix as shown in figure 2.20 (d). If the field is further increased the dielectric coupling will become great enough to force the molecules to align parallel to the field producing the homogeneous texture, figure 2.20 (e). The optical textures for these alignments are shown for the 7/11 bimesogen mixture in figure 2.21.

The flexoelectric properties of tilt angle and response time can be measured in the uniformly lying helix texture as describe fully in chapter 3.

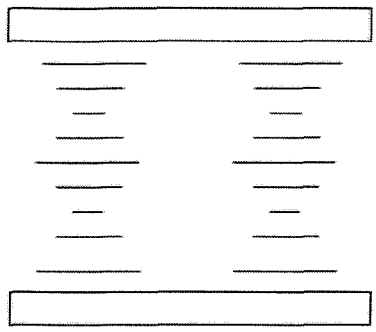

(a) Grandjean texture

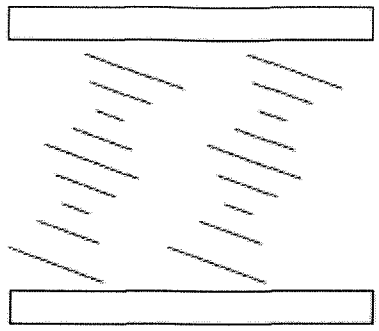

(b) Grid and Stripe texture

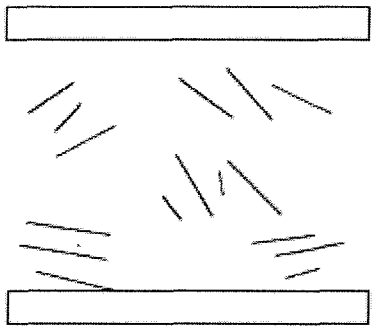

(c) Focal Conic Texture

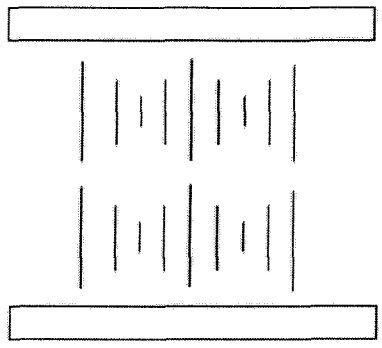

(d) Uniformly Lying Helix

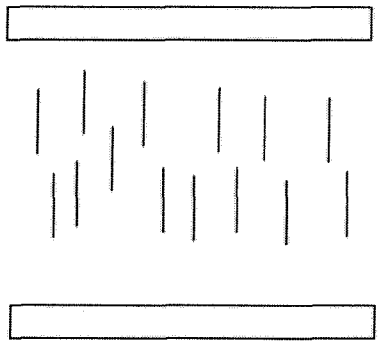

(e) Homeotropic texture

Figure 2.20 Schematic alignment of the chiral nematic effect observed in thin cells with planar alignment

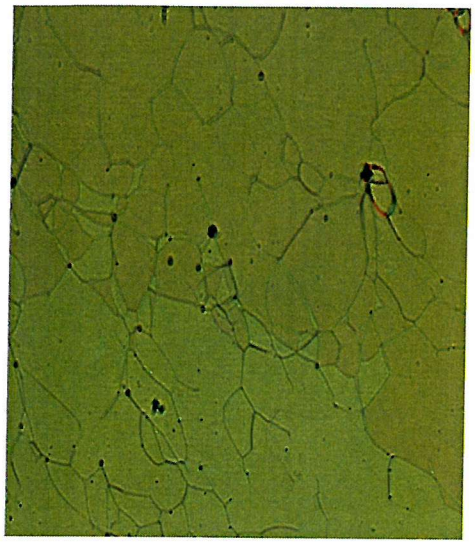

(a) Grandjean texture

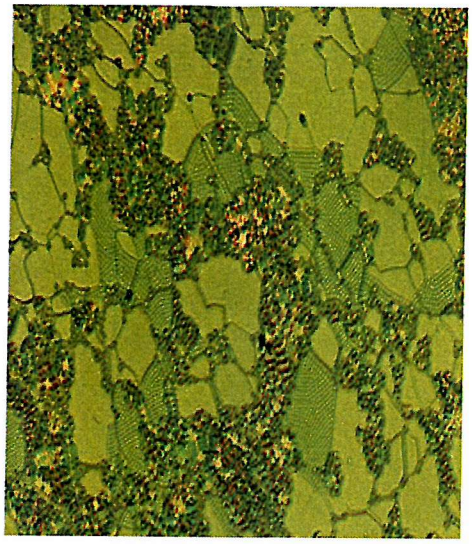

(b) Grid and stripe texture 9V/□m

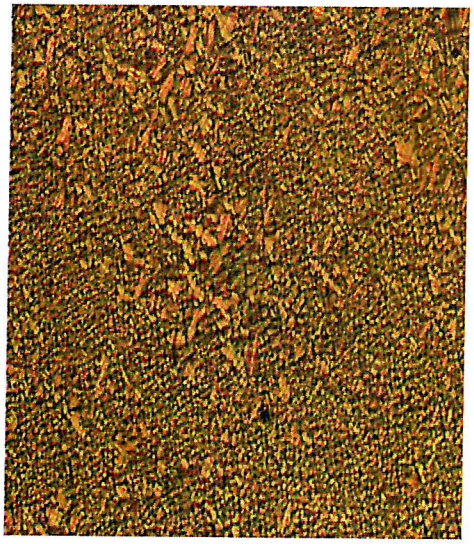

(c) Focal Conic texture

(d) Uniformly Lying Helix texture

Figure 2.21 Textures of the chiral nematic mixture 7/11 bimesogen plus BDH1281 observed in thin cells with planar alignment

There has been much interest in the flexoelectric effect in chiral nematic liquid crystals because of possible uses in display applications and optical switches and modulators. The switching has been found to be linear with the applied field and independent of temperature (as long as the pitch is constant). The thresholdless switching gives the possibility of greyscale applications. The response times are short, often of the order of microseconds to milliseconds. The chiral nematic molecules must have a strong electric dipole and an asymmetric shape to exhibit flexoelectric properties. A pear shaped molecule contributes to the splay deformation, while a banana shaped molecule contributes to the bend deformation. To exhibit a large polarisation the material will ideally have a short pitch, a high elastic constant and a small but positive dielectric anisotropy. Much work has been done to optimise these properties by engineering the shape of the molecules. The bimesogen materials[29,30,31,32] that will be studied in this thesis have been developed in house to attempt to combine the pear and banana shapes to produce large flexoelectric coefficients.

2.8 Photoisomerisation

Photoisomerising dye molecules will be added to liquid crystal systems in this thesis. A photochromic species can be defined as one that changes between two states having distinguishably different absorption spectra, such a change being induced in at least one direction by electromagnetic radiation.[33] The photochromic changes that are of most interest in this thesis involve a steric, or shape change, of the molecule. This involves the reversible change from one isomer to another of higher energy and will be called photoisomerising. The molecules will incorporate an azo linkage which photoisomerises from the straight trans to the bent cis isomer when illuminated by ultra violet radiation in the region 290-350 nm as shown schematically in figure 2.22. The absorption maximum for the simple azobenzene molecule is ~310 nm and the addition to the benzene rings of extra groups causes a minor change of this range.

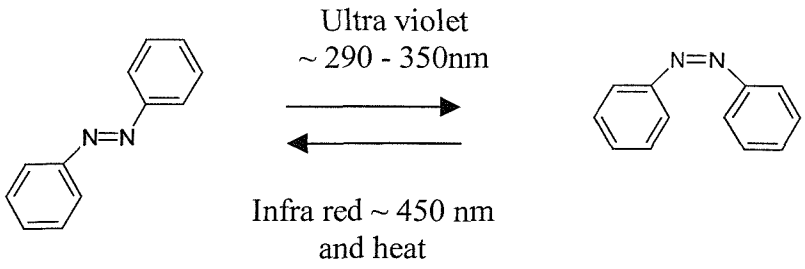

Figure 2.22 The straight trans isomer converts to the bent cis isomer under ultra violet illumination and is returned by heat and longer wavelengths

Liquid crystal systems incorporating photisomerising materials have been investigated to determine the effect of the steric change of the molecules and for potential applications in optically addressed devices[34,35] and as a method of alignment[36]. The first record of such a phenomenon was the increase in pitch of a chiral nematic doped with azobenzene, which was photoisomerised from the trans to the cis isomer.[37] Liquid crystals have been used for electro-optic applications because small changes in the applied field result in large changes in the optical modulation properties of the liquid crystal. The aim of the use of photoisomerising materials is to modulate light with light. A short summary will be given of what has been done in several liquid crystalline phases and with a number of photoisomerising species.

Initial investigation concentrated on materials having the nematic phase. The effect of ultra violet illumination on many photoisomerising liquid crystals is to suppress the phase transition temperatures. It is often possible to induce an isothermal transformation from the nematic phase to the isotropic phase. The presence of a soluble photoisomerising dye in the liquid crystal will cause the same effects in the properties of the host. A homogeneous monodomain alignment of the nematic phase has a high transmission when the director is at 45 ° to the axis of crossed polarisers. When in the isotropic phase the random structure reduces the transmission close to zero. Polymer liquid crystal phases often have a glass transition from the nematic phase to a glass phase in which the polymer backbone is frozen prohibiting molecular reorientation. If the transformation from nematic to isotropic can be made below the

glass transition temperature the random structure of the isotropic phase will be maintained after the ultra violet illumination is ceased.[38]

Photisomerising molecules can also be incorporated in the alignment materials to reorient the nematic liquid crystal at the cell surfaces.[36] They can also be added as a dye to the bulk liquid crystal to again change the alignment upon ultra violet illumination.[39]

Re-writable storage devices have been investigated using smectic A liquid crystal polymers. Large area homeotropic mono-domains with a clear, non-scattering appearance and high transmittance can be prepared by applying a high frequency electric field. This texture is stable for a wide range of temperatures in the smectic phase. A contrasting scattering texture with a low transmittance can be produced by two methods.

Local heating into the isotropic phase by a high power laser[40,41] followed by rapid cooling back to the smectic phase produces an area with a scattering texture and low transmittance. The main problems with this technique are the high intensities 100 – 1000 W/cm^2 required and the limit of spatial resolution of the laser. The photochromic transition from the smectic phase to the isotropic can be used in place of the laser heating. The advantages of using ultra violet illumination over laser heating are that a lower power is required and the ultra violet can be focussed with a better spatial resolution.

Secondly, if an electric field, above a characteristic threshold voltage, is applied to a smectic A liquid crystal the electrohydrodynamic instabilities in the phase produce a scattering texture. When the field is removed a scattering texture remains as the phase relaxes in to a focal conic texture. The illumination of the sample with ultra violet light inducing the trans to cis isomerisation reduces the threshold voltage necessary to produce a scattering texture.[42,43]

Work has been done to control the spontaneous polarisation of the smectic C* phase. The illumination of the sample by ultra violet reduces the threshold voltage from one

polarisation state to the other and can produce a photo-induced flip in polarisation.[44,45,46]

Antiferroelectric materials have also been used, also to reduce the threshold voltage for switching from one polarisation state to the other because the threshold is often sharper than for ferroelectric materials[44,47]

Two studies[48,49] by the Chalmers and Tokyo Institute of Technology groups have been made of the effect of photoisomerisation of flexoelectric chiral nematic materials containing azo dyes. Both reports found an increase in the effective flexoelectric coefficient as would be suggested if there was an increase in the shape anisotropy of the dye molecules in the cis form.

Other photoisomerising molecules have been investigated as dyes in liquid crystalline systems. These include Thionindigo,[50] Dithieylethene[51] and Cinimate ester[52].

Photoisomerising molecules containing an azo will be used as dyes in this work. The shape change of the dye will be investigated in ferroelectric, antiferroelectric, electroclinic and flexoelectric systems.

References for Chapter 2

[1] Reinitzer, F., Monatsch, Chem., **9**, 421, (1888)

[2] Gray, G.W., Goodby, J.W., Smectic Liquid Crystal Textures and Structures, Leonard Hill, Glasgow, 1984

[3] Chandrasekhar, S., Ch. 2, Liquid Crystals, Cambridge University Press, (1977)

[4] Maier, W., Saupe, A., Z. Naturforsch, **13a**, 564, (1958)

[5] de Gennes. P.G., Ch 3, The Physics of Liquid Crystals, Oxford University Press (1974)

[6] Chandrasekhar, S., Ch. 5, Liquid Crystals, Cambridge University Press, (1977)

[7] de Gennes, P.G., Mol. Cryst. Liq. Cryst., **21**, 49, (1973)

[8] de Gennes. P.G., Ch. 7, The Physics of Liquid Crystals, Oxford University Press (1974)

[9] Lagerwall, S.T., Ch. 2, Handbook of Liquid Crystals Volume 2B, Wiley-Vch, (1998)

[10] Meyer, R.B., Lirbert, L., Strzelecki, L., Keller, P., J. Phys. Lett. **36**, L69-L71, (1975)

[11] Martinot-Lagarde, P.H., J.Phys.Lett., Paris, **38**, 17, (1977)

[12] Clark, N.A., Lagerwall, S.T., Appl. Phy. Lett., **36(11)**, 899-901, (1980)

[13] Lagerwall. S.T., Dahl, I., Mol. Cryst. Liq. Cryst. **114**, 151, (1984)

[14] Goodby, J.W., J.Mater.Chem., **1(3)**, 307, (1991)

[15] Rieker, T.P., Clark, N.A., Smith, G.S., Parmer, D.S., Sirota, E.B., Safinya, C.R., Phys. Rev. Lett., **59(23)**, 2658, (1987)

[16] Patel, J.S., Goodby, J.W., Optical Engineering, **26(5)**, 373-384, (1987)

[17] Goodby, J.W., J.Mater.Chem., **1(3)**, 307-318, (1991)

[18]Chandini, A.D.L., Gorecka, R., Ouchi, Y., Takezoe, H., Fukuda, A., Jpn. J. Appl. Phys, **28**, L1265-L1268, (1989)

[19] Fukuda, S., Takanishi, Y.. Isozaki, T., Ishikawa, K., Takezoe, H., J.Mater.Chem, **4**, 997-1016, (1994)

[20] Inui, S., Iimura, N., Suzuki, T., Iwane, H., Miyachi, K., Takanishi, Y., Fukuda, A., J.Mater.Chem., **6(4)**, 671-673, (1996)

[21] Garoff, S., Meyer, R.B., Phys.Rev.Lett, **38**, 848-851, (1977)

[22] Elston, S.J., Sambles, J.R., Ch 8, The Optics of Thermotropic Liquid Crystals, Taylor and Francis Ltd, (1998)

[23]Funfschilling, J., Schadt, M., J.Appl.Phys, **66(8)**, 3877-3882, (1989)

[24] Meyer, R.B., Phys.Rev.Lett., **22(18)**, 918-921, (1969)

[25] Patel, J.S., Meyer, R.B., Phys. Rev. Lett. **58(15)**, 1538-1540, (1987)

[26] Rudquist, P., Buivydas, M., Komitov, L., and Lagerwall, S.T., J. Appl. Phys., **76(12)** 7778-7783 (1994)

[27] de Gennes. P.G., Ch. 3, The Physics of Liquid Crystals, Oxford University Press (1974)

[28] Chandrasekhar, ch 3, Liquid Crystals, Cambridge University Press, (1977)

[29] Musgrave, B., Lehmann,P., Coles,H.J., Liquid Crystals, **26(8)**, 1235-1249, (1999)

[30] Musgrave, B., Lehmann, P., Coles, H.J., Mol.Crys.Liq.Cryst, **238**, 309-316(1999)

[31] B.Musgrave, M.J.Coles, S.P.Perkins, H.J.Coles, Mol.Cryst.Liq.Cryst. Vol 364-8, (2001)

[32] H.J.Coles, M.J.Coles, S.Perkins, B.Musgrave, D.Coates, E.U. Patent EP 99119114, (1999)

[33] Photochromism, Ch 1, Ed. G.H.Brown, Wiley Interscience (1971)

[34] Gibbins, W.M., Kosa, T., Palffy-Muhoray, P., Shannon, P.J., Sun, S.T., Nature, **377**, 43-46, (1995)

[35] Moriyama, T., Kajita, J., Takanishi, Y., Ishikawa, K., Takezoe, H., Fukuda, A., Japn. J. Appl. Phys., **32**, L589-L592, (1993)

[36] Gibbons, W.M., Shannon, P.J., Sun, S.T., Swetlin, B.J., Nature, **351**, 49-50, (1991)

[37] Sackman, J. Am. Chem. Soc., **93**, 7088-7090, 1971

[38] Ikeda, T., Tsutsumi, O., Science, **268**, 1873-1875 (1995)

[39] Komitov, L., Ruslim, C., Matsuzawa, Y., Ichimura, K., Liq.Cryst., **27(8)**, 1011-1016, (2000)

[40] Kahn, F.J., Appl.Phys.Lett., **22(3)**,111-113, (1973)

[41] Coles, H.J., Simon, R., Polymer **26** 1801-1806 (1985)

[42]Ogura, K., Hirabayashi, H., Uejima, A., Nakamura, K., Jpn. J. Appl. Phys, **21(7)**, 969-973, (1982)

[43] Yu, J-W., Lee, S-N., Materials Letters, **34**, 202-207, (1998)

[44] Ikeda, T., Sasaki, T., Ichimura, K., Nature, **361,** 428-430 (1993)

[45] Walton, H.G., Coles, H.J., Guillon, D., Poeti, G., Liq. Cryst., **17(3)**, 333-349, (1994)

[46] Joly, G., Anakkar, A., Nguyen, H.T., Liq. Cryst., **26(8)**, 1251-1255, (1999)

[47] Moriyama, T., Kajita, J., Takanishi, Y., Ishikawa, K.,Jpn. J. Appl. Phys., **32** L589-L592, (1993)

[48] Herman, D.S., Rudquist, P., Ichimura, K., Kudo, K., Komitov, L., Lagerwall, S.T., Phys. Rev. E, **55**, 2857-2860, (1997)

[49] Komitov, L., Ruslim, C., Ichimura, K., Phys. Rev. E., **61**, 5379-5384, (2000)

[50] Dinescu, L., Lemieux, R.P., J. Am. Chem. Soc. **119**, 8111-8112, (1997)

[51] Maley, K.E., Lemieux, R.P., Mol.Cryst.Liq.Cryst. **364-8**, (2001)

[52] Legge, C.H., Whitcombe, M.J., Gilbert, A., Mitchell, G.R., J.Mater. Chem., **1(2)**, 303-304 (1991)

Chapter 3

Experimental Overview

Chapter 3 Experimental Overview

3.1 Introduction

The experimental techniques used to investigate the liquid crystal systems presented in this thesis are described. Section 3.2 details the microscope set-up with which the electro-optic measurements were made, and by which the sample was illuminated with ultra violet light. The transition temperatures and phase sequence must be determined for all liquid crystals. Measurement of these temperatures and phases are described in section 3.3. For the ferroelectric and antiferroelectric materials the spontaneous polarisation, optical tilt angle and response time must be measured as detailed in sections 3.5, 3.6 and 3.7 respectively. For these measurements the liquid crystal is contained in a glass cell designed so an electric field can be applied across the liquid crystal as described in section 3.4. For the flexoelectric materials the tilt angle and response time are again measured. In addition to this, measurements of the helix pitch of flexoelectric liquid crystals are explained in section 3.8.

3.2 Microscope Set up

The experiment set up, centred around a microscope, is shown schematically in figure 3.1. The microscope[1] was used to observe the sample optically and as a way to illuminate the sample with ultra violet. The sample was placed in a Linkam[2] hotstage, allowing temperature control between –200 and +600°C. This hot stage was mounted on the rotating stage of the microscope between a polariser and adjustable analyser allowing observation between crossed polarisers. The photodiode was used to monitor the intensity of light transmitted by the liquid crystal sample.

Electrical contacts could be made to the surfaces of the cells containing the liquid crystalline materials as described in section 3.4. A signal generator[3] and high voltage amplifier were used to apply square and triangular waveforms to the cell in the range 0-200Vp-p and 0-13MHz. A current to voltage amplifier translates the current through the cell to a voltage that can be displayed on the oscilloscope.[4] The

driving waveform and the photodiode output or I-V voltage can be displayed on a digitising oscilloscope or transferred to a PC to analyse the data using HPVEE software.[5]

The law of Malus for two polarisers was used to confirm that the photodiode response is linear with the intensity of incident light. The magnitude of light transmitted through a pair of polarisers depends on the angle between their axes as given in equation 3.1. The output voltage of the photodiode was measured as a function of the angle, θ, between the polariser and analyser as the analyser was rotated. The recorded intensity, I, follows the law of Malus as shown in figure 3.2.

$$I = I_0 \sin^2(\theta - \theta_0) \qquad \text{equation 3.1}$$

The sample was illuminated by ultra violet from a side arm mercury lamp.[1] The switching on and off of the ultra violet illumination was controlled by a manual shutter. The intensity could be varied from 5 mW/cm^2 to 350 mW/cm^2 by means of a ND6 and a ND25 neutral density filter.

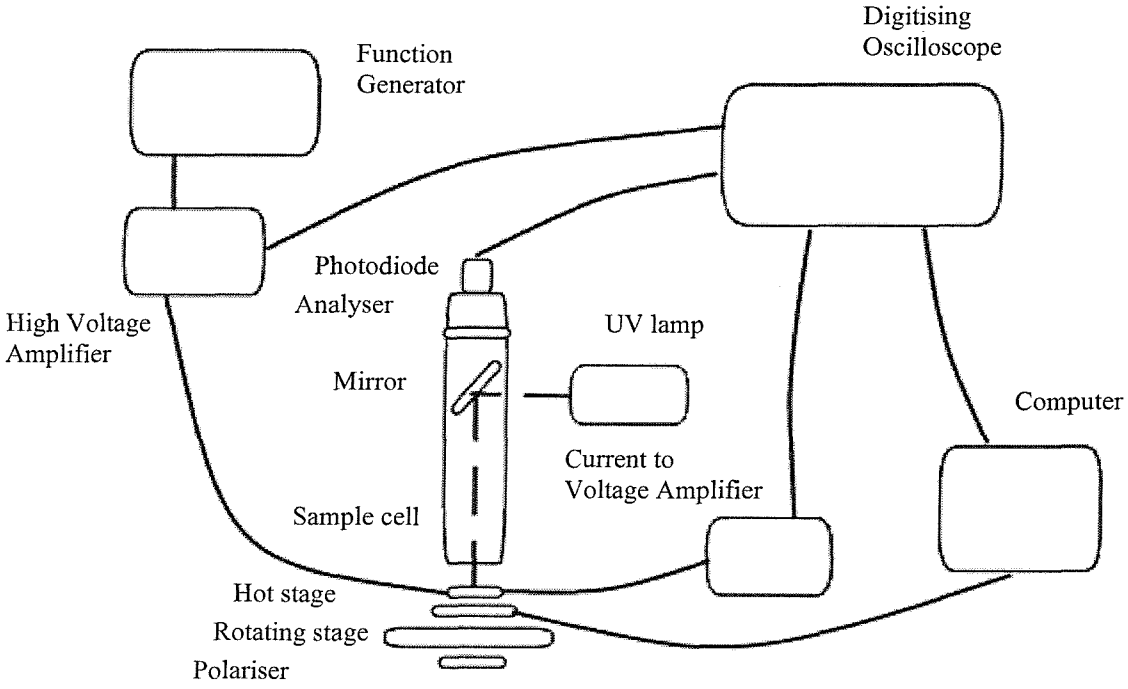

Figure 3.1 Electro-optic measurement – Schematic diagram of equipment centred around the optical microscope

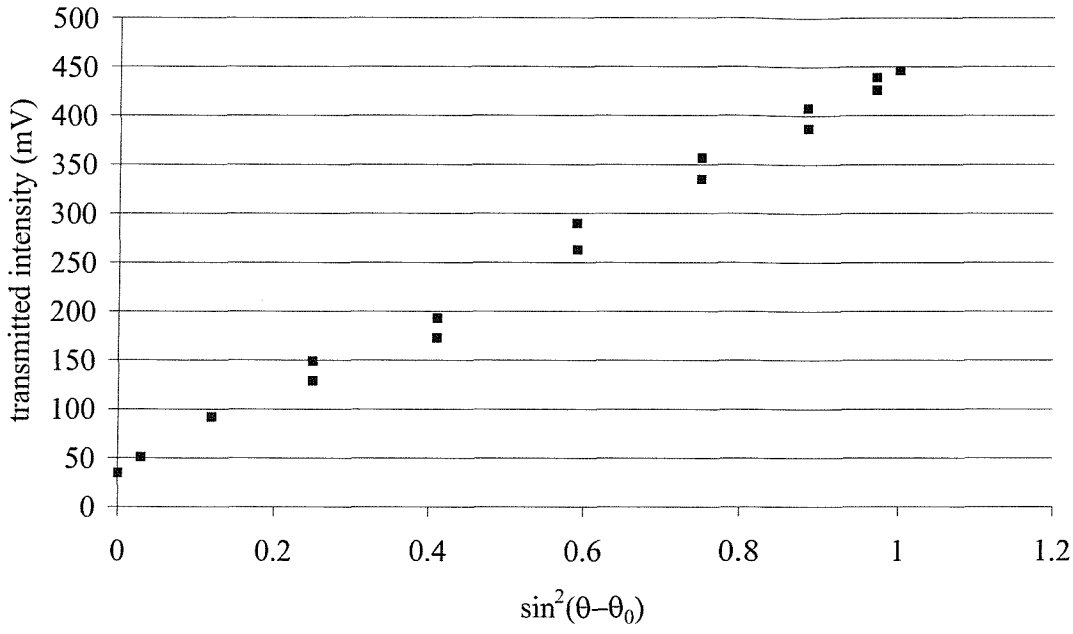

Figure 3.2 Photodiode characteristics – Detected intensity against the angle between two polariser axes

3.3 Phase characterisation

The sequence of liquid crystalline phases and the temperatures of the transitions between phases must be determined. As even small amounts of impurities can change the transition temperatures, comparisons of reduced temperatures, defined as the temperature below the phase transition, are often made. The mesophase type is usually identified by optical microscopy and could be more accurately identified by x-ray scattering.[6] Precise transition temperatures can be obtained from differential scanning calorimetry and changes in the birefringence of the material. These techniques are described in more detail below.

When observed through crossed polarisers the birefringence and defect structure of each phase forms characteristic textures. Observation of the textures formed in the sample as it is cooled from the uniform isotropic phase can be used to identify many of the phases present. A more detailed explanation of the textures of liquid

crystalline phases is given in the book by Gray and Goodby.[7] Two main orientations of the mesophases can be observed, homogeneous (or planar) with the optic axis perpendicular to the viewing direction and homeotropic with the optic axis parallel to the viewing direction. For the non chiral phases the optic axis is parallel to the director and for the chiral phases the optic axis is parallel to the helix axis. The sample can be viewed between a glass slide and cover slip to allow observation of both the homogeneous and homeotropic textures.

The phases studied in this report include nematic phases which posses orientational order and smectic phases which posses both orientational and positional order. Chiral phases contain optically active isomers that add a twisted orientational order to the material and have extra optical properties.

The isotropic, liquid phase is dark between crossed polarisers because there is no macroscopic ordering of the molecules to interact with the transmitted polarisation.

If a nematic phase is present, it is the first to form. Spherical droplets of birefringent material emerge from the dark isotropic material indicating the fluidity of the nematic phase. Imperfections in the homogeneous director pattern give rise to a schlieren texture with 2 or 4 brushes as shown in figure 3.3a. The nematic phase is easily sheared to the homeotropic alignment which appears black between crossed polarisers.

When the chiral nematic phase is viewed with the optic axis parallel to the viewing direction a grandjean texture (figure 3.3b) is observed, which can also exhibit oily streaks(figure 3.3b). A random mixed orientation of the helix axis produces the focal conic texture as shown in figure 3.3c and if the optic axis is constrained to lie perpendicular to the viewing direction the fingerprint texture is observed. These textures are discussed further with respect to flexoelectric switching in chapter 2.

The transition from the isotropic to smectic A phase often occurs by the growth of batonettes (figure3.3d) indicating the more crystalline nature of the phase. The focal conic structure (figure 3.3e) is present with homogeneous alignment but will easily shear to a dark homeotropic texture.

The smectic C* phase also has a focal conic texture with homogeneous alignment with the addition of striations across the fans (figure 3.3f). This can be sheared into a dark homeotropic texture.

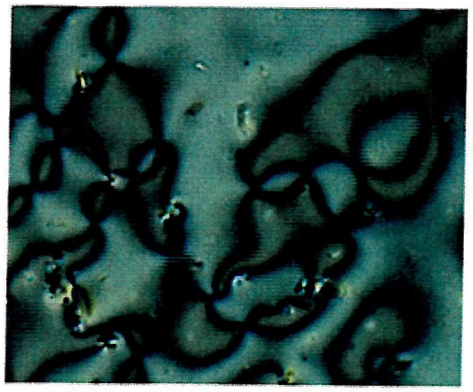

(a) N schlieren

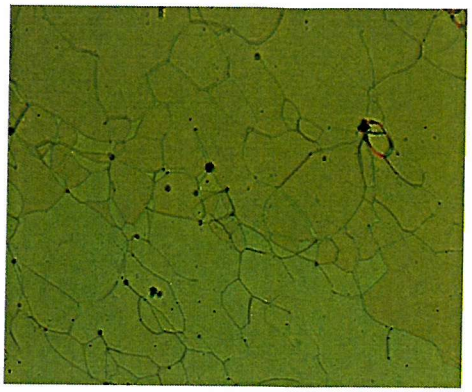

(b) N* grandjean

(c) N* focal conic

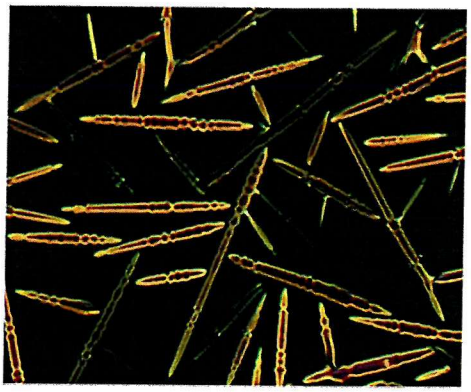

(d) SmA battonettes

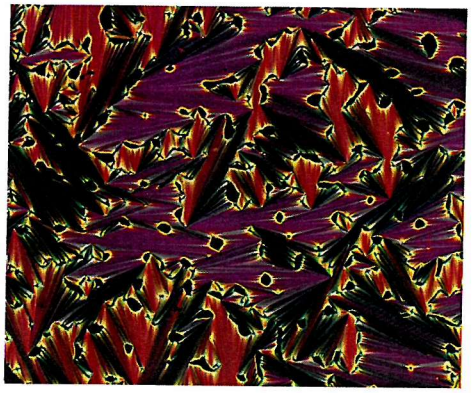

(e) SmA focal conic

(f) SmC* striated focal conic

Figure 3.3 Characteristic textures of phases

An optical method of measuring the transition temperatures is the thermo-optic analysis of the transmitted intensity between crossed polarisers. Each liquid crystalline phase has a different value of birefringence. This alters the intensity of light transmitted between crossed polarisers. A plot of the photodiode output against temperature as shown in figure 3.4 clearly shows the phase transitions. The transition temperatures can be measured to an accuracy of 1 °C. This method is particularly useful for smectic A to smectic C* transitions which can be difficult to observe optically if there is only a minor change in colour between the phases. To maximise the change in transmission between the smectic A and smectic C the sample can be rotated in the smectic A phase to its minimum intensity. At the transition to the smectic C phase the director tilts away from the polariser axis producing a large change in intensity.

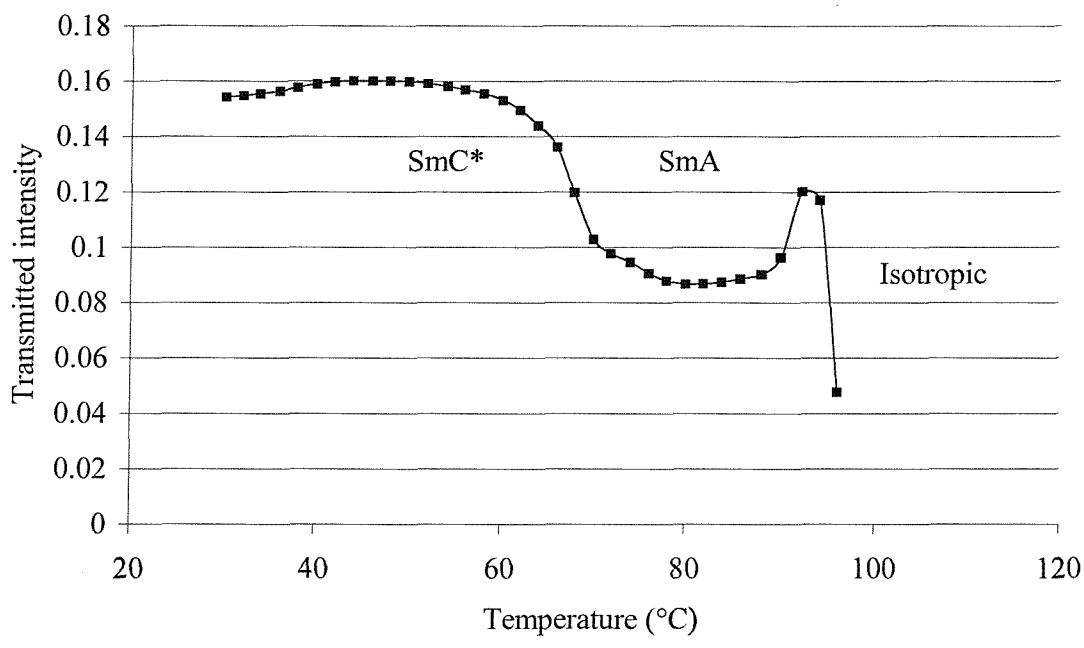

Figure 3.4 Thermo-optic analysis – Trace of photodiode output against temperature for the Br11-Si3 + 40% NA11-Si3 mixture described fully in chapter 4.

Differential scanning calorimetry (DSC)[8] can be used to accurately measure the transition temperatures and enthalpy changes of phase transitions. A standard mass of a known metal is heated at a controlled rate. The differential heat flow required to maintain the sample at the same temperature is assessed. Phase transitions appear as endotherms or exotherms in the trace as shown in figure 3.5 for Br11-Si3.

In principle, the smectic A to smectic C transition is second order so should have no latent heat of transition. In practise the transitions are often found to not be perfectly second order and will show a small peak when heated rapidly, for example 5°C/min.

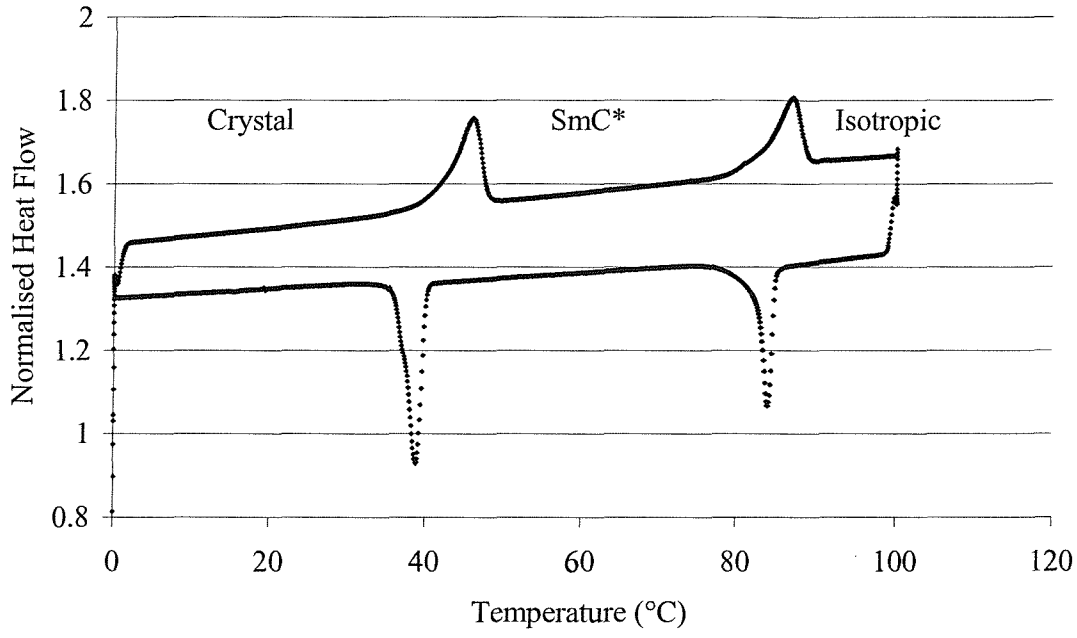

Figure 3.5 Differential scanning calorimetry – Trace of normalised heat flow against temperature for the ferroelectric Br11-Si3 also described in chapter 4.

3.4 Sample Cells

Most of the electro-optic measurements were made in commercially made lucid cells.[9] As shown in figure 3.6 each cell is made of two glass plates separated by glass spacers of a nominal thickness of 5 or 7.5μm. An electrically conductive indium tin oxide (ITO) electrode pattern was applied to each glass plate. This was then coated with a polyimide alignment layer rubbed anti-parallel on each face to promote planar alignment. Copper wires were indium soldered to the overlapping edges of the cell to allow electric connections.

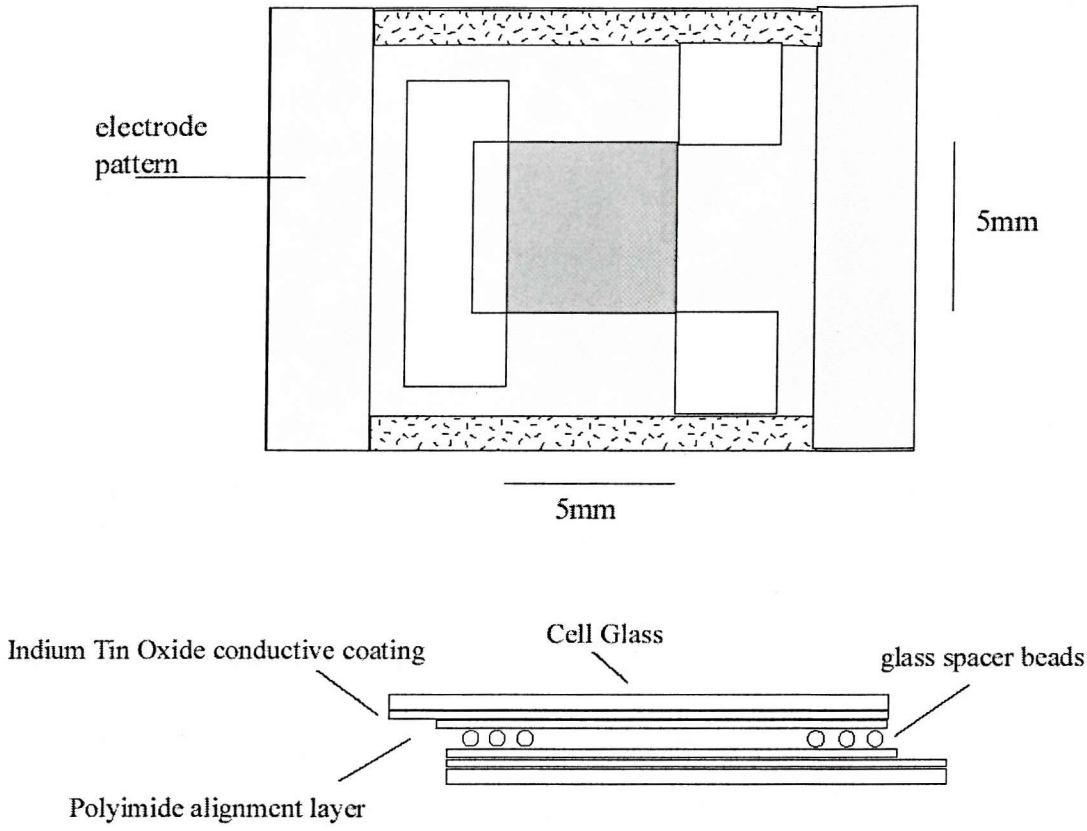

Figure 3.6 Lucid Cell – plan view and side view of commercially made cell.

The cell thickness can be measured accurately using a UV-visible spectrometer.[10] The cell is masked so that a small area to be measured is left uncovered. The cell acts as an etalon producing the peaks and troughs of an interference pattern in the absorbance spectrum as shown in figure 3.7. The cell thickness, d, is related to the number of peaks, m, and the wavelengths of the first and last peaks, λ_1 and λ_2 by equation 3.2.

$$d = \frac{m}{2} \frac{\lambda_1 \lambda_2}{\lambda_1 - \lambda_2} \qquad \text{equation 3.2}$$

The cells are capillary filled while heated on a hot plate to a temperature where the liquid crystal is in its isotropic phase. The ends of the cell are sealed with an ultra violet curing adhesive[11] and the active area is covered while they are cured to prevent damage caused by the ultra violet. Cells made to other specifications; for

example larger cell gap, different alignment layers or wedge shaped were made by hand and are described in the appropriate sections.

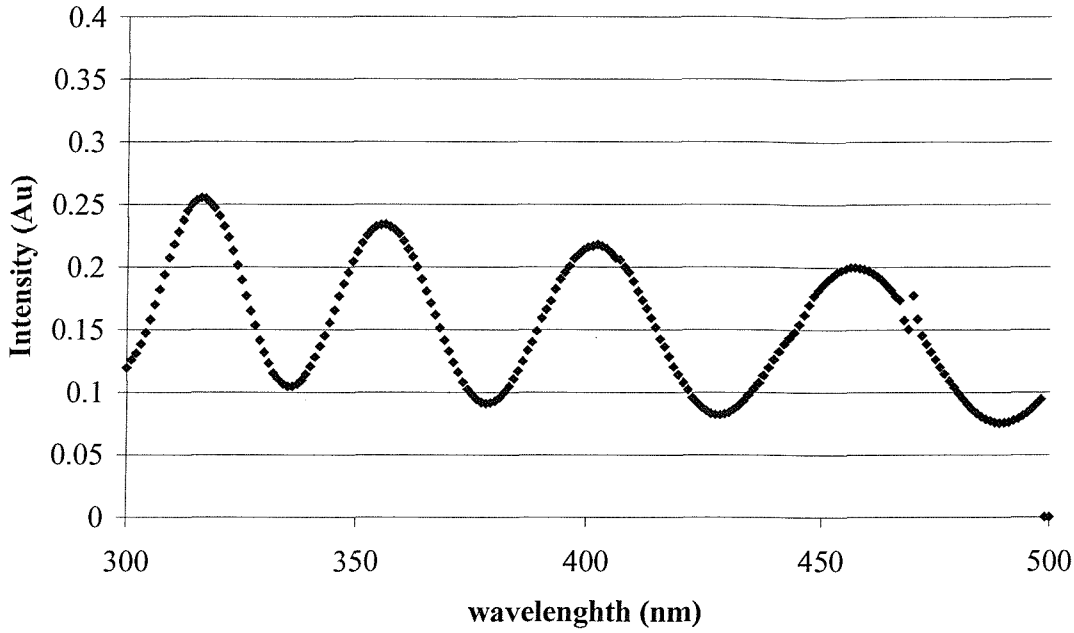

Figure 3.7 Measurement of cell thickness – absorption against wavelength

3.5 Spontaneous polarisation

The current pulse method[12,13] with a triangular driving wave was used to measure the spontaneous polarisation of the ferroelectric and antiferroelectric samples. This method was chosen because the calculation of the area of the current pulse could be easily computerised.[14] Other methods to calculate the spontaneous polarisation in solid ferroelectrics and liquid crystals include the Sawyer–Tower[15,16] capacitance method and use of the pyroelectric effect.[17] The Sawyer-Tower or Diamont bridge method is commonly used and is found to be very accurate, but it produces hysteresis loops, the area of which must be measured to calculate the spontaneous polarisation and this is not easy to do computationally.

In the current pulse method an alternating voltage is applied to the conducting plates of the cell while the current through the cell is measured. A current to voltage converter is used so that the current can be displayed as a voltage on a digitising oscilloscope. There are three main components[12] to the current through the cell shown in figure 3.8. The dielectric charging of the capacitor formed by the

cell plates, which decays exponentially after each voltage reversal. The polarisation reversal current, as the molecules switch around the cone. Finally the electrolytic or ionic current, caused by dissolved charged impurities moving in the applied field.

The use of a triangular wave separates the polarisation reversal and ionic peaks and generates a flatter baseline than a square wave as shown in figure 3.8. Figure 3.9 shows a typical current pulse trace for the material Br11-Si3.

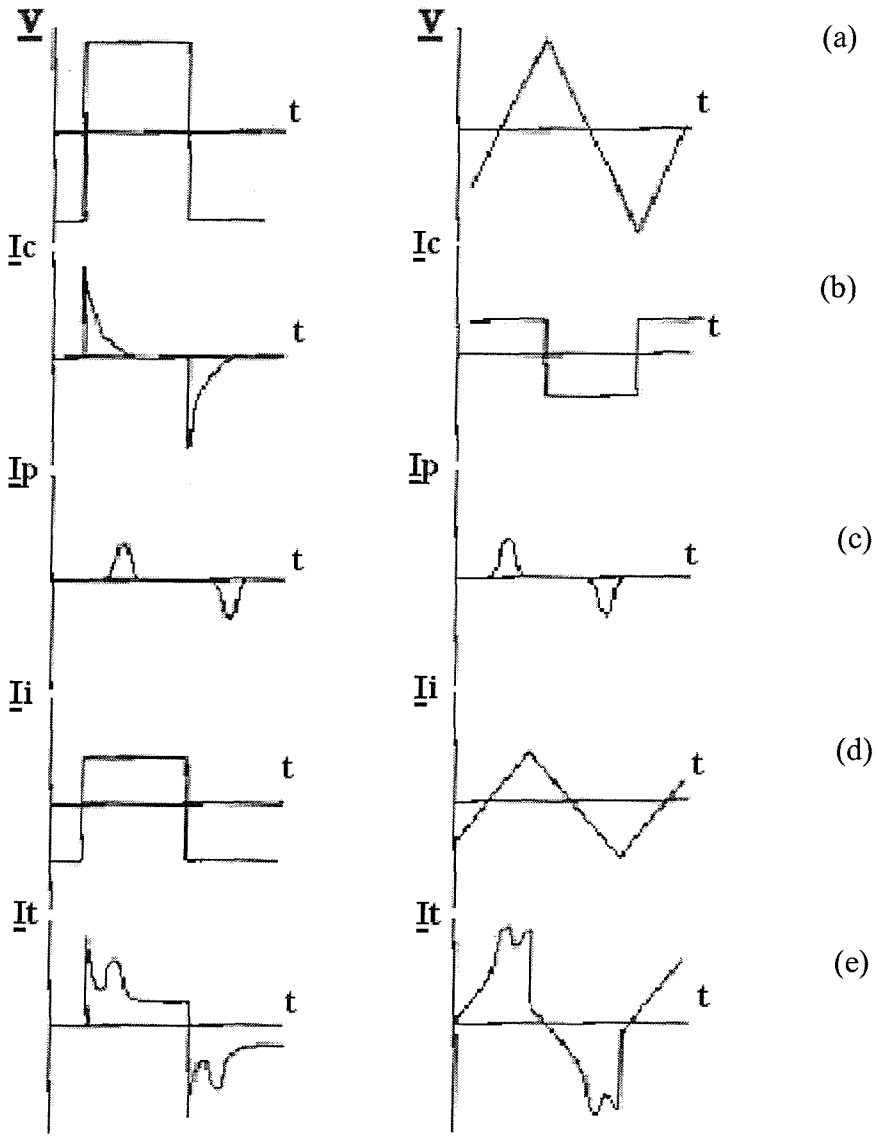

Figure 3.8 Components of current pulse measurement

(a) square and triangular driving voltages

(b) capacitive components (c) polarisation reversal

(d) ionic component (e) current pulse responses

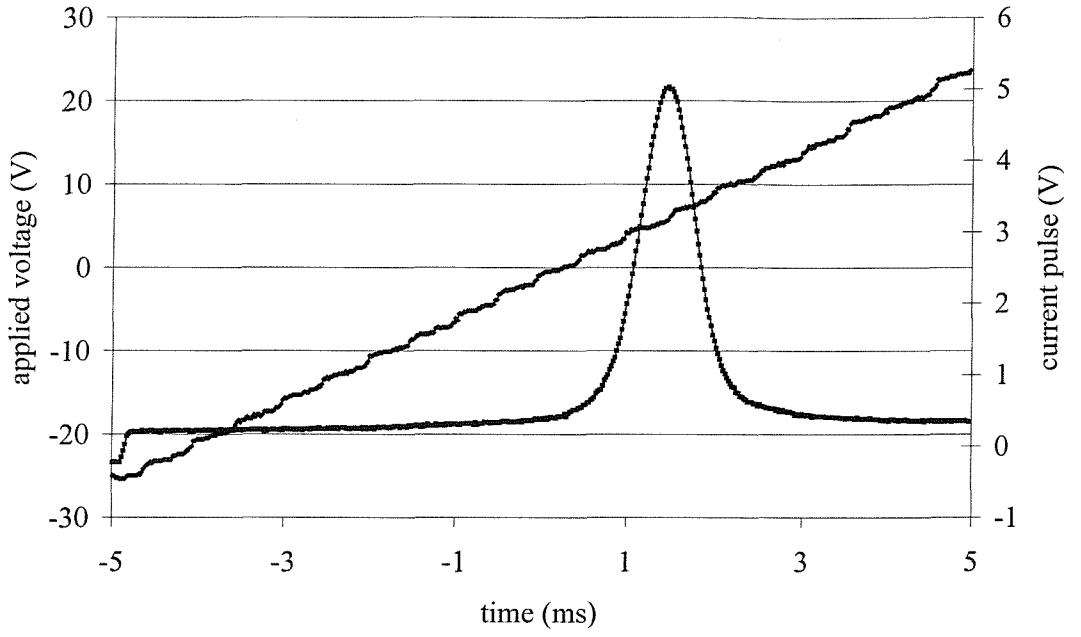

Figure 3.9 Example of the current pulse response for the ferroelectric material Br11Si3 to a triangular waveform.

3.6 Tilt Angle

To measure the tilt angle the material must first be aligned. This means that as many of the molecules as possible must have the same orientation. An aligned sample can be recognised by the absence of defect patterns. Alignment layers on the glass cells can be used to aid alignment. For example polyimide, SiOx, and PVA are commonly used to produce planar alignment. For both the ferroelectric and flexoelectric work commercially made cells with anti-parallel rubbed surfaces of polyimide were used.

For the ferroelectric materials the samples were held just below the isotropic transition while the amplitude and frequency of the applied ac field was altered until the liquid crystalline chevrons oscillated. The material was then cooled at rates of 0.1 to 0.5°C/min to align the sample. The flexoelectric materials were cooled into the chiral nematic phase. The magnitude of the applied filed was increased until the focal conic structure appeared. The cell was then sheared by unidirectional rubbing to produce the uniformly lying helix texture.

The tilt angle can be measured optically or by x-ray measurement of the smectic layer spacing. These two methods do not measure exactly the same properties of the molecules so will often give different values of the angle. The optical tilt is defined as the angle between the layer normal and the optic axis, while the x-ray measurement evaluates the mass axis of the molecules. These axes may not be equal, leading to the different observed values of the tilt angle. However both measurements will follow the same dependence on properties of the phase and the sample temperature.

The tilt angles of the materials described in this these were measured optically. A square wave was applied to the sample causing the director to switch through twice the tilt angle. The sample is rotated between crossed polarisers. The transmitted intensity depends upon the orientation of the director with respect to the polariser and analyser. When the switching is equidistant from either side of a polariser the optical response is that shown in figure 14(a), with equal transmission at the switched positions and a dark spike as the molecules switch. The maximum change in transmission occurs when the director switches equidistantly about the 22.5° position. To find the intensity at the 22.5° position the sample is rotated 22.5° from position (a) as shown in figure 14(b). The mid-point of this switching is the 22.5° level. The sample is rotated so first the maximum and then the minimum switching are level with the 22.5° position as shown in figures 14(c) and (d). The angle between these two positions is equal to twice the tilt angle.

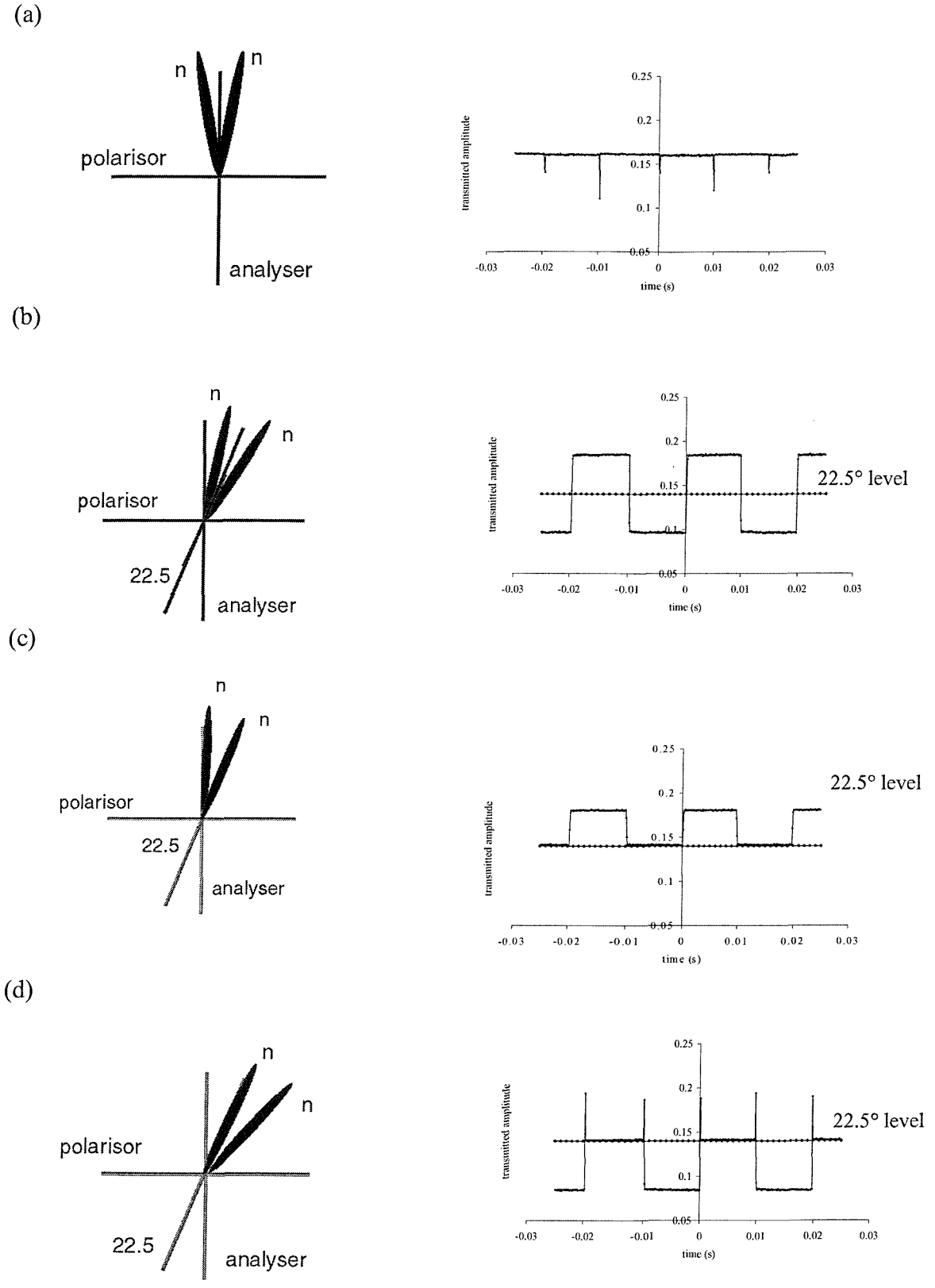

Figure 3.10 Description of tilt angle measurement

(a) equidistant about polariser (b) switching about 22.5°

(c) extremity of switch at 22.5° (d) other extremity of switch at 22.5°

3.7 Response time

The response of a liquid crystal to an applied electric field may be measured optically or electrically. The two methods may give slightly different magnitudes but have been shown to be equivalent for many liquid crystal systems. The optical method is the most commonly quoted. As for the measurement of tilt angle the liquid crystal must be prepared in a cell with its optic axis perpendicular to both the applied field and the observation direction. This is the planar texture for ferroelectric materials and the uniformly lying helix for flexoelectric materials.

To measure the optical response time a square wave is applied to the cell. The magnitude and frequency are altered to ensure complete switching. The sample is rotated so that it is switching symmetrically about an angle of 22.5° to one of the polarisers as shown in figure 3.10b. The optical response time is defined as the 10 to 90% change in the optical transmission as shown in figure 3.11. This method is difficult to define for materials with a tilt angle greater than 22.5° because there is a peak in the trace immediately before the switch as shown in figure 3.12. This makes definition of the 10 to 90% measurement ambiguous.

A square wave is also applied to the cell to measure the current response time. This is defined as the time between field reversal and the maximum of the resulting current peak as shown in figure 3.13. The current response time can be measured for materials with a tilt angle greater than 22.5° and in samples with poor alignment where the optical response cannot be measured.

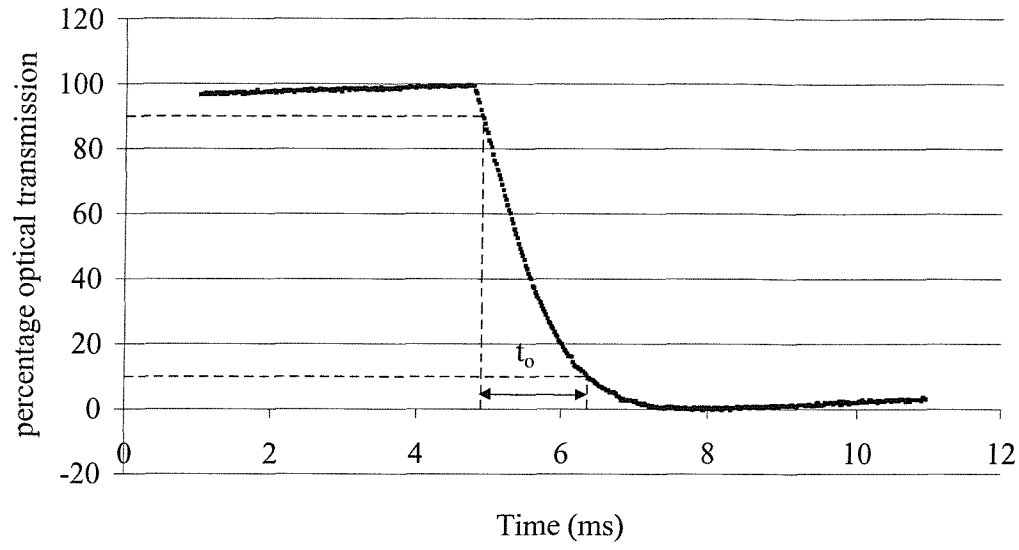

Figure 3.11 Optical response time – defined as the 10 to 90% change in optical transmission.

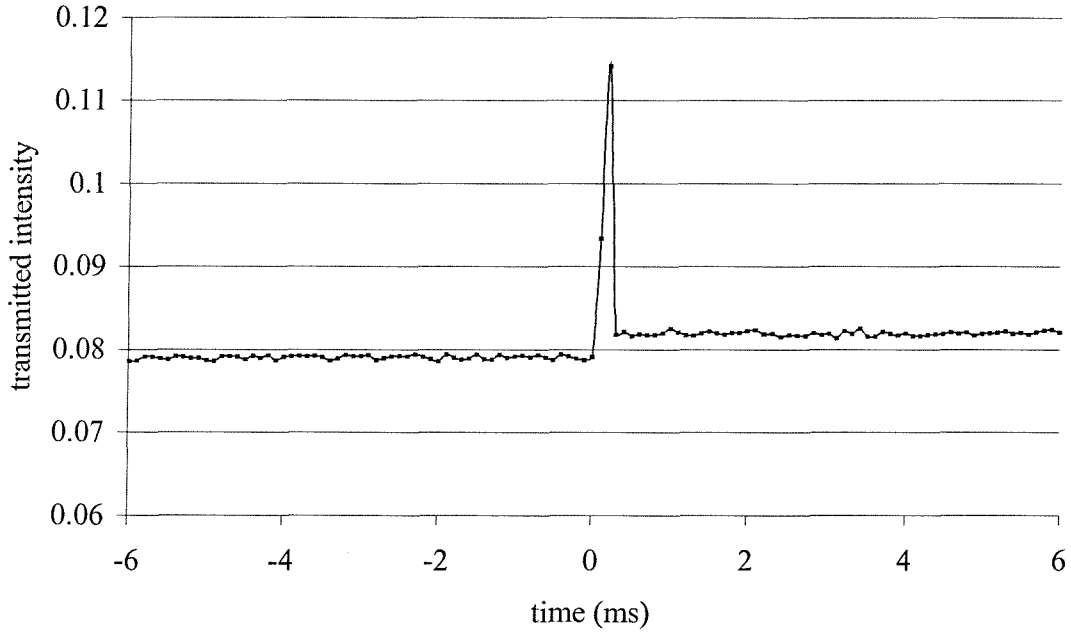

Figure 3.12 Optical response for tilt greater than 22.5° - showing a large peak as the material switches

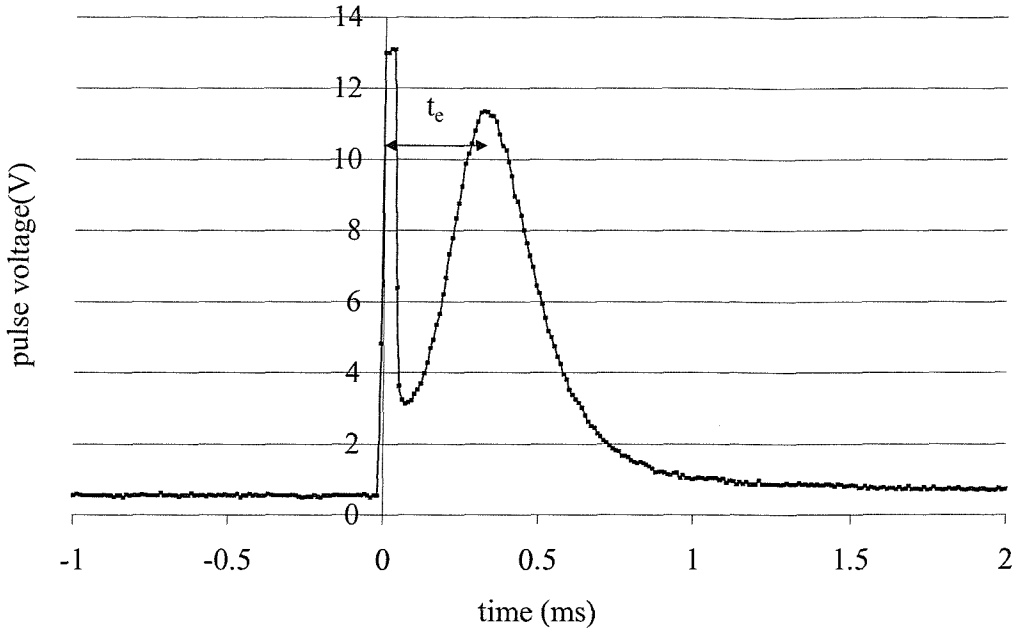

Figure 3.13 Current pulse response time – defined as the time between field reversal and the resulting current pulse.

3.8 Pitch measurements

All the methods for measuring the pitch of a chiral nematic material depend upon the periodicity of the helix. There are three main methods. Measurement of the distance between adjacent Grandjean disclinations in a cano wedge[18], measurement of the selective reflection of wavelengths close to the pitch length and observation of the diffraction pattern from a laser beam incident on the helix.

A cano wedge is formed with planar alignment layers that quantise the standing helix structure as shown in figure 3.14. This produces a stepped texture with distinct disclination lines. The pitch, p, is related to the distance between disclination lines, l, and the wedge angle, ϕ, as shown in equation 3.3.

$p = 2l\tan\phi$ equation 3.3

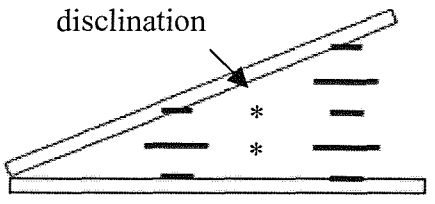

Figure 3.14 The discrete number of turns of the standing helix in a cano wedge.

The selective reflection from a Grandjean or standing helix texture was used to measure the pitch in this thesis. When a chiral nematic is illuminated with white light almost parallel to the pitch axis the wavelengths that are close to the pitch length are selectively reflected[19] as shown schematically in figure 3.15.The maximum reflected wavelength and bandwidth are defined in equations 3.4 and 3.5. The typical refractive index, n, is approximately equal to one for many liquid crystalline materials.

$$\lambda_{max} = \bar{n}p \qquad \text{equation 3.4}$$

$$\delta\lambda = \lambda_{max}\frac{\delta n}{\bar{n}} \qquad \text{equation 3.5}$$

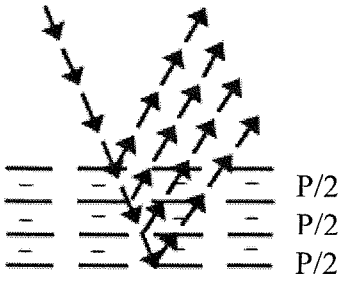

Figure 3.15 Schematic diagram of selective reflection of a wavelengths close to the pitch length, p.

A wedge cell with anti-parallel rubbed planar alignment was used to achieve the standing helix or Grandjean texture. The pitch axis was then perpendicular to the

cell surfaces. Two spectrometers were used to measure the maximum reflected wavelength. In one case the sample was held in a Metler[20] hotstage in an UV–visible spectrometer.[10] A spectrometer[21] mounted above the objective of the microscope was also used to measure the wavelength at which maximum reflection occurred. It was also possible with this arrangement to illuminate the sample with ultra violet light while taking measurements.

3.9 Conclusion of Chapter Three

The microscope and associated equipment to make electro-optic observations of liquid crystalline materials and to enable ultra violet illumination have been described. Some common liquid crystalline phases and the methods of identifying them have been detailed.

The glass sample cells and the methods of aligning smectic and chiral nematic materials have been described. The measurement of spontaneous polarisation, tilt angle and response time have been defined for smectic C* phases. In addition to these measurements the determination of the helix pitch was described for the chiral nematic phase.

References for chapter 3

[1] Olympus Optical Company(UK) Ltd, 2-8 Honduras Street, London, EC1Y 0TX

[2] Linkam Scientific Instruments, 8 Epson Downs Metro Centre, Waterfield, Tadworth, Surrey, KT20 5HT

[3] Thurlby Thandar Insruments, Glebe Road, Huntingdon, Cambrideshire, PE29 7DX

[4] Hewlett-Packard Ltd., Test and Measurement, Cain Road, Bracknell, Berkshire RG12 1HN http://www.hewlett-packard.com/ghp/european.html

[5] Agilent, 395 Page Mill Road. P.O. Box 10395, Paulo Alto CA USA

[6] Collings, P.J., Hird, M., Chp 9, Introduction to Liquid Crystals, Taylor and Francis, (1997)

[7] Gray, G.W., Goodby, J.W., Smectic Liquid Crystal Textures and Structures, Leonard Hill, Glasgow, 1984

[8] Perkin Elmer Chalfont Road, Seer Green, Beaconsfield, Bucks, HP9 2FX

[9] EEV Limited, 106 Waterhouse Lane, Chelmsford, Essex, CM1 2QU, UK

[10]Anachem Ltd., 20 Charles Street, Luton, Bedfordshire LU2 0EB

[11] Norlan Optical Adhesive, Norland Products, 695 Joyce Kilmer Avenue, New Brunswick, New Jersey, 08902, USA

[12] Miyassato, K., Abe, S., Takezoe, H., Fukuda, A., Japn J. appl. Phys, **22**, L661 (1983)

[13] Dahl, I., Lagerwall, S.T., Skarp, K., Phys.Rev.A., **36(9)**, 4380-4389, (2987)

[14] Walton, H.G., Ph.D. Thesis, University of Manchester, (1994)

[15] Sawyer, C.B., Tower, C.H., Physical Review, **35**, 269-273, (1930)

[16] Diamont, H., Drenck, K., Pepinsky, R., Rev. Sci. Inst. , **28(1)**, 30-33, (1957)

[17] Blinov, L.M., Beresnev, L.A., Shtykov, N.M., Elashvili, Z.M., J. de Phys., **C3**, 269-273, (1979)

[18] Coles. H.J., Ch. 2A, Handbook of Liquid Crystals Volume 2B, Wiley-Vch, (1998)

[19] de Gennes. P.G., Ch. 6, The Physics of Liquid Crystals, Oxford University Press (1974)

[20] Mettler-Toledo Ltd., 64 Boston Road, Beaumont Leys, Leicester LE4 1AW

[21] Ocean Optics Inc. supplied by Knight Optical Technologies Ltd., PO Box 142, Leatherhead, Surrey

Chapter 4

Monomesogenic Azo dye added to a Ferroelectric Monomesogenic Organosiloxane Host

Chapter 4
Monomesogenic Azo dye added to a Ferroelectric Monomesogenic Organosiloxane Host

4.1 Introduction

The liquid crystalline mesogens investigated in this chapter all belong to a family of low molar mass organosiloxanes. These organosiloxane materials have been designed to create a compromise between the extremes of low molar mass liquid crystals and side chain polymer liquid crystals.[1,2,3] Low molar mass ferroelectric liquid crystals have been synthesised with very fast response times but they do not produce rugged displays. At the opposite extreme the polymerisation of side chain polymer liquid crystal molecules stabilises the smectic layers, yielding a more rugged display, but as a consequence they have a much slower response time than low molar mass mesogens[4,5,6,7,8].

The low molar mass organosiloxane materials studied here incorporate a molecular group that has been shown to produce a liquid crystalline phase and a siloxane unit that is commonly found in polymer materials. The liquid crystalline mesogenic moiety is attached to the siloxane unit via a flexible hydrocarbon chain, to allow a degree of independent movement, as shown schematically in figure 4.1(a). Each different part of the molecule has an affinity for the same part of the other molecules causing them to cluster together. In particular the siloxane core units are thought to agglomerate, shown schematically in figure 4.1 (b), forming a pseudo siloxane backbone.[1,9,10] This backbone promotes the formation of smectic phases and produces more robust[11] phases than other low molar mass mesogens while allowing the functional part of the molecule to switch freely. Hence a combination of the rugged structure resembling that of polymers and the fast switching times of low molar mass mesogens is achieved.

An organosiloxane molecule with a chiral end group hydrosilylated onto a three siloxane group by an eleven carbon alkyl chain that produces a wide ferroelectric phase is used as the host material[12]. Dyes have been synthesis by Dr S.Perkins at Southampton University containing the same three silicone core as the host to attempt

to produce good miscibility and lessen the effect of the dye mesogen on the host's properties.

Novel dyes with nitrostilbene and azobenzene moieties have recently been synthesised.[13] The dye containing the azo moiety has been investigated in this work because of its photoisomerising effects[14], which will be discussed in later chapters.

The notation used to describe the organosiloxane materials includes the type of liquid crystalline mesogen, the length of the methylene spacer chain and the number of siloxane atoms in the siloxane core. For example the 2-Bromo-4-(1-methylheptyloxy)benzoic acid 4'-(11-{heptamethylsiloxyl}undecyloxy)biphenyl-4-yl ester mesogen, with an eleven methylene chain and three siloxane atoms is denoted Br11-Si3.

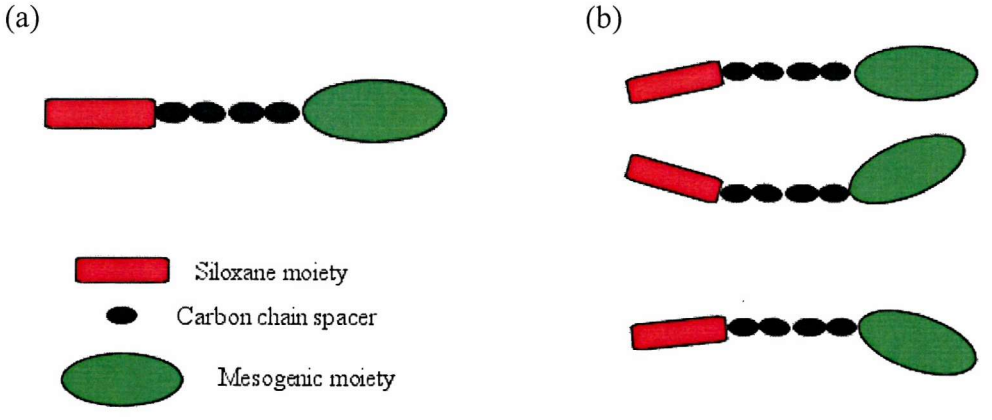

Figure 4.1 (a) schematic siloxane molecule (b) siloxane units agglomerate to form smectic phases

4.2 Host and Dye Characteristics

The ferroelectric bromine substituted mesogen 2-Bromo-4-(1-methylheptyloxy)benzoic acid 4'-(11-{heptamethylsiloxyl}undecyloxy)biphenyl-4-yl ester denoted Br11-Si3[13,15,16], with a three siloxane unit and a bromine substituted biphenylyl benzoate mesogenic unit is used as the host material in this study. The schematic molecular structure and phase transition temperatures are shown in figure 4.2. The material has a broad smectic C* phase ranging over 42°C. Both the

spontaneous polarisation, with a maximum value of 90nC/cm^2, measured by the current pulse technique, and the optical tilt angle, held at 44° are widely independent of temperature as shown in figures 4.5 and 4.8. The high tilt angle, close to 45°, and high spontaneous polarisation makes this material suitable for 45° tilt display applications requiring only one polariser. The absence of a smectic A or nematic phase in organosiloxane materials means that the alignment of the smectic C* phase is not straightforward. Slow cooling in the presence of an electric field produces tolerable alignment but this is not as good as that achieved in a phase with a smectic A* phase as shown in figure 4.19.

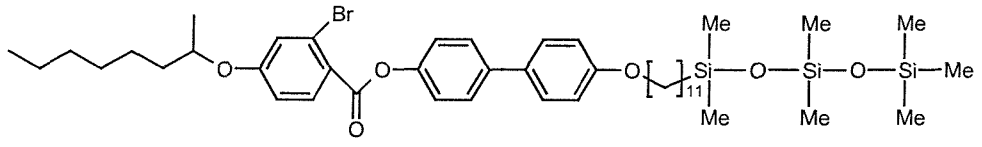

Crystal – 46°C – Smectic C* - 88°C –Isotropic

Figure 4.2 Schematic diagram and transition temperatures of ferroelectric host Br11-Si3 measured by optical microscopy.

A liquid crystalline dye incorporating the same three-siloxane unit as the host material and a nitro-azo group has been synthesised by S. Perkins in an attempt to produce dyes that are miscible in the host material. The dye, α,ω-bis(4-nitroazobenzene-4'-oxyundecyl)hexamethylsiloxane, is denoted NA11-Si3. The schematic diagram of the dye molecule and phase transition temperatures are shown in figure 4.3. The dye has a smectic A phase over a 30°C range which also suggests that it should be highly miscible with a smectic C* host. Other dye moieties also show corresponding high solubility when attached to the same siloxane core.[13] The effect of dye concentration on the spontaneous polarisation, the tilt angle, the response time and the phase sequence of a range of mixtures have been investigated and shown in this chapter. The photoisomerising effect of ultra violet illumination on Br11-Si3 and NA11-Si3 mixtures will be examined in chapter six.

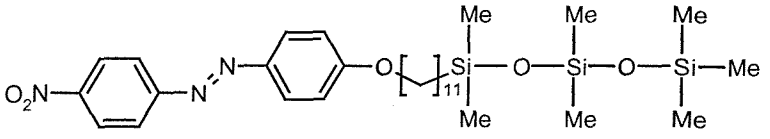

Crystal – 49°C – Smectic A – 83°C – Isotropic

Figure 4.3 Schematic diagram and phase sequence of the photoisomerising dye NA11-Si3 measured by optical microscopy.

4.2 Effect of dye addition

4.2.1 Phase Characteristics

An extensive range of mixtures have been made between the ferroelectric host Br11-Si3 and the photoisomerising dye NA11-Si3 by heating the weighed mixtures to above both component's isotopic transition temperatures for up to 12 hours. Cells of 5μm thickness with anti-parallel rubbed polyimide alignment layers were used for all the observations and measurements described in this chapter. A phase diagram of the phase transition temperatures plotted against molar concentration is shown in figure 4.4. The transition temperatures were measured by optical microscopy and the switching type determined by the response to a triangular waveform.

Dye concentrations of up to 20% are shown not to greatly change the transition temperatures from that of the pure host material. Furthermore a smectic C* phase is present in mixtures with a dye concentration of up to 80%. For the concentration range between 25% and 80% both a smectic A* and a smectic C* phase are present. The presence of this smectic A* phase aids the alignment of the smectic C* phase and exhibits a marked electroclinic effect shown later in this chapter.

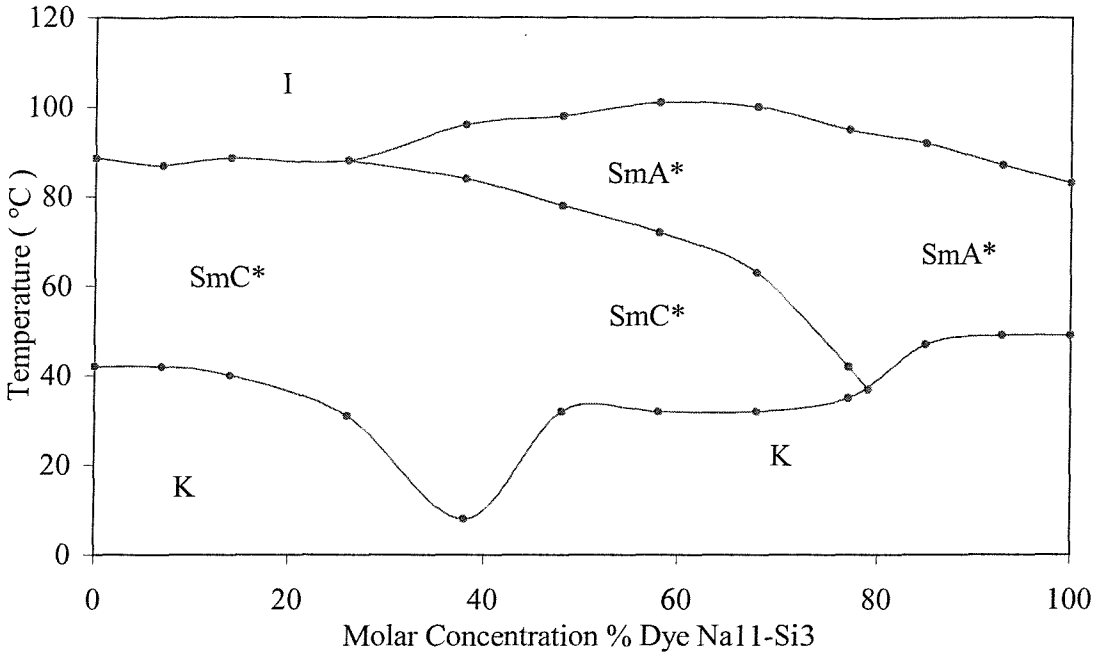

Figure 4.4 Phase diagram for molar concentration of dye addition against temperature measured by optical microscopy, where an asterisk denotes a mixture containing a chiral molecule.

4.2.2 Spontaneous Polarisation

The variation of the spontaneous polarisation, measured by the current pulse technique, with temperature for the range of mixtures possessing a smectic C* phase is shown in figure 4.5. These show that the spontaneous polarisation of the mixtures maintains the broad temperature independence of the host. Figure 4.6 shows that the maximum magnitude of the spontaneous polarisation scales linearly with concentration.

While there is a sharp reduction of the spontaneous polarisation to zero for the mixtures with a smectic C* to isotropic transition, the change is seen to be more gradual once a smectic A* phase is present. The transition from a smectic C* to smectic A* phase can theoretically be second order and follow a Curie-Weiss dependence[17]. The theoretical Curie-Weiss relationship between the spontaneous

polarisation and temperature is compared with the experimental results for dye concentrations of 40%, 50% and 60% in figure 4.7. The spontaneous polarisation, P_S, equation 4.1, is related to the sample temperature, T, by the constants, K_P, T_0 and β. The exponent β is equal to a half in a mean field approximation[18] and the constant T_0 is approximately equal to the smectic A* to smectic C* transition temperature. The constant k_p used in figure 4.7 was calculated from the gradient of the graph of the spontaneous polarisation against the ratio of transition and sample temperatures given in equation 4.1.

$$P_s = k_p\left(\frac{T_0 - T}{T_0}\right)^{\beta} \qquad \text{equation 4.1}$$

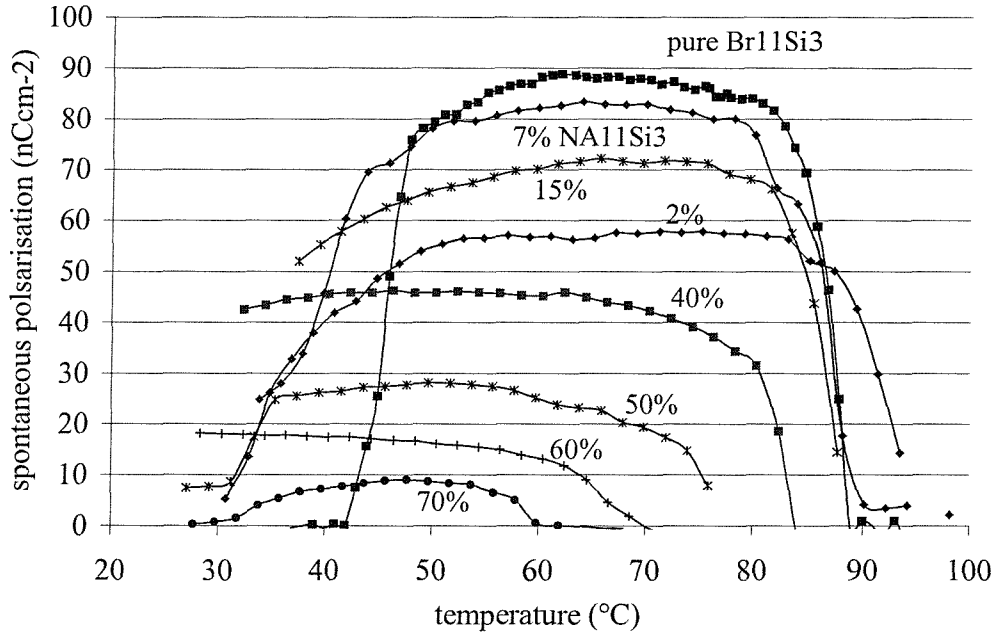

Figure 4.5 Spontaneous polarisation against temperature for Br11-Si3 and NA11-Si3 (molar dye concentration quoted) mixtures measured at 50Hz and 20Vp-p/μm.

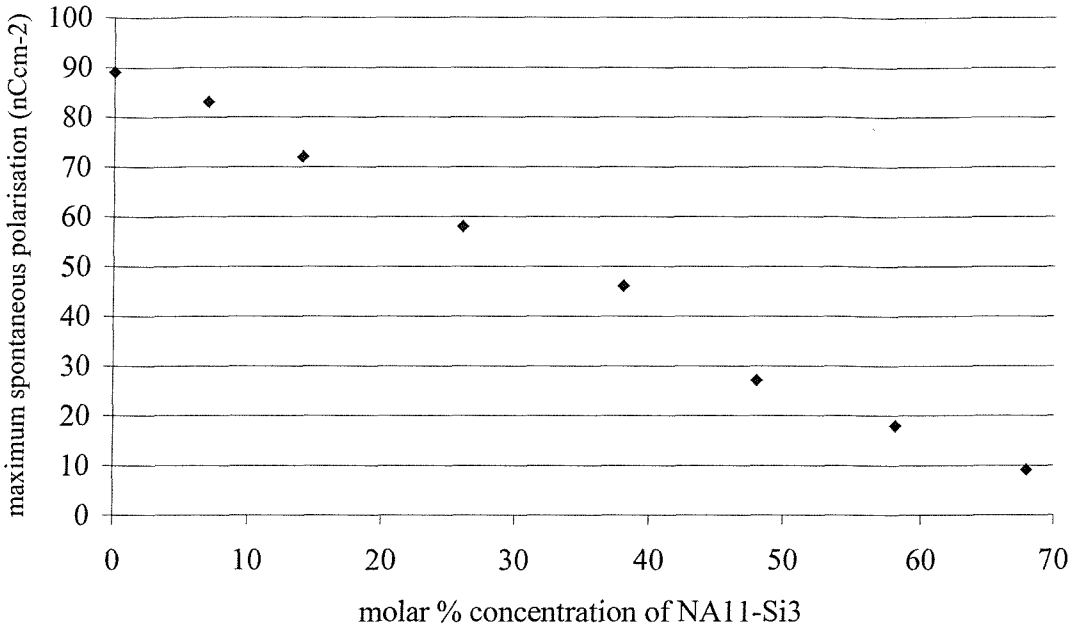

Figure 4.6 The maximum value of the spontaneous polarisation as measured in figure 4.5 as a function of dye molar % concentration

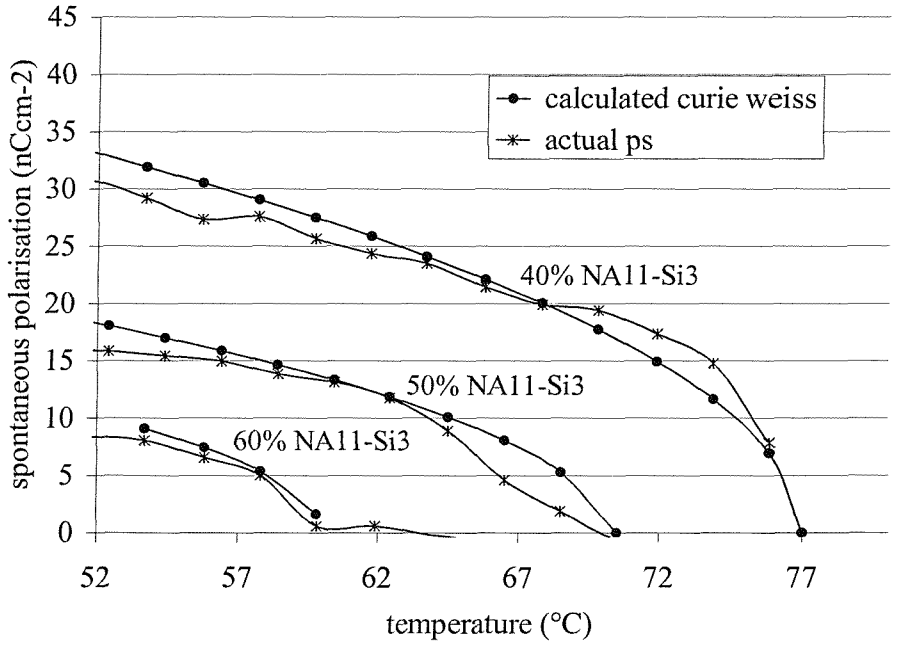

Figure 4.7 Curie Weiss fits of spontaneous polarisation data against temperature close to the smectic C*-smectic A* transition (molar dye concentration quoted).

4.2.3 Tilt angle

Figures 4.8 and 4.9 show that the tilt angles of the mixtures are also reduced by increasing dye concentration, while maintaining a uniform value across the temperature range. However this does not have the same linear dependence on dye concentration as the spontaneous polarisation. For small dye concentrations, before a smectic A phase is induced the tilt angle is held close to 45°. It is then reduced for mixtures with a smectic A phase.

For the pure ferroelectric material Br11-Si3 and after NA11-Si3 dye addition the ratio of the spontaneous polarisation to the tilt angle is constant across the main temperature range of the ferroelectric phase. This is shown for a range of dye concentration in figure 4.10. This shows that the magnitude of the spontaneous polarisation is proportional to the tilt angle, this association is further investigated in chapter 6 as the tilt angle and spontaneous polarisation are altered by photoisomerising ultra violet illumination.

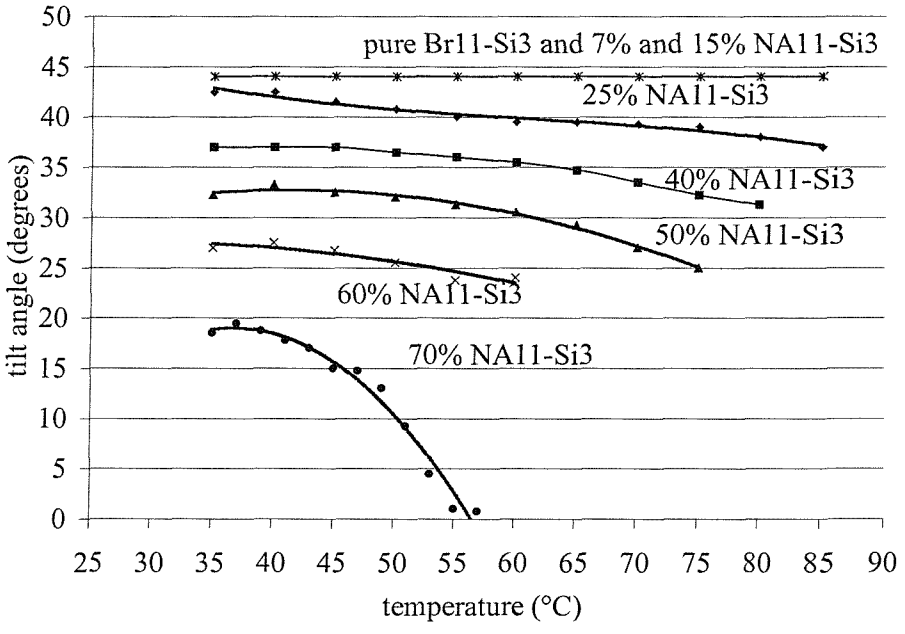

Figure 4.8 Optical tilt angle against temperature for the Br11-Si3 and NA11-Si3 mixtures(molar dye concentration quoted). Measured by polarised microscopy at 120 Hz, 40 Vp-p /μm.

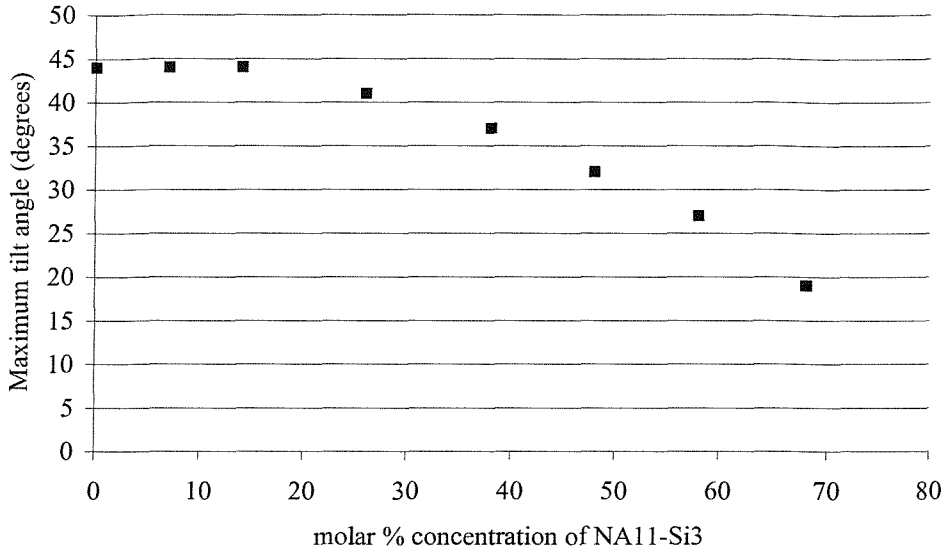

Figure 4.9 The maximum value of the tilt angle as measured in figure 4.8 as a function of molar % dye concentration.

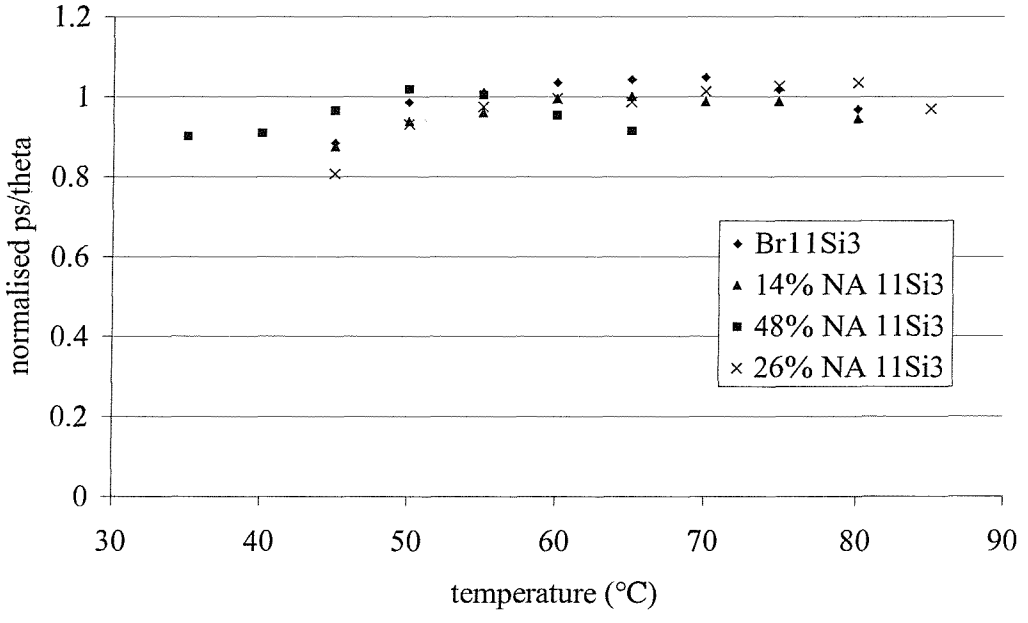

Figure 4.10 Ratio of spontaneous polarisation to tilt angle against temperature for a range of NA11-Si3 dye concentrations.

4.2.4 Response time

Figure 4.11 shows that the current pulse response times are slightly decreased by the addition of the nitroazo dye. The response time, τ, is exponentially related to the inverse of the sample temperature, T, by the activation energy, E_A, and the constants τ_0 and R as shown in equation 4.2.

$$\tau = \tau_0 \exp^{\frac{E_A}{RT}} \quad \text{equation 4.2}$$

The linearity of the log of the response time with temperature is shown in figure 4.12. The gradient, of the best fit line, as shown in table 4.1, indicates a decrease in the activation energy, as the dye concentration is increased. There is a significant change in the gradient and hence the activation energy corresponding to the shift from a first order crystal to smectic C* transition to the second order smectic A* to smectic C* phase transition.

Figures 4.13 and 4.14 show that the response time is inversely proportional to the applied field, E, for a constant polarisation, P, equation 4.3, at temperatures well below the transition for both the pure host and the 40% dye mixture. However this becomes less linear closer to the transition. The increase in the gradient as the temperature is increased indicates that the viscosity, γ, is decreasing.

$$\tau = \frac{\gamma}{P.E} \quad \text{equation 4.3}$$

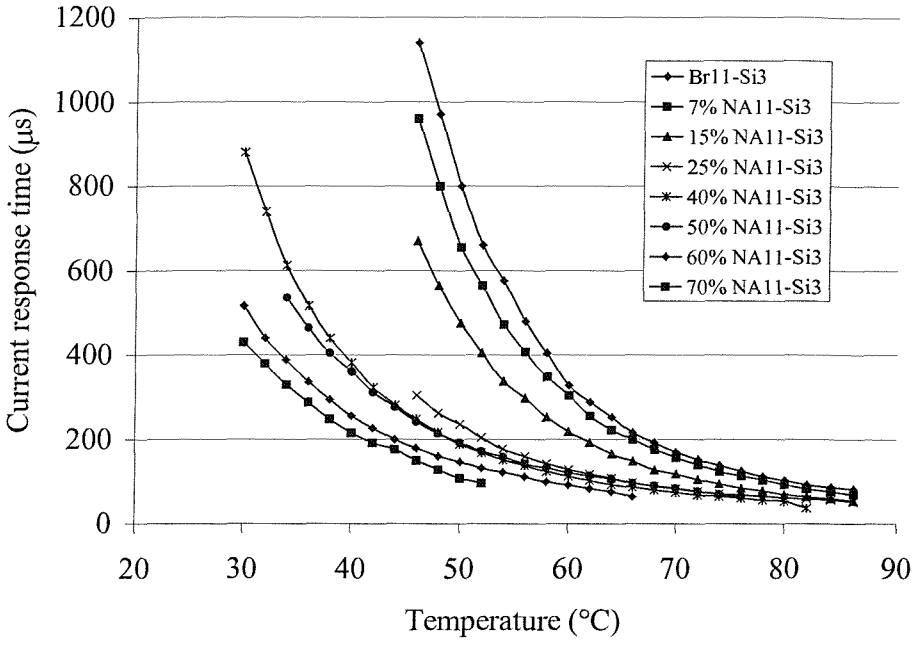

Figure 4.11 Current pulse response time against temperature for the Br11-Si3 and NA11-Si3 mixtures measured at 10 Hz, 10 $V_{pp}/\mu m$.

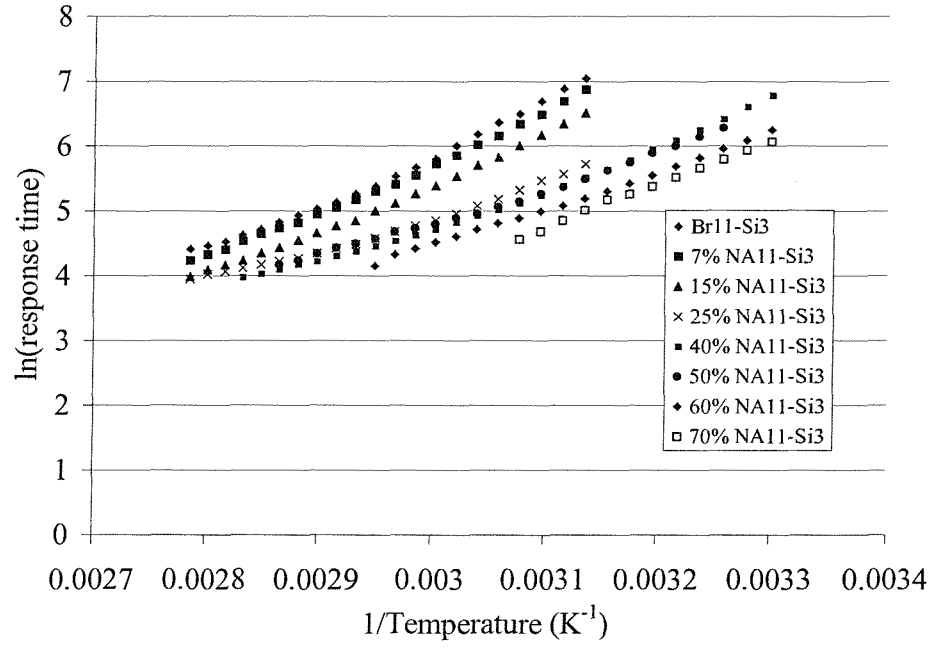

Figure 4.12 Ln(response time) against 1/temp for data presented in figure 4.10.

Concentration of NA11-Si3	Gradient of ln(response time) against temperature (J mol^{-1})
0% (SmC*)	7700 ± 100
7% (SmC*)	7500 ± 100
15% (SmC*)	7200 ± 100
25% (SmC*-SmA)	5000 ± 100
40% (SmC*-SmA)	5800 ± 100
50% (SmC*-SmA)	5300 ± 100
60% (SmC*-SmA)	5700 ± 100
70% (SmC*-SmA)	6500 ± 100

Table 4.1 Gradient of the graph of ln(response time) against temperature corresponding to activation energies for the mixtures possessing a smectic C* phase.

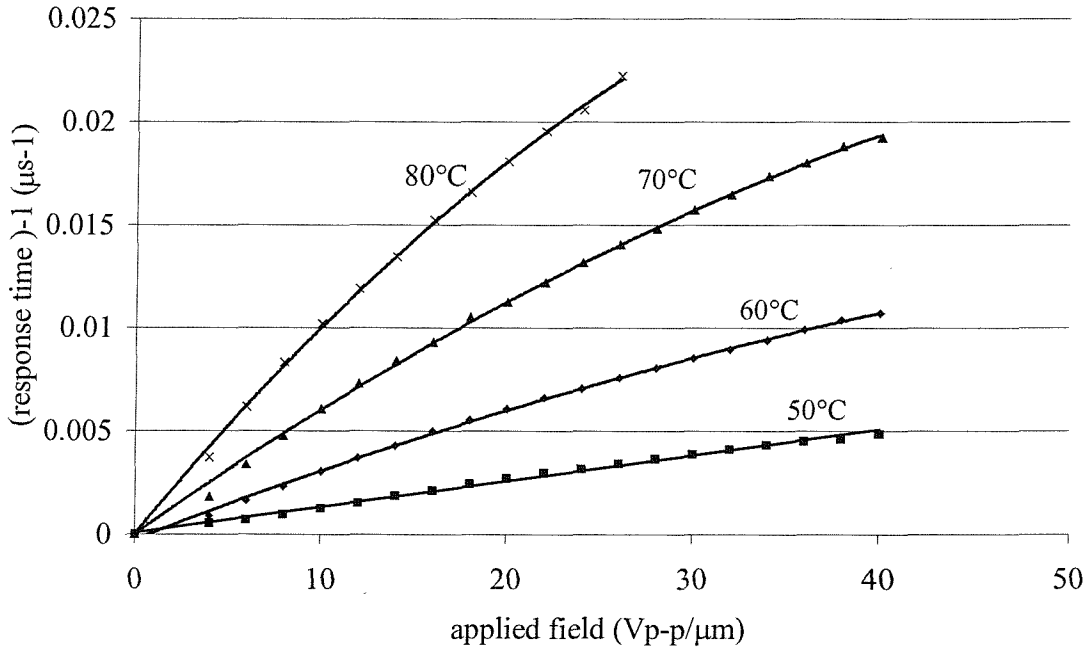

Figure 4.13 1/response time against voltage for pure Br11-Si3 measured at 35 Hz.

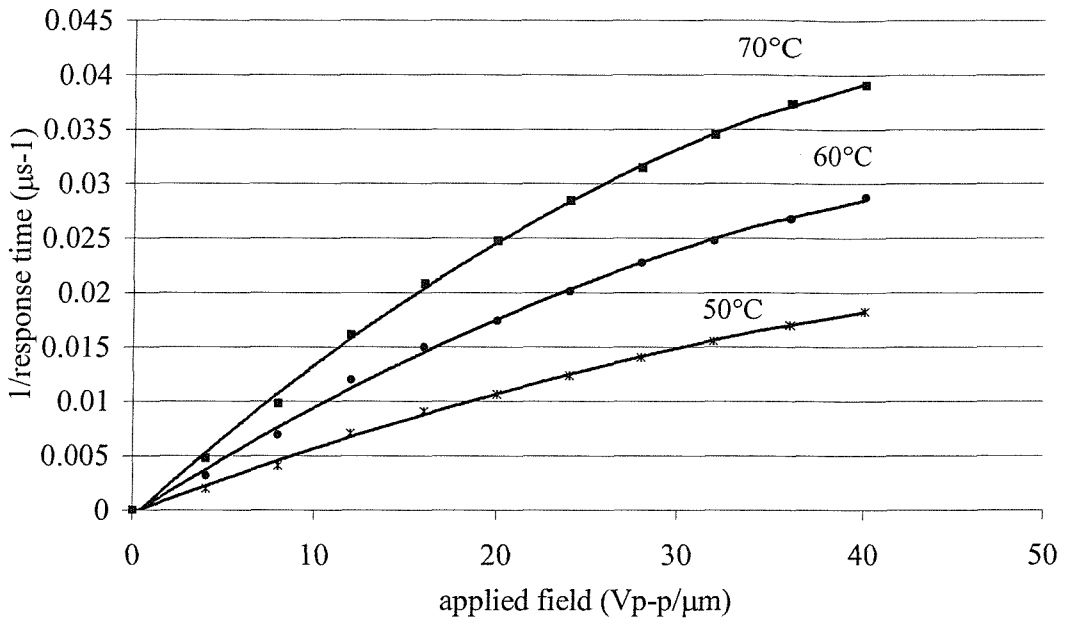

Figure 4.14 1/response time against applied voltage for Br11-Si3 + 40% NA11-Si3 taken at35 Hz.

4.2.5 Electroclinic Smectic A* Switching

Electroclinic switching has been observed in the smectic A* phase of all of the mixtures with an isotropic to smectic A* to smectic C* phase sequence. As shown in figure 4.15 for the 40% NA11-Si3 mixture the optical response of the electroclinic switching is linearly dependant on the applied field in the smectic A* phase. The optical hysteresis loops in figure 4.16 show the transition from Goldstone switching with hysteresis to the linear electroclinic soft mode switching in the same mixture. Figure 4.17 shows the change in tilt angles for the 40%, 50% and 60% mixtures as they pass through the smectic C* - smectic A* transition. The magnitude and range of the electroclinic switching decreases as the concentration of dye increases. As described by equation 4.4 the electroclinic switching angle, θ, is linearly dependant on the applied field, E, where μ and α are constants, T is the sample temperature and T_C is the smectic A* to smectic C* transition temperature. Figure 4.18 shows that the switching of the 40% dye mixture is linearly dependent on the applied electric field away from the smectic C* to smectic A* transition but becomes less linear close to

the transition. Close to the smectic C*-smectic A* transition there is a coupling between the soft mode switching and the Goldstone switching in the ferroelectric phase[19] resulting in coupling that is not linear in this region.

$$\theta = e_c E \qquad \theta = \frac{\mu}{\alpha(T - T_c)}\mathrm{E} \qquad \text{equation 4.4}$$

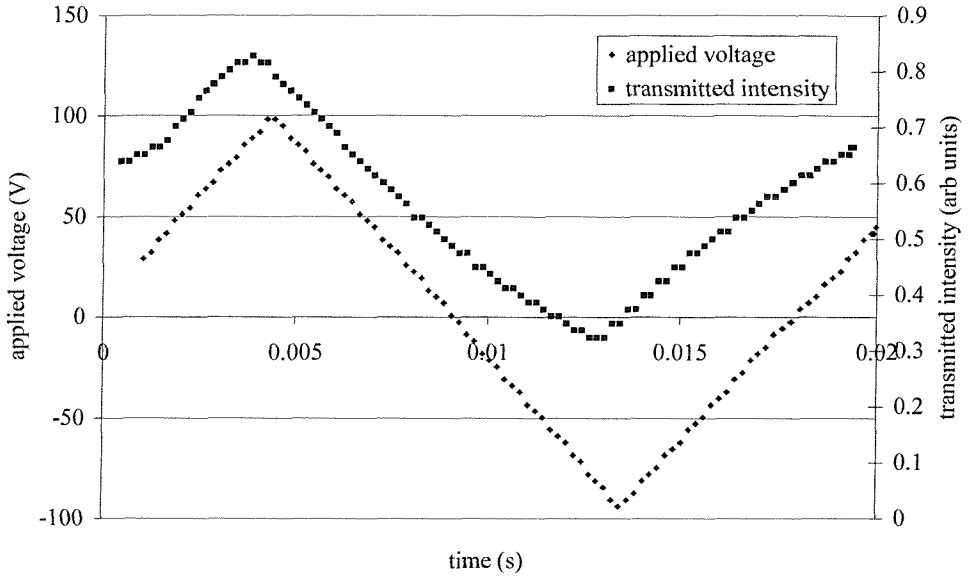

Figure 4.15 Comparison of the applied waveform and transmitted switching intensity plotted against time for the 40 % molar dye concentration measured at 95°C, 55Hz and 40 Vp-p/μm.

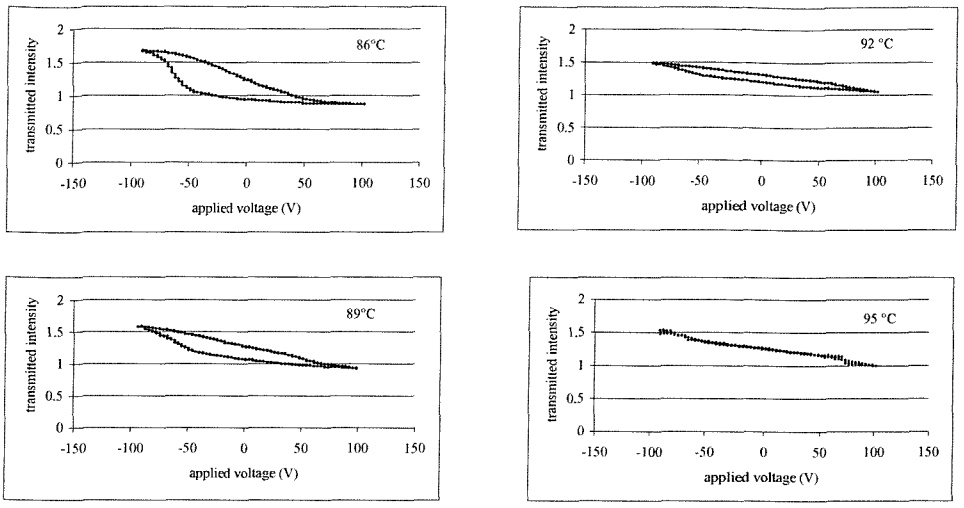

Figure 4.16 Optical hysteresis loops for the 40% dye concentration, measured at 86°C to 95°C, where the smectic A* to smectic C* transition temperature occurs at 92°C, taken at 55Hz and 40 Vp-p/μm.

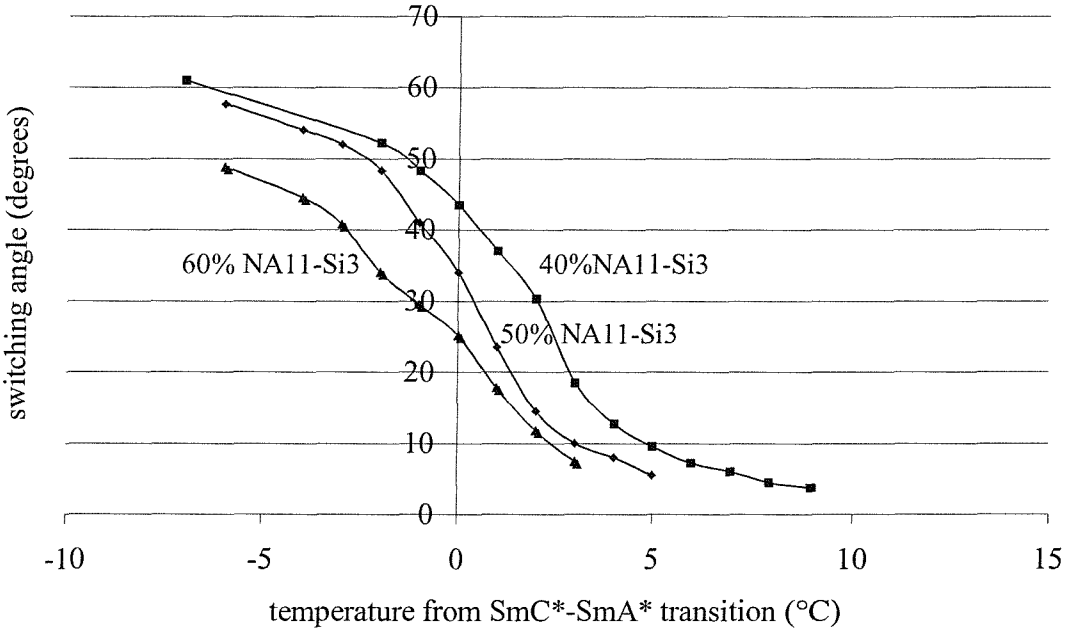

Figure 4.17 Switching angle against temperature for the 40%, 50% and 60% mixtures measured at 120 Hz and 40 $V_{p-p}/\mu m$.

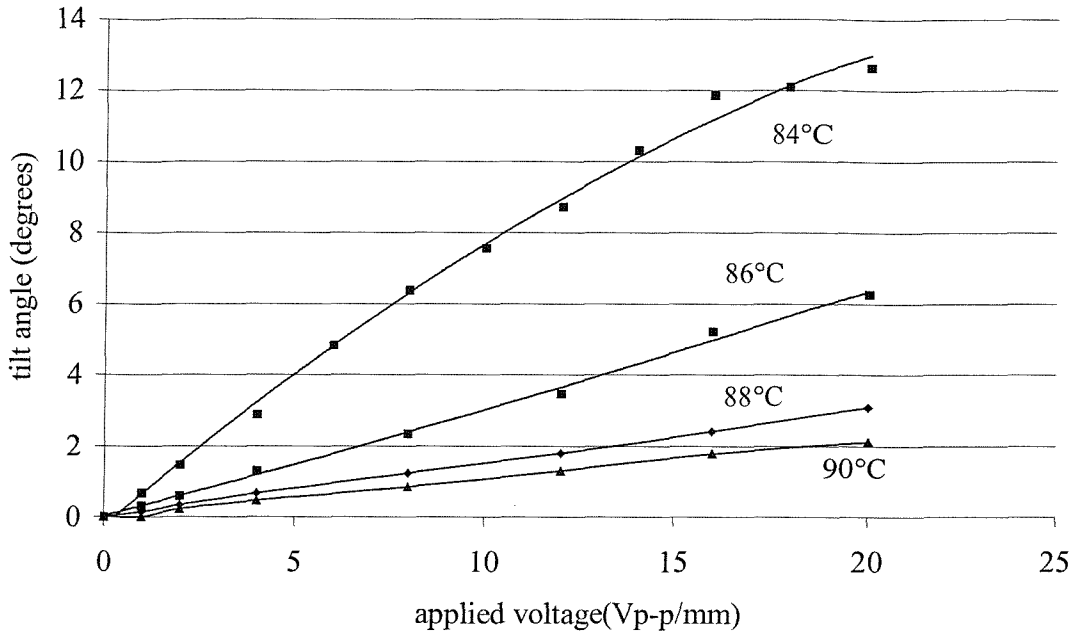

Figure 4.18 Plot of electroclinic tilt against applied voltage in the smectic A* phase of the 40% NA11-Si3 mixture measured at 35 Hz. The transition to smectic C* occurs at 82°C.

4.2.6 Improved Alignment

The presence of the smectic A* phase at temperatures above the smectic C* phase aids alignment. Representative examples of alignment observed in the centre of the stable temperature range with and without a smectic A* phase are given in figure 4.19.

Figure 4.19 (a) poor alignment of Br11-Si3 host at 60°C (b) Br11-Si3 + 40% NA11-Si3 at 60°C good alignment cooled from the smectic A* phase to the smectic C* phase at 0.1°C/min. 50 x magnification.

4.3 Conclusion of Chapter Four

In this chapter the properties of a ferroelectric organosiloxane host and a complementary azo dye were investigated. The organosiloxane materials are of great interest because they combine the ruggedness of polymers with the fast switching of low molar mass liquid crystals. The ferroelectric host material has a wide smectic C* phase with a temperature invariant spontaneous polarisation, close to 90 nC/cm^2, and tilt angle close to 45°. This chapter presents the properties of a completely new set of organosiloxane materials.

The nitroazo organosiloxane dye material was shown to be completely soluble in the ferroelectric host. This miscibility is attributed to the compatibility of the siloxane units of the dye and host materials. Concentrations of the dye up to 20% show only a

minor change in transition temperatures, spontaneous polarisation, tilt angle and response time compared to the host material. Dyed mixtures with a large dye concentration of up to 20% and a high polarisation (~90nCcm^{-2}) and a tilt angle close to 45° are a possibility. This is a substantial dye concentration compared to what is possible using many non-liquid crystalline materials[20]. The 40% NA11-Si3 mixture has a broad smectic C* phase, greater than 70°C, that is wider than either the host or the dye material and more than adequate for many applications. It is also possible to add up to 80% dye without destroying the ferroelectric properties of the host. These very high dye concentrations prove to be useful when examining the photomechanical properties of the azo dyes.

Both the spontaneous polarisation and the tilt angle scale with dye concentration. The reduction of the spontaneous polarisation scales linearly with dye concentration with dye concentration as would be expected as the fraction of chiral molecules is reduced. The optical tilt angle stays close to 45° for mixtures without a smectic A* phase but for dye concentrations above where this phase appears the tilt angle reduced as a linear function of the dye concentration. A material with a particular polarisation or tilt angle could be engineered by altering the dye concentration. For small concentrations, before a smectic A phase appears, the tilt angle is held close to 45°C so could be used for 90° switching applications.

The mixtures with a smectic A* phase at temperatures above the smectic C* phase are of interest because of improved alignment in the smectic C* phase and a strong electroclinic effect in the smectic A* phase. Organosiloxane materials without a nematic or smectic A phase can be hard to align. It has been shown that the presence of a smectic A* phase above the smectic C* phase produces better aligned samples than the mixtures without this phase.

The smectic A* phase also shows a significant electroclinic effect. The magnitude of switching angles (of up to 35°) and range (up to 7° C into the smectic A* phase) of this effect is greatest in the lowest concentrations in which a smectic A* phase is present and is reduced with increasing dye concentration. At temperatures away from the interference from the smectic C* phase the switching angle is linear with the

applied electric field giving rise to the possibility for high contrast grey scale applications.

The use of dye and host materials with the same three siloxane unit produced systems enabling a large dye concentration, giving a range of controllable values for the spontaneous polarisation and tilt angle and, where a smectic A* phase is present, aiding the alignment of the phase. An interesting electroclinic region with a large soft mode switch exists in the smectic A* phases.

The investigations carried out in this chapter will be advanced further in two directions. First the effect of a bimesogenic dye with the same three silicone core with a mesogenic unit attached, via the same eleven methylene spacer, at either end will be investigated. Secondly the photomechanical properties of the mixtures upon ultra violet illumination will be described.

References for Chapter 4

[1] Coles, H.J., Owen, H., Newton, J., Hodge, P., Liquid Crystals, **15(5)**, 739-744, (1993)

[2] Newton , J., Coles, H.., Owen, H., Hodge, P., Ferroelectrics, **148**, 379, (1993)

[3] Coles.H.J., Qwen.H., Newton.J., Hodge.P., SPIE, **2408**, 22, (1995)

[4] Coles, H.J., Gleeson. H.F., Scherowsky. G., Schliwa. A., Mol.Cryst.Liq.Cryst., **7(4)**, 117 (1990)

[5] Finkelmann. H., Kiechle. U., Rehage. G., Mol.Cryst.Liq.Cryst., **94**, 343, (1983)

[6] Uchida. S.,Morita. K., Miyoshi. K., Hashimoto. K., Kawasaki. K., Mol.Cryst.Liq.Cryst., **155**, 93, (1998)

[7] Hopwood. A.I., Coles. H.J., Polymer, **26,** 1312, (1985)

[8] Lester. G.A., Coles. H.J., Murayama. A., Ishikawa. M., Ferroelectrics, **148**, 389, (1993)

[9] Ibn-Elhaj. M., Skoulios. A., Guillon. D., Newton. J., Hodge. P., Coles. H.J., Liq.Cryst., **19(3)**, 373, (1995)

[10] Newton.J., Coles.H.J., Hodge.P., Hannington.J., J.Mater.Chem., **4(6)**, 869, (1994)

[11] Poths.H., Zentel. R., Liq.Crysy., **16(5)**, 749, (1994)

[12] Kloess, P., McComb, J., Coles, H.J., Ferroelectrics, **180**, 233, (1996)

[13] Shoosmith, D.E., Remnant, A., Perkins, S.P, , Coles, H.J., Ferroelectrics, **243(1-4),**75, (2000)

[14] A.M.Remnant, S.P.Perkins, H.J.Coles, Mol.Cryst.Liq.Cryst. **Vol 364-8**, (2001)

[15] Robinson, W.K., Kloess, P.S., Carboni,C., Coles, H.J., Liquid Crystals, **23(2)**, 309-312, (1997)

[16] Robinson,W.K., Carboni, C., Kloess, P., Perkins, S.P., Coles, H.J., Liquid Crystals, **25(3)**, 301-307, (1998)

[17] Lagerwall, S.T., Ch. 2, Handbook of Liquid Crystals Volume 2B, Wiley-Vch, (1998)

[18] de Gennes. P.G., Ch. 7, The Physics of Liquid Crystals, Oxford University Press (1974)

[19] Andersson, G., Dahl, I., Komitov, L., Lagerwall, S.T., Skarp, K., Stebler, B., J.Appl.Phys., **66(10)**, 4983-4995, (1989)

[20] Coles. H.J., Lester, G.A., Owen, H., Liquid Crystals. **14(4)**, 1039-1045, (1993)

Chapter 5

Bimesogenic Azo Dye added to Monomesogenic Ferroelectric Organosiloxane Host

Chapter 5
Bimesogenic Azo Dye added to Monomesogenic Ferroelectric Organosiloxane Host

5.1 Introduction

This chapter is a continuation of the work on dye guest host mixtures of low molar mass organosiloxane liquid crystals from chapter four. In the previous work a monomesogenic nitroazo dye[1] was added to a ferroelectric monomesogenic host[2]. The monomesogenic molecules consist of a liquid crystalline mesogenic unit attached, via a hydrocarbon chain to a siloxane unit as depicted in figure 5.1(a). In this chapter a bimesogenic dye incorporating the same nitroazo mesogenic moieties is added to the monomesogenic host. In the bimesogenic molecule a mesogenic unit is attached, via hydrocarbon chains, to either end of the siloxane unit as shown schematically in figure 5.1(b). There are two main reasons for this investigation: to compare and contrast the results with those for the monomesogenic dye and to investigate the effect of the dye's bimesogenic conformation on the host's ferroelectric switching properties.

It was shown in chapter four that a very high dye concentration was possible with a ferroelectric phase present at concentrations of up to 80%. The effect of monomesogenic dye addition on the ferroelectric host was to diminish the switching properties in proportion to the concentration of dye molecules phase without loosing the temperature independence of the host material. For a range of mixtures a smectic A* phase was present at temperatures above the smectic C* phase. This smectic A* phase exhibited substantial electroclinic switching and aided the alignment of the ferroelectric phase.

The monomesogenic and bimesogenic molecules are denoted using the type of liquid crystalline mesogen, the length of the methylene spacer chain and the number of siloxane atoms in the siloxane core as described in chapter four. For example the 2-Bromo-4-(1-methylheptyloxy)benzoic acid 4'-[11-(11-{4'-[4-(1-methylheptyloxy)benzoyloxy]biphenyl-4-yloxy}undecylhexamethylsiloxane)undecyloxy]biphenyl-4-yl ester bimesogen,

with an eleven methylene chain and three siloxane atoms is denoted Br11-Si3-11Br.

The switching properties of a range of monomesogenic and bimesogenic chiral organosiloxane mesogens comprising of a chiral end group attached via a range of different length hydrocarbon chains to a variety of siloxane cores all having a smectic C* phase, has been carried out by the Southampton group.[2,3,4] Homologous series with fluorine, chlorine or bromine as the halogen in the chiral groups have been synthesised. The effect of the number of silicone atoms in the bimesogen compounds is of particular interest here. It has been found that for two or four silicone atoms the smectic C* phase exhibits ferroelectric switching while for three or five silicone atoms the switching is antiferroelectric.

This tristable switching does not occur in the monomesogenic molecules or in the vinyl terminated precursers, so cannot be attributed to the chiral functional groups. The anticlinic arrangement that gives rise to the antiferroelectricity must come from the attachment of the two mesogens to the siloxane unit. This arrangement is shown schematically in figure 5.2.

The hypothesis that the addition of a bimesogenic dye with three silicon atoms in the siloxane unit to a ferroelectric monomesogenic host could change the switching characteristics from bistable to tristable antiferroelectric will be investigated.

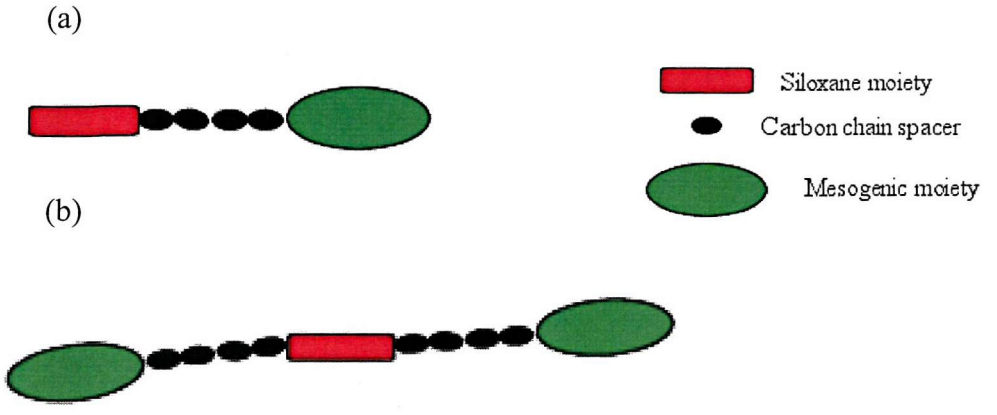

Figure 5.1 Schematic diagram of (a) monomesogenic and (b) bimesogenic organosiloxane

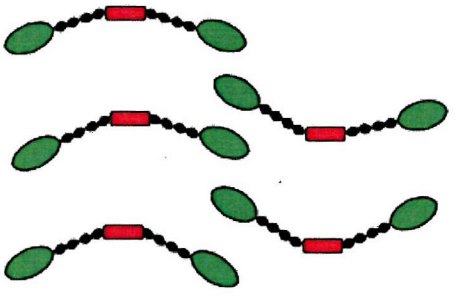

Figure 5.2 Anticlinic ordering of the mesogenic

5.2 Dye and Host Characteristics

A bimesogenic nitro-azo dye, α,ω-bis(4-nitroazobenzene-4'-oxyundecyl)hexamethylsiloxane, denoted NA11-Si3-11NA shown schematically in figure 5.3, has been synthesised by S.Perkins**Error! Bookmark not defined.** at Southampton University with the same functional group as the monomesogenic dye NA11-Si3 studied in chapter four. It has a smectic A phase which, in addition to the presence of the three siloxane unit, should produced good miscibility with Br11-Si3.

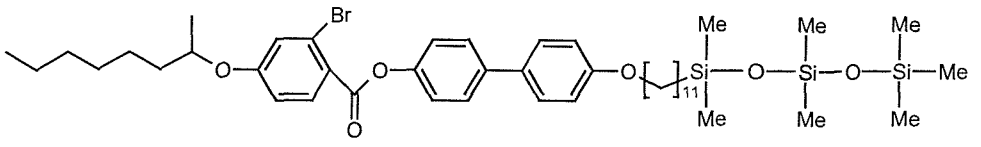

Crystal – 46°C – Smectic C* - 88°C – Isotropic

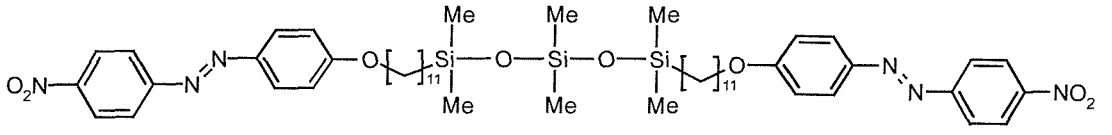

Crystal – 60°C – Smectic A – 126°C – Isotropic

Figure 5.3 Schematic diagram of the monomesogenic ferroelectric host Br11-Si3 and the bimesogenic dye molecule NA11-Si3-11NA. The phase transition temperatures were measured by optical microscopy.

5.3 Effect of bimesogenic dye addition

5.3.1 Phase Characteristics

A full range of mixtures have been made between the ferroelectric host Br11-Si3 and the dye NA11-Si3-11NA by heating the weighed mixtures to above both component's isotopic transition temperatures for up to 12 hours. Cells of 5μm thickness with anti-parallel rubbed polyimide alignment layers were used for all the observations and measurements described. A phase diagram of transition temperatures against molar concentration is shown in figure 5.4. The transition temperatures were measured by optical microscopy and the switching type determined by the response to a triangular waveform. Phases denoted with an asterisk include chiral molecules. For dye concentrations less than 15% the only effect of dye addition is a small increase in the temperature range of the smectic C* phase. For concentrations between 15% and 45% the smectic C* phase becomes antiferroelectric (smectic C_A*) and a smectic A* phase is also present. The double current pulse peak, shown in figure 5.5, and double hysteresis loop, figure 5.6,

show that the material switches between three states in the antiferroelectric phase[5,6,7]. The presence of a smectic A* phase improves the alignment of the smectic C_A* phase. For dye concentrations greater than 45% the mixtures are all smectic A.

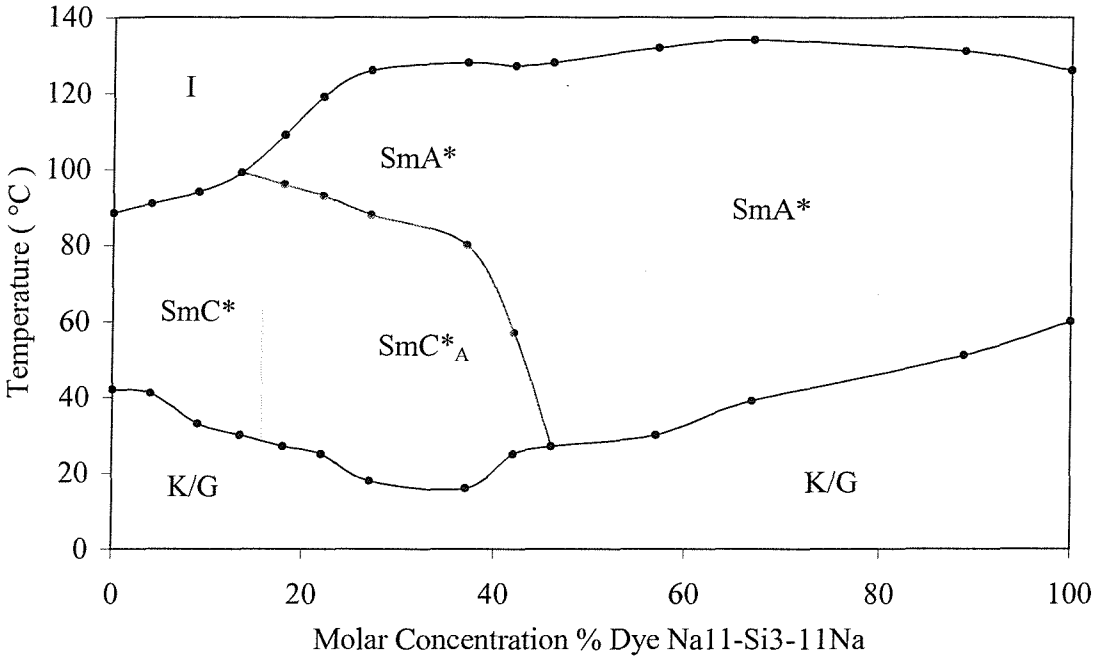

Figure 5.4 Phase diagram for dye addition against temperature measured by optical microscopy where the phases denoted by an asterisk contain a chiral molecule.

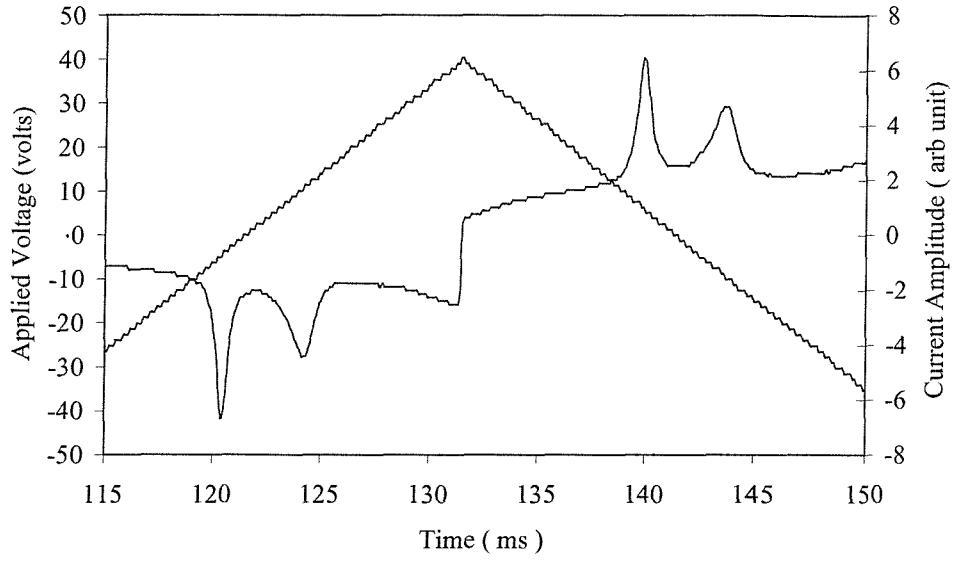

Figure 5.5 The antiferroelectric double current pulse for 30% NA11-Si3-11NA mixture at 60°C, 25 Hz and 8 Vp-p/μm

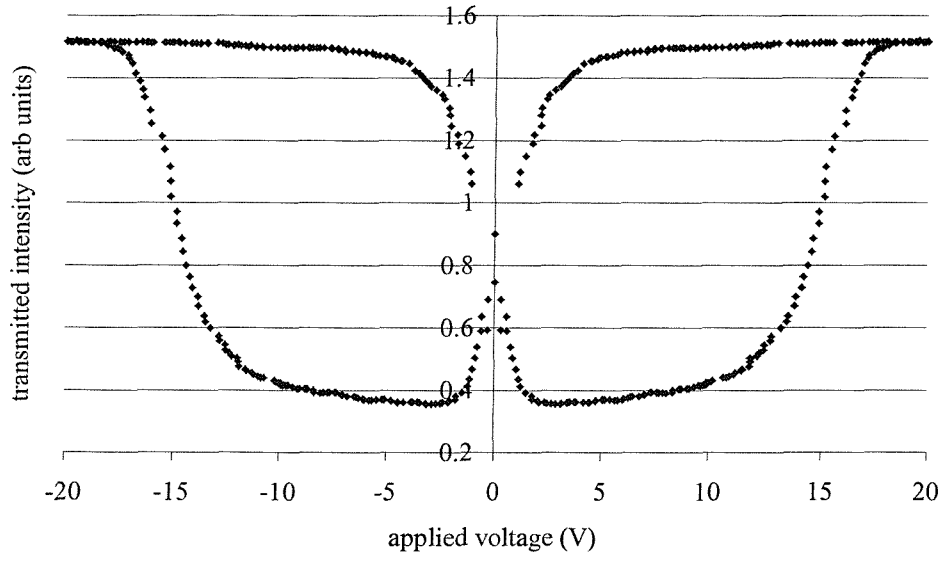

Figure 5.6 Double hysteresis loop for 30% NA11-Si3-11NA mixture at 60°C, 25 Hz and 8 Vp-p/μm

5.3.2 Spontaneous Polarisation

Figure 5.7 shows that the spontaneous polarisation of the mixtures maintains the broad temperature independence of the host. The spontaneous polarisation was measured by the current pulse method in 5 μm cells. The maximum value of the spontaneous polarisation decreases linearly with dye concentration as shown in figure 5.8.

It can be seen for the mixtures with a smectic A* phase above the smectic C* phase that the spontaneous polarisation reduces more gradually to zero close to the transition. The theoretical Curie-Weiss relationship between the spontaneous polarisation and temperature is plotted transition for dye concentrations of 40%, 50% and 60% in figure 5.9.The spontaneous polarisation, P_S, equation 5.1, is related to the sample temperature, T, by the constants, K_P, T_0 and β. The exponent β is equal to a half in a mean field approximation[8] and the constant T_0 is approximately equal to the smectic A* to smectic C* transition temperature. The constant k_p was calculated from the gradient of the graph of the spontaneous polarisation against the ration of transition and sample temperatures given in equation 5.1 and compared to the experimental dependence in figure 5.9. The fitted curves show that for the mixtures where a smectic A* phase is present the spontaneous polarisation follows the Curie Weiss dependence close to the smectic C* - smectic A* transition.

$$P_s = k_p\left(\frac{T_0 - T}{T_0}\right)^{\frac{1}{2}} \quad \text{equation 5.1}$$

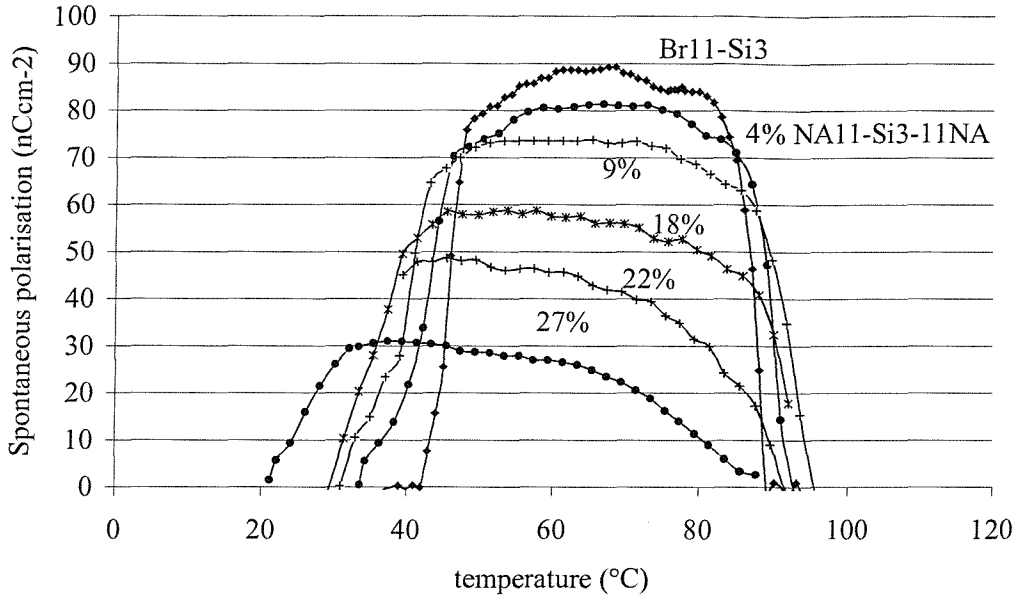

Figure 5.7 Spontaneous polarisation against temperature for the Br11-Si3 and NA11-Si3-11NA mixtures. Measured using the current pulse technique at 50 Hz, 20Vp-p/μm.

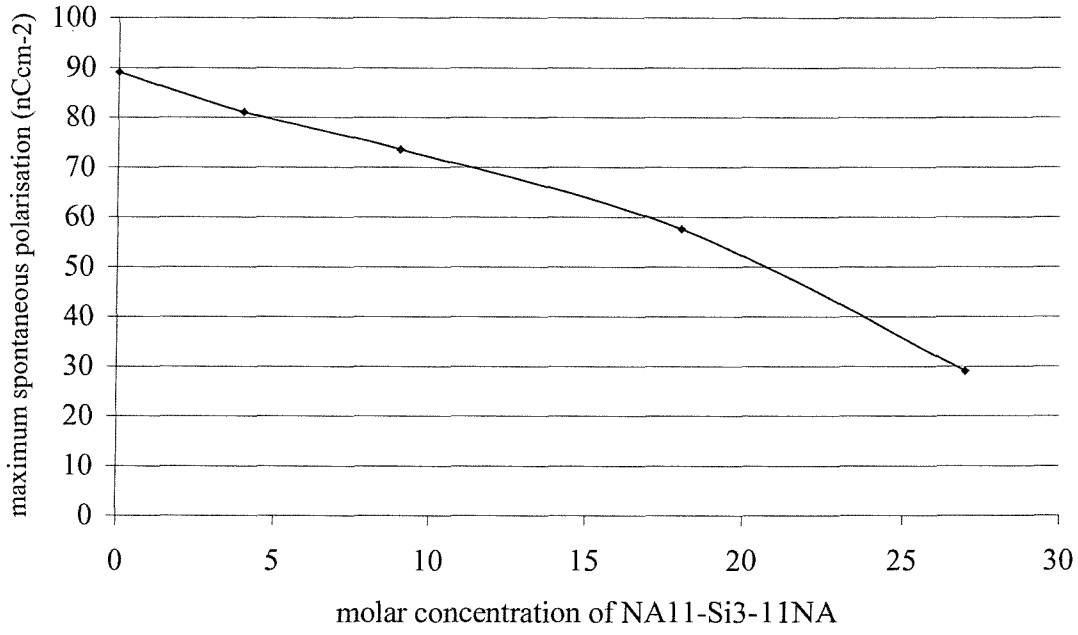

Figure 5.8 The maximum value of the spontaneous polarisation as measured in figure 5.7 as a function of dye concentration.

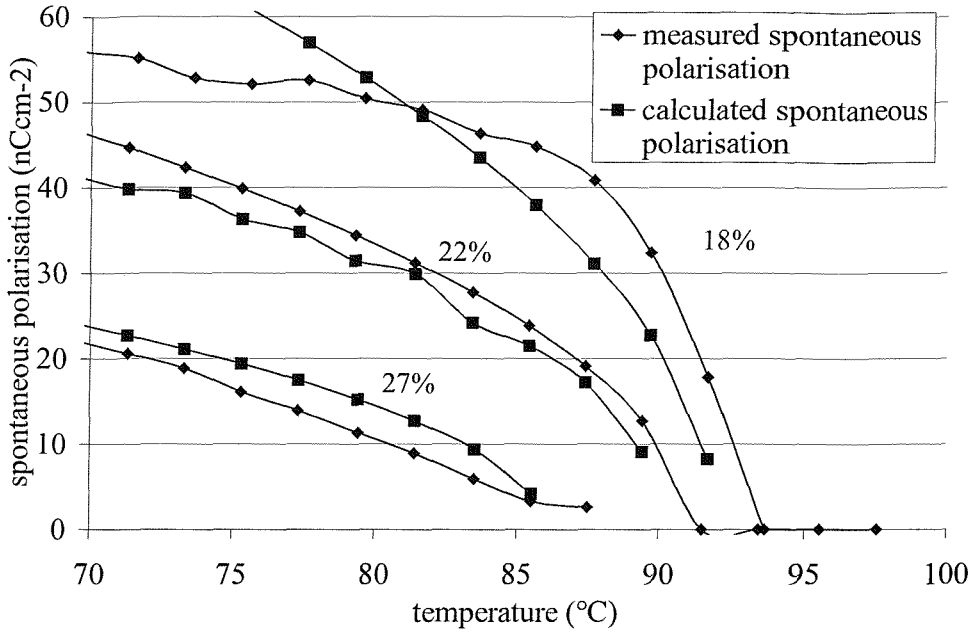

Figure 5.9 Curie Weiss fits of spontaneous polarisation data against temperature close to the smectic C* - smectic A transition.

5.3.3 Tilt Angle

The optical tilt angles of the mixtures were measured by polarised microscopy in aligned cells as shown plotted against temperature in figure 5.10. These tilt angles maintain the broad temperature independence across the phase range of the host material. The magnitude of the maximum tilt angle is reduced by increased dye concentration as shown in figure 5.11. The tilt angle is held close to 45° for concentrations without a smectic A* phase, reducing linearly with concentration after the smectic A* phase is induced.

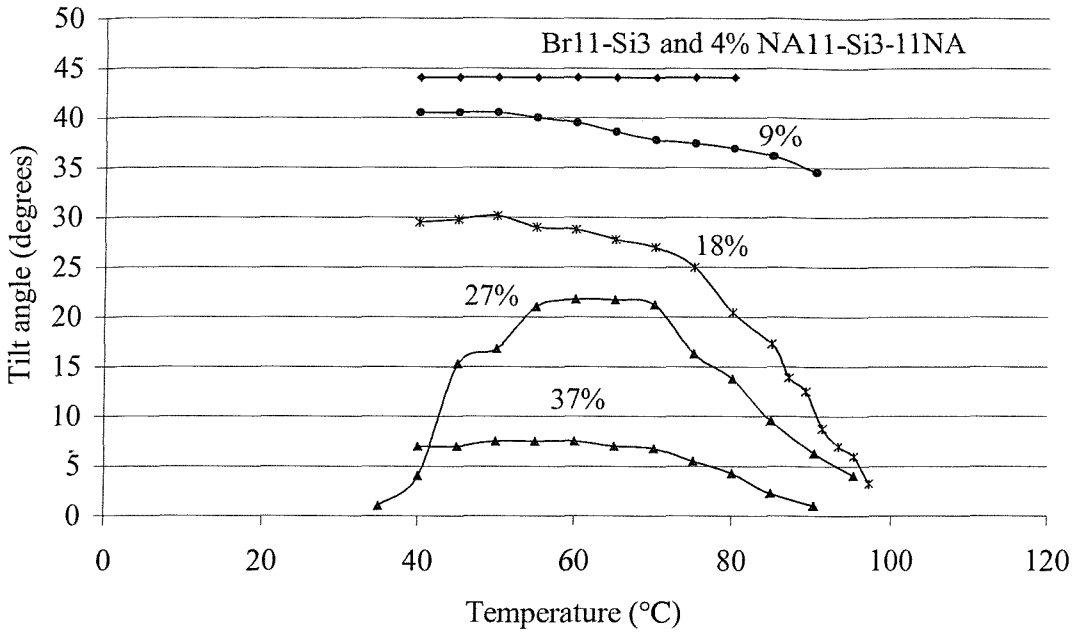

Figure 5.10 Tilt angle against sample temperature for the Br11-Si3 and NA11-Si3-11NA mixtures. Measured by crossed polarisor microscopy at 120 Hz, 40 V/μm.

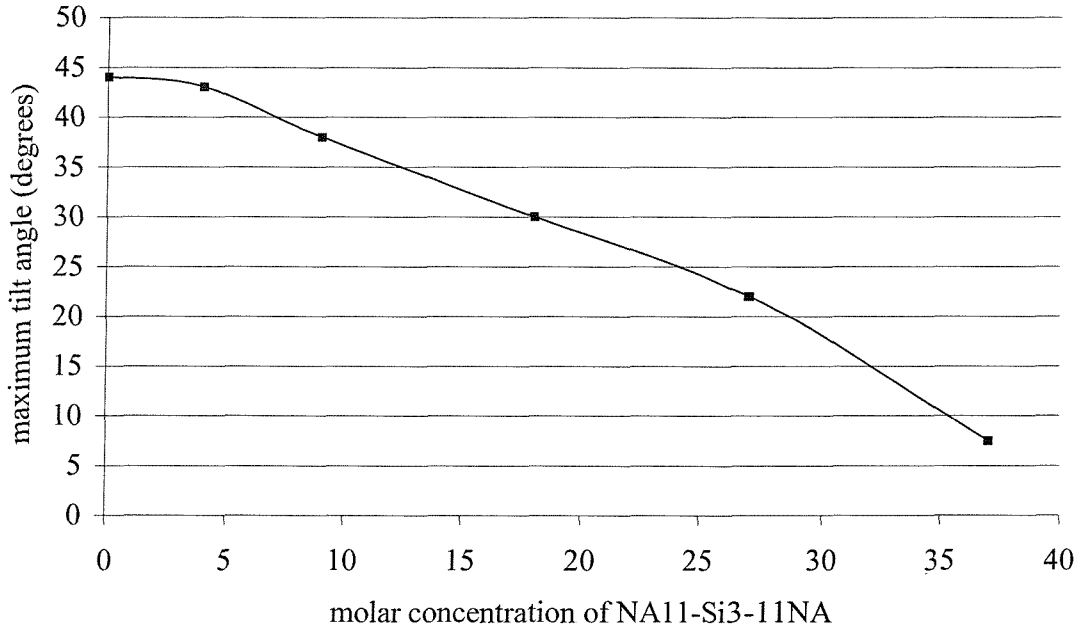

Figure 5.11 The maximum value of the tilt angle as measured in figure 5.10 as a function of dye concentration.

5.3.4 Response Time

The response times, measured as the time between the reversal of a square wave and the resulting current maximum, as shown in figure 5.12, are slightly reduced with increasing dye concentration. The response time, τ, is exponentially related to the inverse of the sample temperature, T, by the Ahhrenius relationship involving the activation energy, E_A, and the constants τ_0 and R as shown in equation 5.2.

$$\tau = \tau_0 \exp^{\frac{E_A}{RT}} \quad \text{equation 5.2}$$

The linearity of the log of the response time with temperature is shown in figure 5.13. Figure 5.14 shows that the response time of the 20% mixture is inversely proportional to the applied field, E, at temperatures well below the isotropic transition for a constant polarisation, P, as predicted by equation 5.3. However this becomes less linear closer to the transition. The increase in the gradient as the temperature is increased indicates that the viscosity, γ, is decreasing.

$$\tau = \frac{\gamma}{P.E} \quad \text{equation 5.3}$$

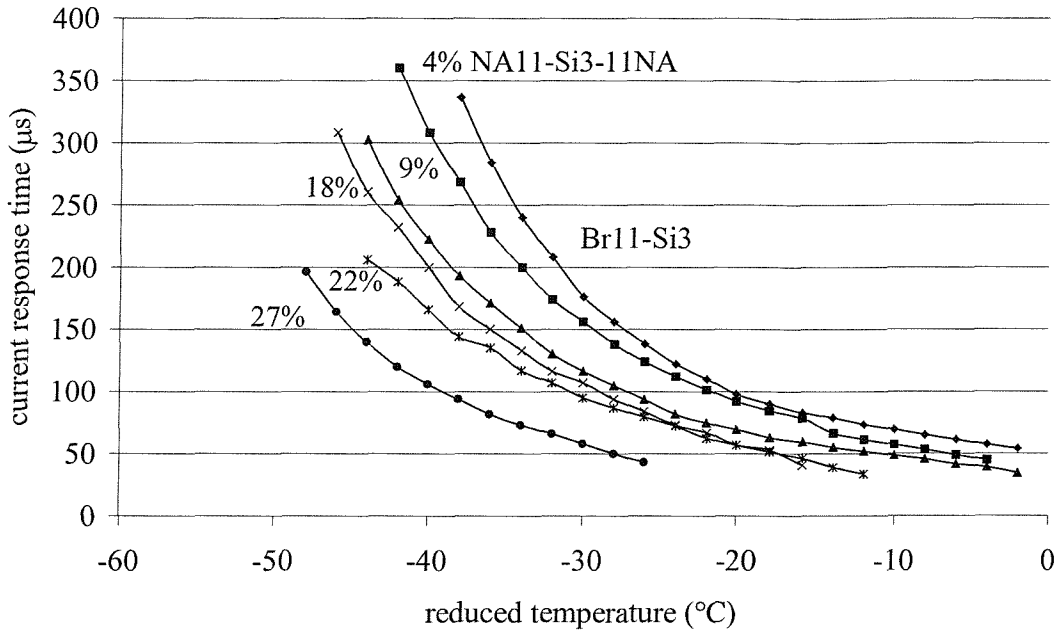

Figure 5.12 Current pulse response time against reduced temperature for the NA11-Si3-11NA mixtures measured at 10Hz 17 Vp-p/µm.

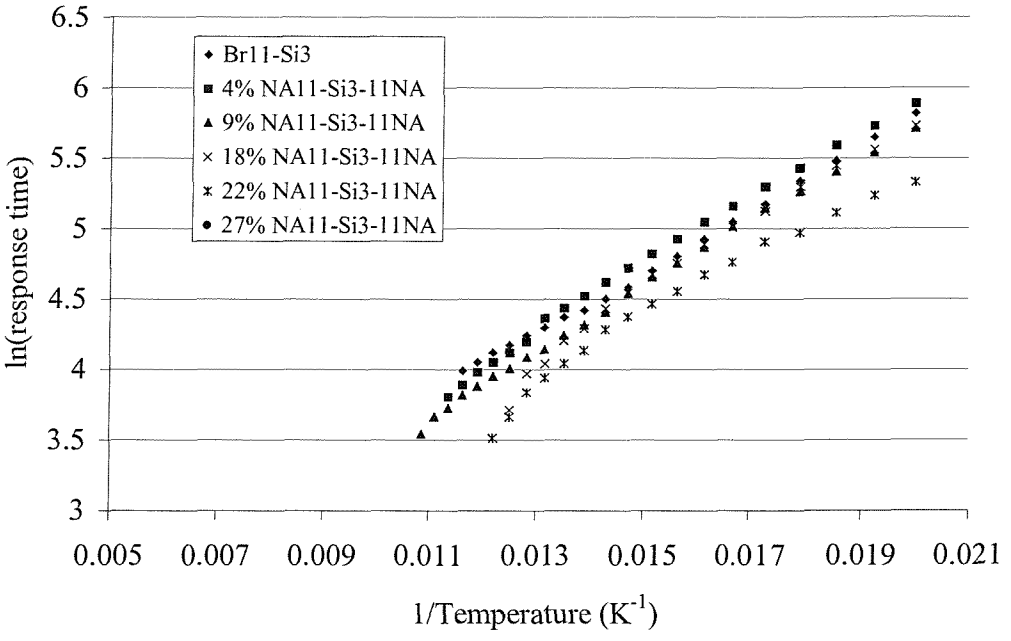

Figure 5.13 Ln(response time) against 1/temperature for the data presented in figure 5.12.

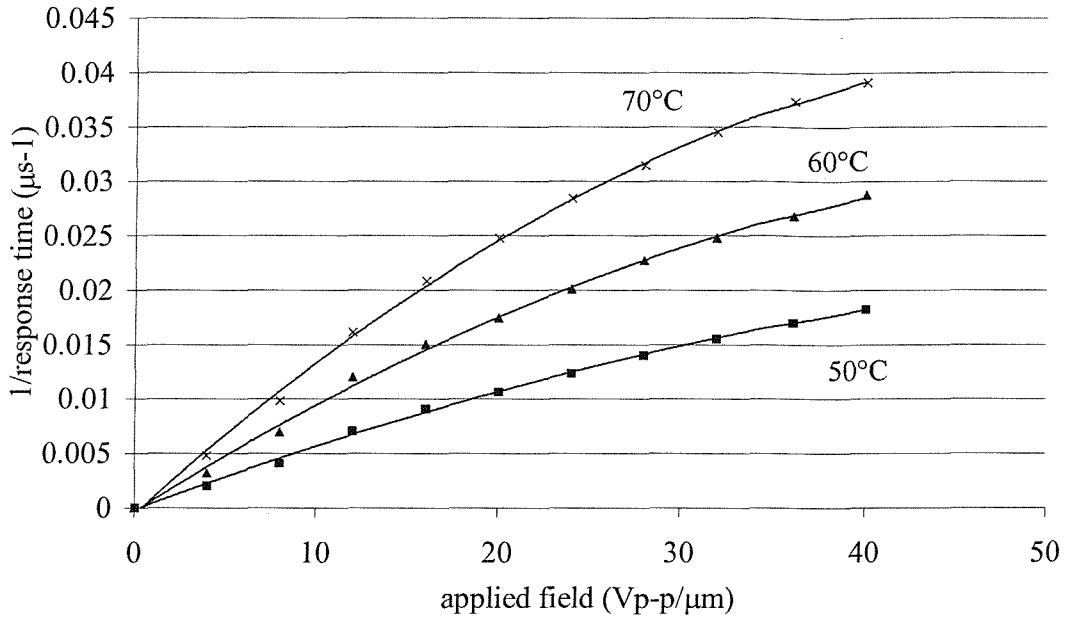

Figure 5.14 1/response time against voltage for Br11Si3 + 20% NA11-Si3-11NA

5.3.5 Electroclinic Switching

Figure 5.15 shows that a switching angle is observed well into the smectic A* phase of the 22% and 27% mixtures. Soft mode or electroclinic switching has been observed in chiral smectic A phases most commonly immediately above a smectic C* phase. Electroclinic switching is dielectric in origin and an induced polarisation grows linearly with the applied field[9]. Whereas in the Goldstone mode the optic axis moves around a cone, in electroclinic switching there is a simple change of tilt causing a linear change in the transmitted intensity. Observations of the switching, figure 5.16, show that the optical response in the smectic A* phase is linearly proportional to a triangular applied field indicating that soft mode electroclinic switching does occur. The transition from smectic C_A* to smectic A* is determined by observing the change in the hysteresis loops from Goldstone to soft mode switching as the temperature is increased. A typical example for the 22% mixture is shown in figure 5.17. The electroclinic switching angle, θ, is linearly related to the applied field, E, equation 5.4, where μ and α are constants, T is the sample temperature and T_C is the smectic A* to smectic C* transition temperature. This

relationship holds well at temperatures well above the transition as shown in figure 5.18 but becomes less linear close to the transition as the ferroelectric switching starts to interfere causing hysteresis.

$$\theta = e_c E \qquad \theta = \frac{\mu}{\alpha(T - T_c)}\mathrm{E} \qquad \text{equation 5.4}$$

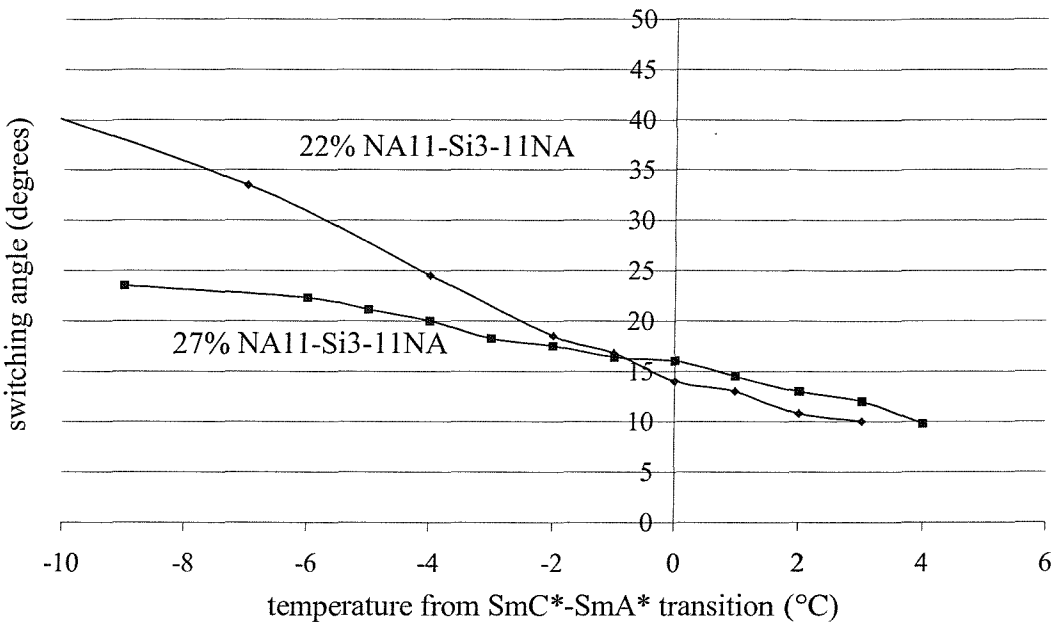

Figure 5.15 Switching occurs well into the smectic A phase for the 22% and 27% mixtures measured at 70V/μm at 100 Hz.

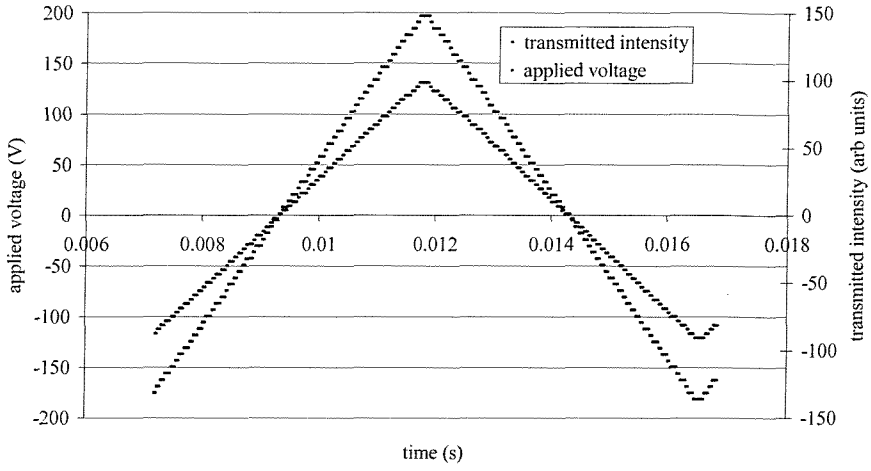

Figure 5.16 The relationship between the transmitted intensity and the applied triangular voltage for the 27 % mixture measured at 100 Hz and at 92C.

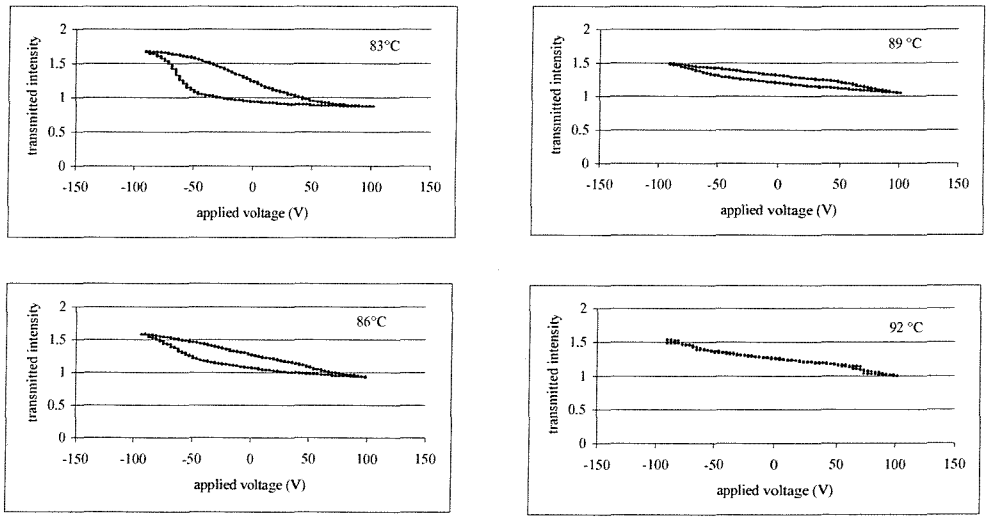

Figure 5.17 Hysteresis loop for the 27% mixture measured from 83 to 92 where the smectic A* to smectic C* transition occurs just above 89 °C, at 40 Vp-p/μm and 200Hz.

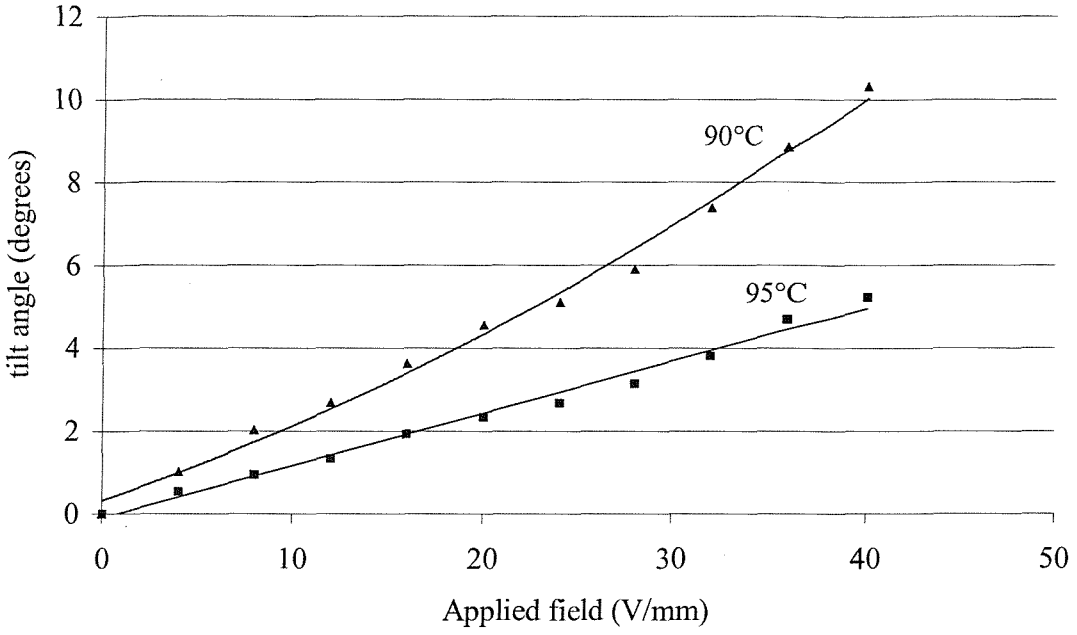

Figure 5.18 Relationship between the tilt/switching angle and the applied electric field for the 27 % mixture measured at 100 Hz.

5.4 Comparison of bimesogenic and monomesogenic dye addition

As well as investigating the templating effect of the bimesogenic dye the effect of dye addition can be compared to the monomesogenic dye NA11-Si3. Molar concentrations are compared. Figures 5.19 to 5.23 compare the transition temperatures, maximum spontaneous polarisation and tilt angle of the two dyes.

A comparison of the phase diagrams, figure 5.19, shows that concentrations up to 15% have a very similar effect on the phase range of the pure ferroelectric host. The bimesogenic dye induces a smectic A phase at approximately half the concentration of the monomesogenic dye. The monomesogenic dye maintains a ferroelectric phase for almost twice the dye concentration as the bimesogenic dye. It can be hypothesised that as each bimesogenic molecule has two mesogens it has twice the tendency to form smectic A phases than the monomesogenic dye.

A comparison of the maximum spontaneous polarisation against molar dye concentration, figure 5.20, shows that the polarisation decreases more rapidly for the bimesogenic dye. If the x-axis is changed so that the concentration of monomesogenic dye is compared to twice the concentration of bimesogenic dye the number of NA11 mesogenic units is being equally compared. Figure 5.21 shows that the decrease is compatible for both the mono and the bimesogenic dyes and the NA11 mesogenic units dilute the switching response of the Br11 mesogenic units.

The tilt angle of the bimesogenic dye also decreases more rapidly than that of the monomesogenic dye with increased concentration. The reduction does not follow the simple linear decrease of the polarisation as shown in figure 5.22, rather it has a strong dependence on the phase sequence of the mixtures. The tilt angle stays close to 45° until the smectic A phase appears above the smectic C* and then decreases. Even when the bimesogenic dye concentration is doubled to compare the number of NA11 units, figure 5.23, the reduction is greater than for the monomesogenic dye.

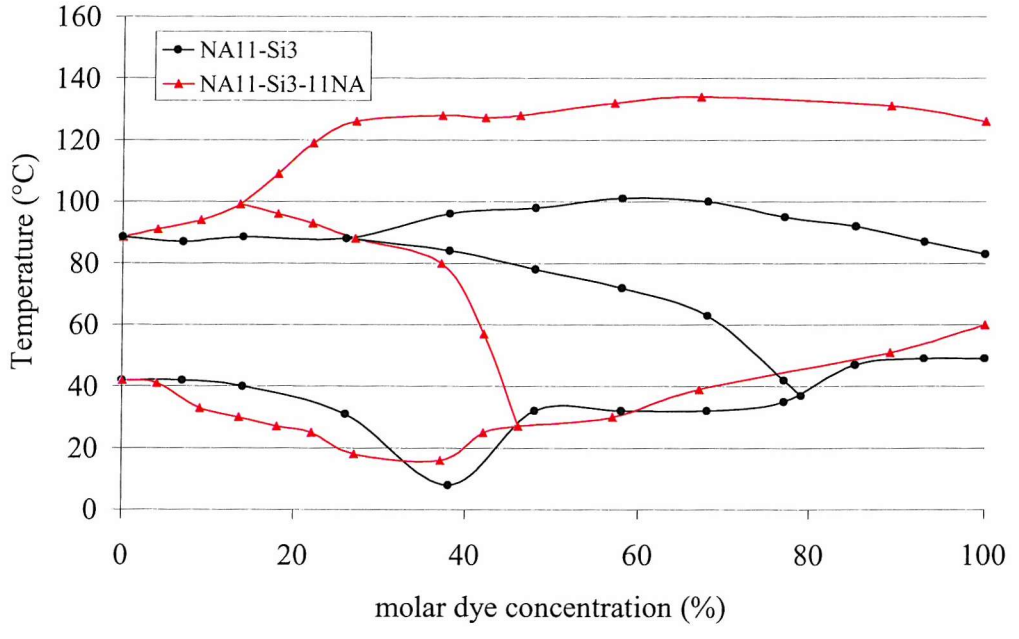

Figure 5.19 Comparison of the phase diagrams for NA11-Si3 and NA11-Si3-11NA against molar dye concentration

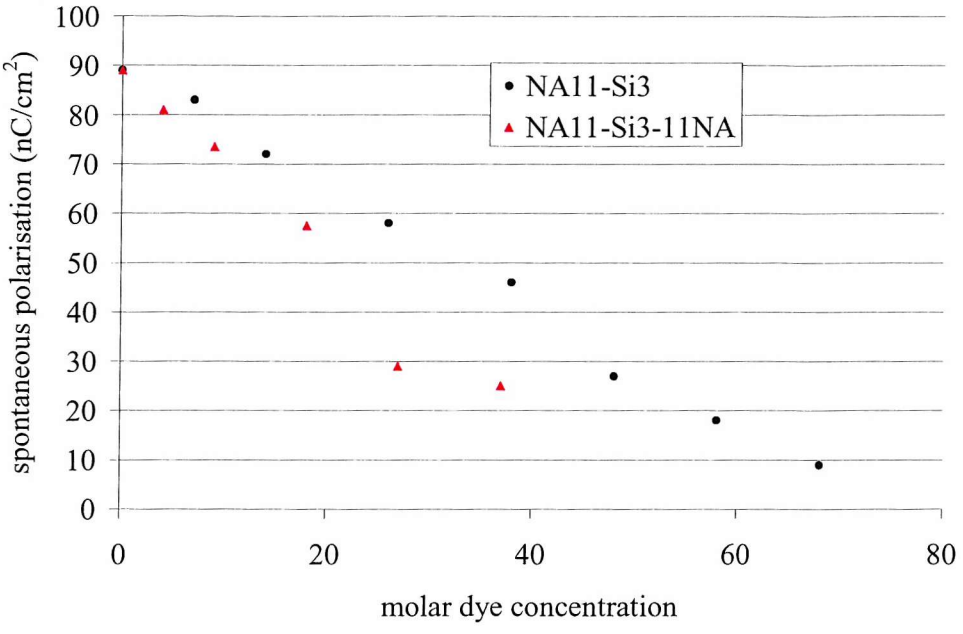

Figure 5.20 Maximum value of spontaneous polarisation plotted against molar dye concentration for the mono and bimesogenic dyes

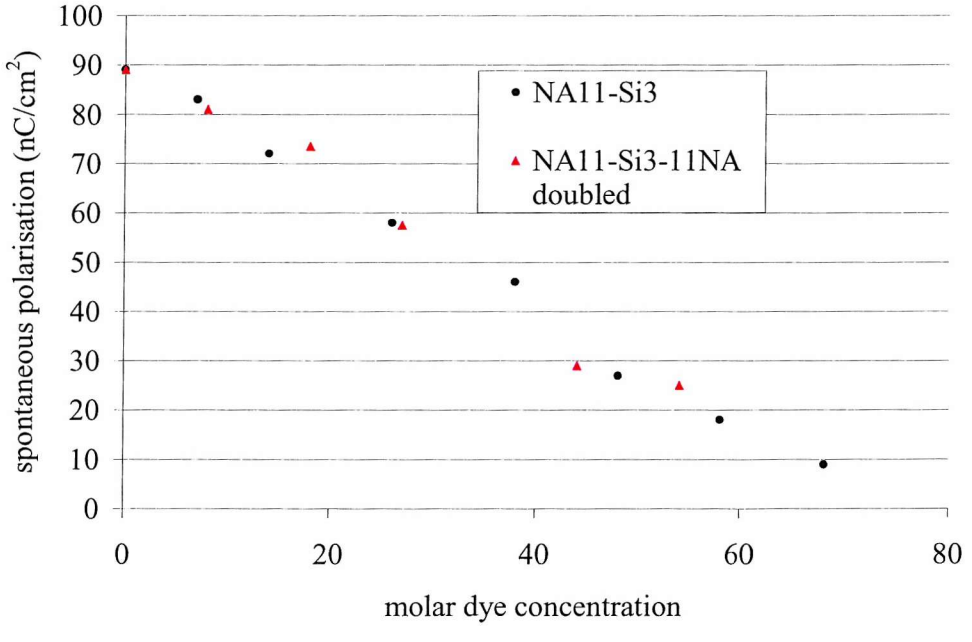

Figure 5.21 Comparison of the maximum spontaneous polarisation plotted against dye concentration for NA11-Si3 and twice the dye concentration for NA11-Si3-11NA

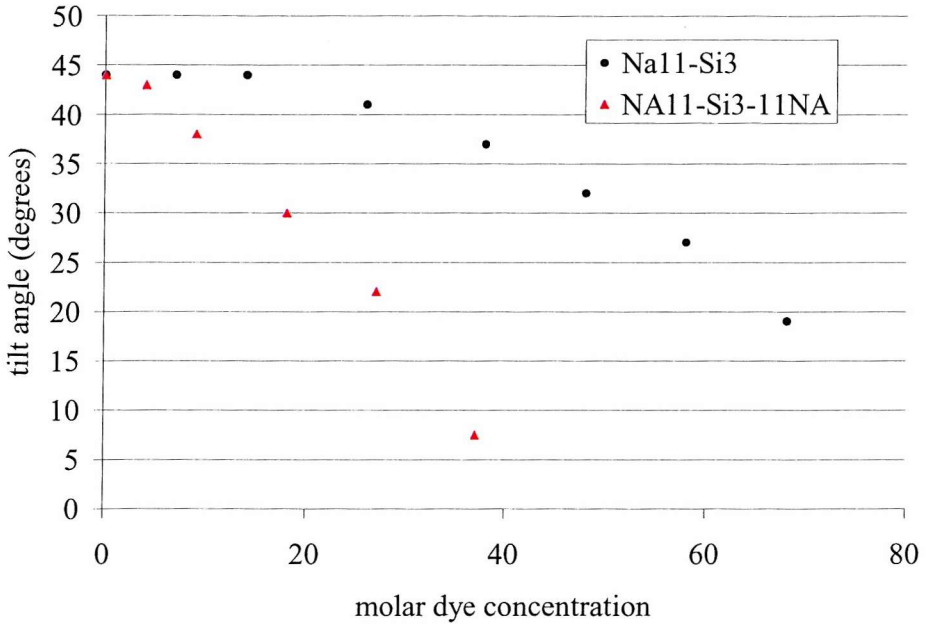

Figure 5.22 Maximum value of tilt angle plotted against molar dye concentration for the mono and bimesogenic dyes

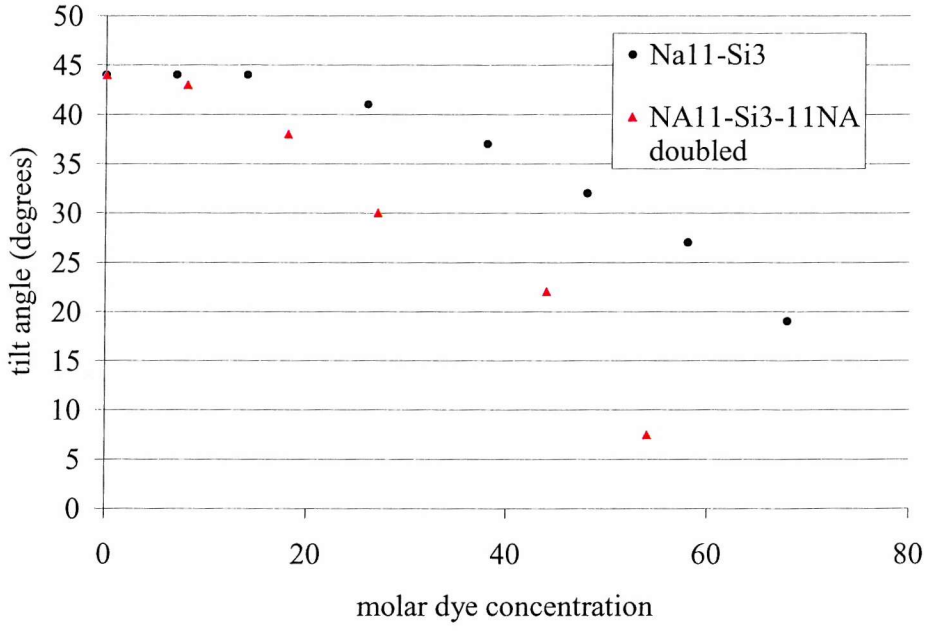

Figure 5.23 Comparison of the tilt angle plotted against dye concentration for NA11-Si3 and twice the dye concentration for NA11-Si3-11NA

5.5 Conclusions of Chapter Five

The results of mixing a novel bimesogenic organosiloxane dye with a monomesogenic ferroelectric host are discussed in this chapter. The bimesogenic organosiloxane dye was found to be completely miscible with the ferroelectric host. This miscibility was attributed to the presence in both the dye and host of a three siloxane unit. As with the monomesogenic dye in chapter four mixtures were produced with both a smectic C* and a smectic A* phase. Interestingly these mixtures exhibited antiferroelectric switching characteristics of the bimesogenic dye rather than of the rather than that of the ferroelectric monomesogenic host, confirmed by the double current pulse and the hysteresis loops.

The presence of the smectic A* phase caused the dependence of the polarisation in the smectic C* to become Curie Weiss in nature and aided the alignment of the smectic C* phase. The smectic A* phase itself showed a substantial electroclinic switching effect.

The effect of the bimesogenic dye addition was compared to that of the monomesogenic dye described fully in chapter four. It was found that the appearance of the smectic A phase and the disappearance of the smectic C* phase happened for the bimesogenic dye at approximately twice the molar concentration as the monomesogenic dye. These would be concentrations with roughly the same amount of NA11 mesogenic units. It was also found that linear reduction of the maximum value of spontaneous polarisation was twice as rapid for the bimesogenic dye as it was for the monomesogenic dye.

This relationship does not hold for the tilt angle, which for both dyes is close to 45° in the phases without a smectic A* phase and then reduces with dye addition. The reduction of the tilt angle in the bimesogen dye is much greater than for the monomesogenic dye

References for Chapter 5

[1] Shoosmith, D.E., Remnant, A., Perkins, S.P, , Coles, H.J., Ferroelectrics, **243(1-4),**75, (2000)

[2] Kloess, P., McComb, J., Coles, H.J., Ferroelectrics, **180**, 233, (1996)

[3] Robinson, W.K., Kloess, P.S., Carboni, C., Coles, H.J., Liquid Crystals, **23(2)**, 309-312, (1997)

[4] Robinson, W.K., Carboni, C., Kloess, P., Perkins, S.P., Coles, H.J., Liquid Crystals, **25(3)**, 301-307, (1998)

[5] Chandini, A.D.L., Gorecka, R., Ouchi, Y., Takezoe, H., Fukuda, A., Jpn. J. Appl. Phys, **28**, L1265, (1989)

[6] Fukuda, S., Takanishi, Y., Isozaki, T., Ishikawa, K., Takezoe, H., J.Mater.Chem, **4**,997, (1994)

[7] Inui, S., Iimura, N., Suzuki, T., Iwane, H., Miyachi, K., Takanishi, Y., Fukuda, A., J.Mater.Chem., **6(4)**, 671, (1996)

[8] Goodby, J.W., J.Mater.Chem., **1(3)**, 307-318, (1991)

[9] Elston, S.J., Sambles, J.R., Ch 8, The Optics of Thermotropic Liquid Crystals, Taylor and Francis Ltd, (1998)

Chapter 6

Effect of Photoisomerisation by Ultra Violet light on the Monomesogenic Host and Monomesogenic Dye mixtures

Chapter 6

Effect of Photoisomerisation by Ultra Violet light on the Monomesogenic Host and Monomesogenic Dye mixtures

6.1 Introduction

In this chapter the photoisomerising properties of the smectic organosiloxane liquid crystals mixtures will be investigated. In chapter four the properties of the system of a ferroelectric host and a photoisomerising nitroazo dye were investigated. The use of the same three siloxane unit for the dye and host material produced complete miscibility. It was found that the mixtures maintained ferroelectric characteristics up to 80% dye concentration. The tilt angle and spontaneous polarisation of the mixtures maintained the temperature independence of the host but decreased in magnitude as the dye concentration was increased.

This chapter describes the effect of ultra violet illumination on the ferroelectric mixtures. As discussed in chapter two the trans-cis isomerisation by ultra violet illumination of the nitrobenzene group should induce a bend into the configuration of the dye.[1] This more bulky configuration could be expected to disrupt the liquid crystalline order[2] and disrupt the phase characteristics and switching properties[3,4,5].

Changes in the phase transition temperatures, the spontaneous polarisation, the tilt angle and the response time will be monitored to assess any changes due to illumination by ultra violet light.

6.2 Photoisomerisation of pure NA11-Si3

The nitro azo dye NA11-Si3[6] synthesised by S. Perkins at Southampton University should exhibit two responses to ultra violet illumination. Ultra violet illumination should be absorbed by the compound at the frequency that causes a trans to cis isomerisation. Secondly the pure dye exhibits a smectic A phase. The phase transition temperatures of this phase should be reduced by ultra violet illumination as the resulting bent isomer should be less inclined to form the phase.

The absorption spectrum of NA11-Si3 was measured in a solution of 100mg of dye per litre of optical DCM using a UV–Vis spectrometer. As shown in figure 6.1 the nitroazo dye absorbs ultra violet across the wavelength range of 350 to 450 nm, the energy range required to induce the trans to cis isomerisation.

The isotropic to smectic A and smectic A to crystal transition temperatures of the dye were measured by optical microscopy. These transition temperatures, shown in figure 6.2, are reduced by ultra violet illumination.

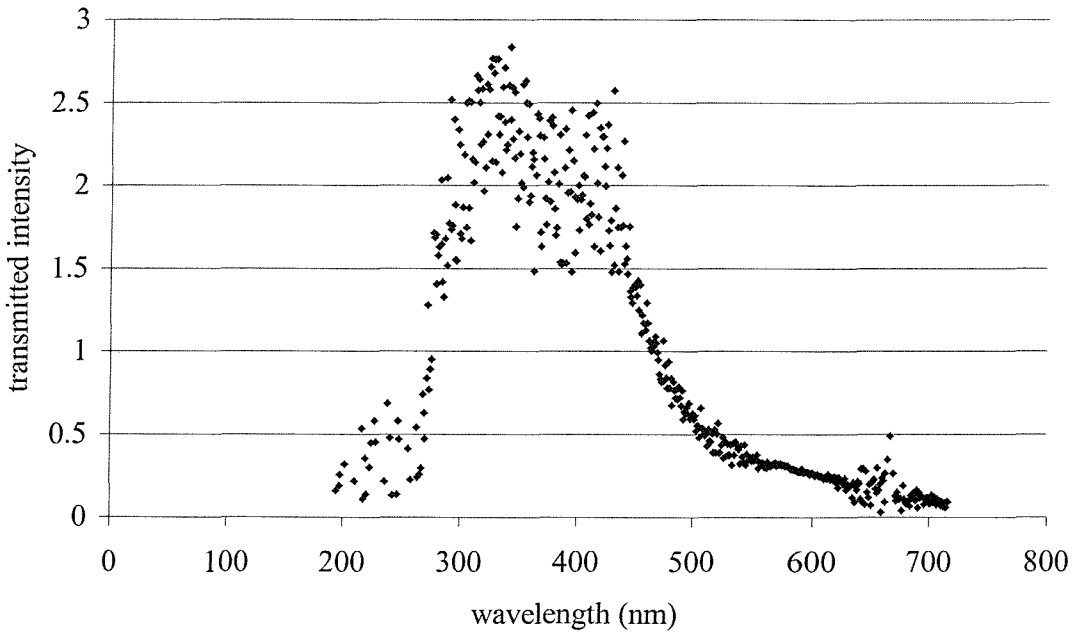

Figure 6.1 Absorption spectrum of the monomesogenic dye NA11-Si3 showing an absorbance peak between 350 and 450 nm.

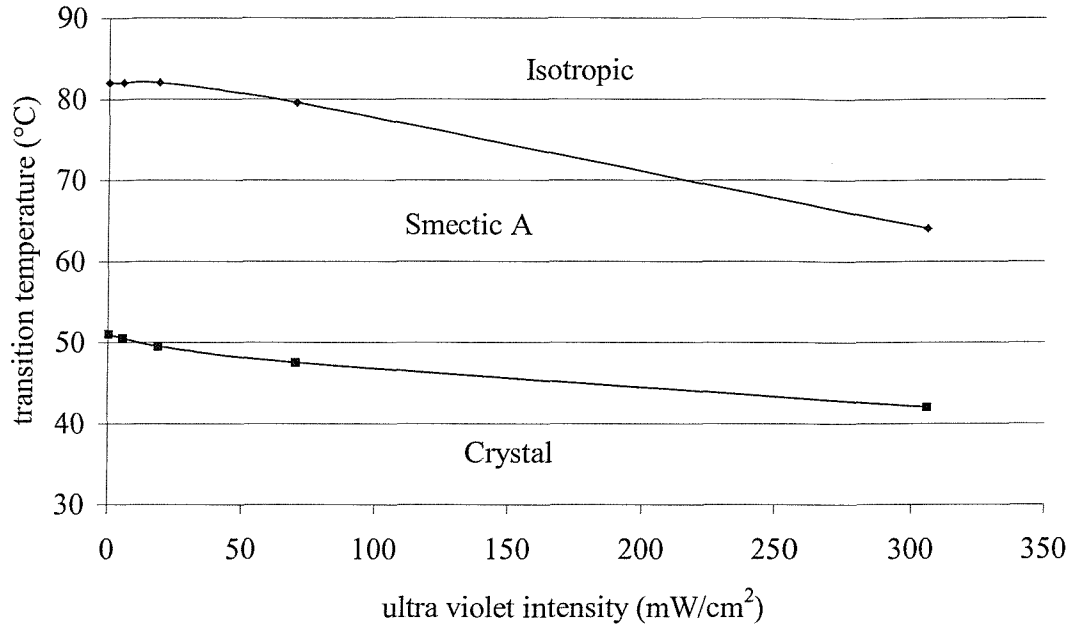

Figure 6.2 The change in the isotropic to smectic A and smectic A to crystal transition temperatures of NA11-Si3 with ultra violet illumination.

6.3 Photoisomerisation of mixtures

6.3.1 Choice of mixtures

The use of mixtures of the ferroelectric host, Br11-Si3[7,8], and the nitro-azo dye, NA11-Si3, allowed a range of dye concentrations to be studied. Photoisomerising effects were investigated in two mixtures, one with an isotropic - smectic A* - smectic C* -crystal phase sequence and one with just a smectic C* phase. The two concentrations are shown in figure 6.3, the 25% dye concentration with the phase sequence isotropic - 88°C –smectic C* - 40° - crystal and the 50% dye concentration with the phase sequence isotropic – 98°C – smectic A* - 78°C – smectic C* - 30°C - crystal. The effect of UV illumination on the transition temperature, spontaneous polarisation and tilt angle of both the samples was reversible as shown later.

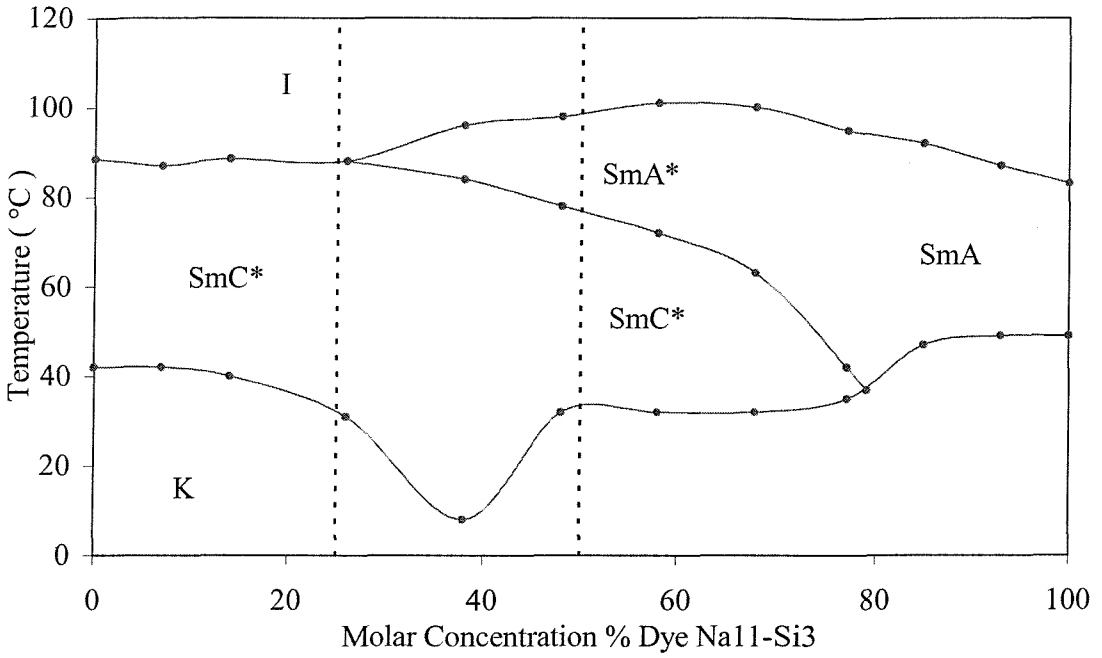

Figure 6.3 Phase diagram of NA11-Si3 dye addition against temperature showing the phase sequences of the two concentrations to be illuminated by ultra violet measured by optical microscopy.

6.3.2 25% NA11-Si3 Isotropic-Smectic C*-Crystal phase sequence

The isotropic to smectic C* transition temperatures of the 25% dye mixture have been measured by observing the transmitted optical intensity through crossed polarisers against temperature. These transition temperatures are reduced by increased intensity of ultra violet illumination as shown in figure 6.4. There is a linear relationship between the ultra violet intensity and the reduction in the transition temperature.

The magnitude of the spontaneous polarisation, measured by the current pulse technique, is isothermally decreased by ultra violet illumination as shown in figure 6.5. The maximum magnitude of the spontaneous polarisation decreases linearly with ultra violet intensity as shown in figure 6.6. The tilt angle could not be measured accurately for this sample as ultra violet illumination disturbed the aligned smectic C* texture so is not discussed here.

The optical micrographs shown in figure 6.7 show how the application of ultra violet illumination affects the focal conic texture of the material. Figure 6.7(a) shows the smectic C* texture of the sample before illumination at 60°C. Figure 6.7(b) shows the same sample area illuminated by 290 mW/cm^{2}of ultra violet. The birefringence has changed and a striped texture has appeared across the focal conic fans. A greater intensity of ultra violet illumination adds defects to the texture. For comparison, figure 6.7(c) shows the sample at 80°C without ultra violet illumination, with an equivalent lowered value of polarisation showing a similar birefringence. The change in birefringence indicates that the tilt of the system is changed leading to the change of spontaneous polarisation.

There is no optical evidence of any phase separation between the host and dye materials upon application of ultra violet illumination. A biphasic region only appears at lower values of polarisation corresponding to those at higher temperatures in the mixture before illumination. In both cases this is very close to the smectic C* to isotropic transition.

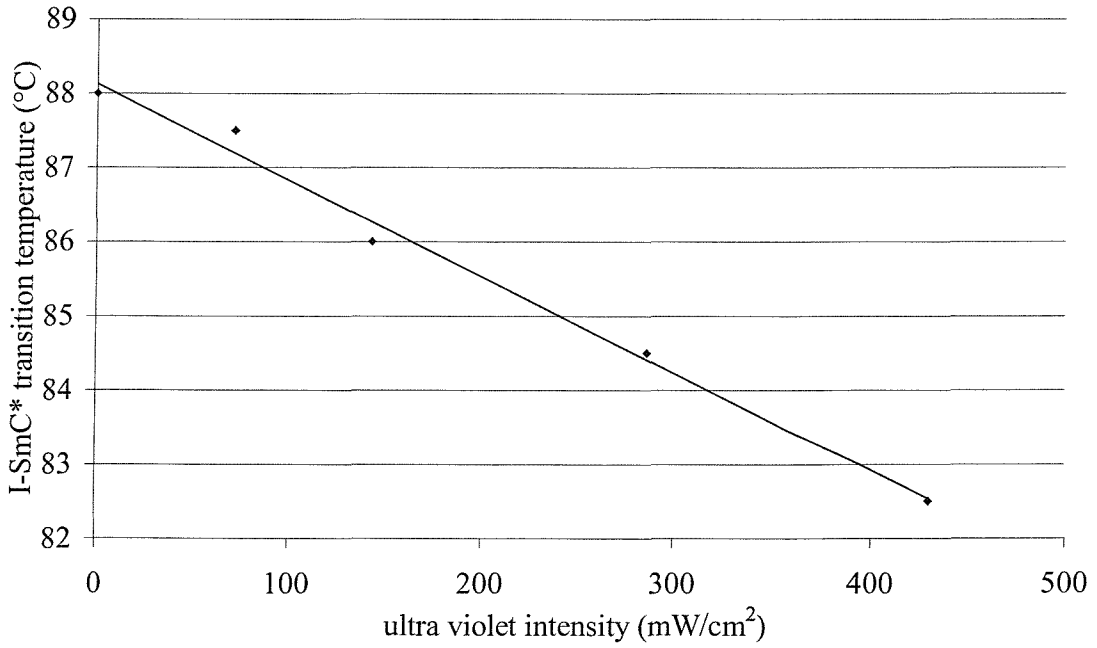

Figure 6.4 Isotropic to smectic C* transition temperature of the 25% mixture plotted against ultra violet intensity.

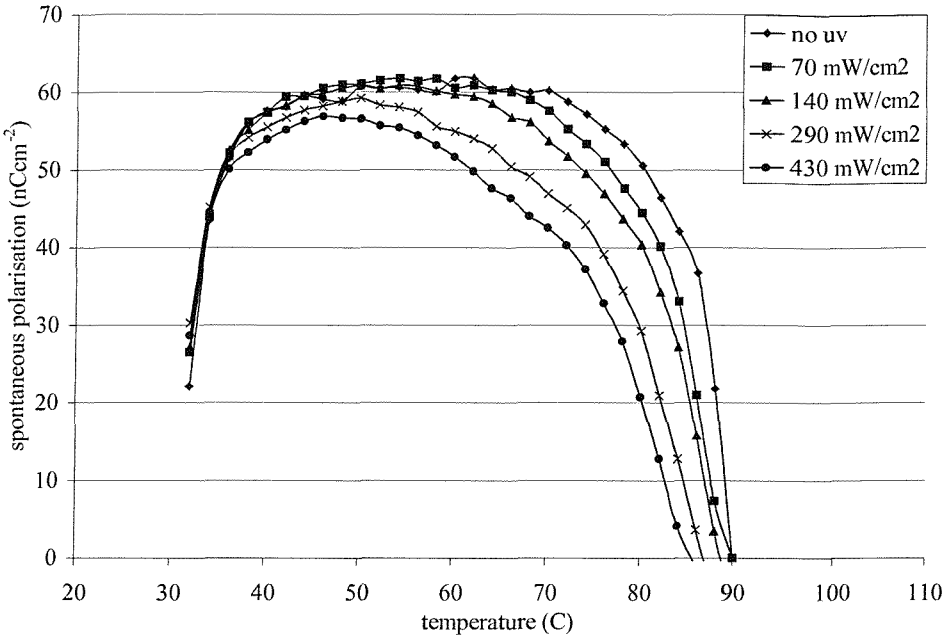

Figure 6.5 Spontaneous polarisation of the 25% sample against sample temperature for a range of ultra violet intensities.

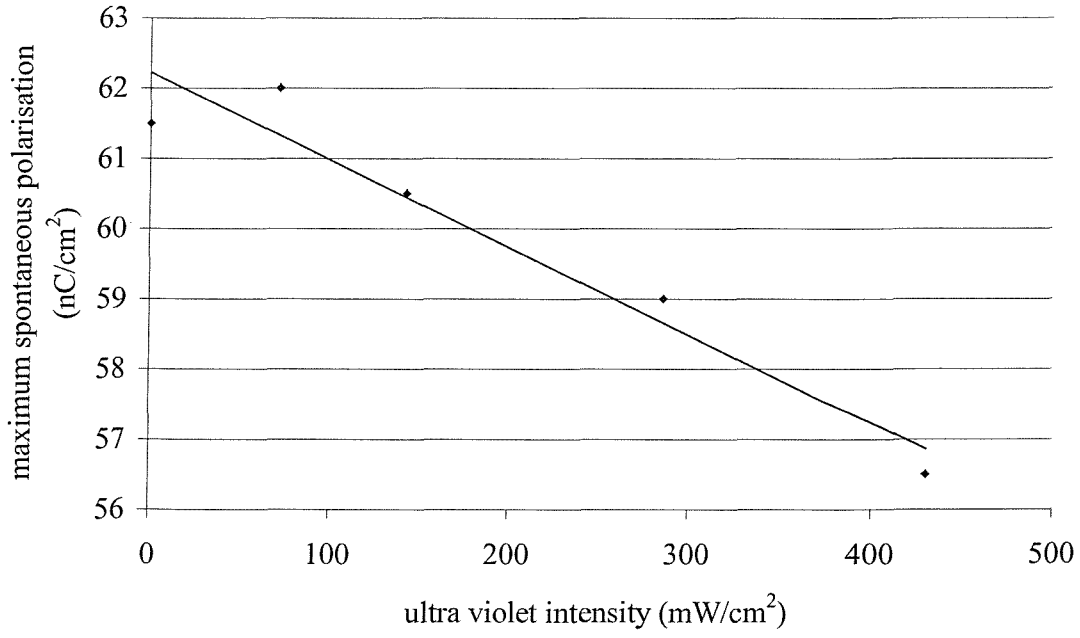

Figure 6.6 Maximum value of spontaneous polarisation plotted against ultra violet intensity for the 25% mixture.

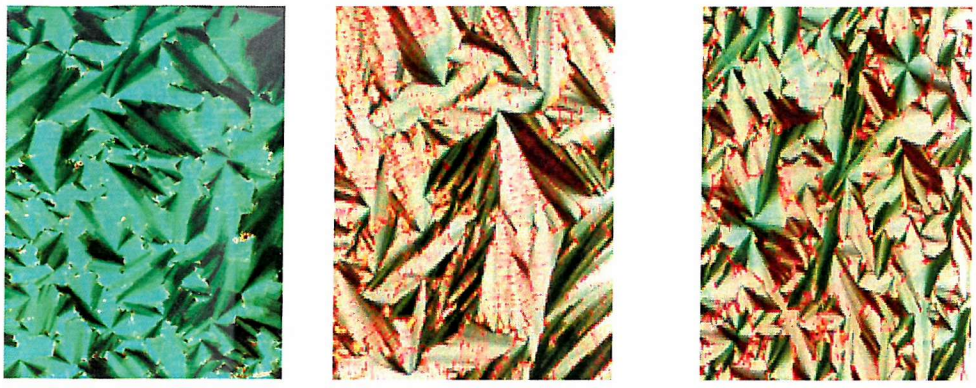

Figure 6.7 a) Smectic C* texture for no illumination at 60°C
b) 286 mW/cm^2 at 60°C c) no illumination at 80°C.

6.3.3 50% NA11-Si3 Isotropic-Smectic A*-Smectic C*-Crystal phase sequence

The isotropic to smectic A* and smectic A* to smectic C* transition temperatures of the 50% dye mixture were also measured by the change in transmitted intensity. The reduction in both these transition temperatures with ultra violet illumination is again linear with ultra violet intensity as shown in figure 6.8.

Both the spontaneous polarisation and the optical tilt angle tilt angle are reduced by ultra violet illumination as shown in figures 6.9 and 6.10. At lower temperatures away from the smectic A* transition the polarisation and tilt angle are almost unchanged by ultra violet illumination. For the lower ultra violet intensities 70 and 140 mW/cm^2 both the polarisation and the tilt angle reduce with a Curie Weiss like relationship with respect to temperature to zero. For the higher intensities of 290 and 430 mW/cm^2 the relationship between the tilt or polarisation and the temperature is different. There is a substantial reduction at temperatures between 45 and 55°C and then a gentle reduction to zero.

In order to demonstrate that the reduction in spontaneous polarisation is related to the primary order parameter, the tilt angle, and not, initially, due to microphase separation we consider the ratio of the spontaneous polarisation to the tilt. This ratio is consistent for all magnitudes of illumination as shown in figure 6.11.

From the sequence of textures and optical hysteresis loops, it is clear that the material is moving from a smectic C* phase to a smectic A* phase and that the electro-optic switching changes from ferroelectric to electroclinic. The optical micrographs and hysteresis loops of figure 6.12 show the changes in the 50% mixture upon UV illumination. The material changes from the smectic C* phase, figure 6.12(a), to a smectic C* phase with a striped appearance and a birefringence similar to that of the smectic A* material, figures 6.12(b) and 6.12(c). Upon further illumination this is transformed to the smectic A* phase, figure 6.12(d).

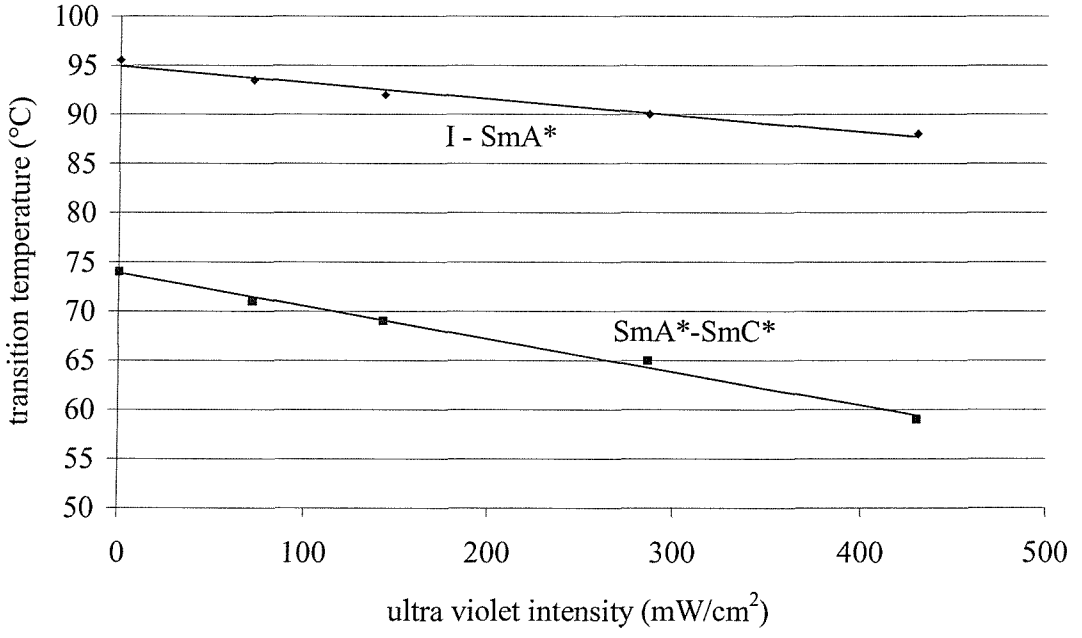

Figure 6.8 isotropic to smectic A* and smectic A* to smectic C* transition temperatures of the 50% mixture plotted against ultra violet intensity.

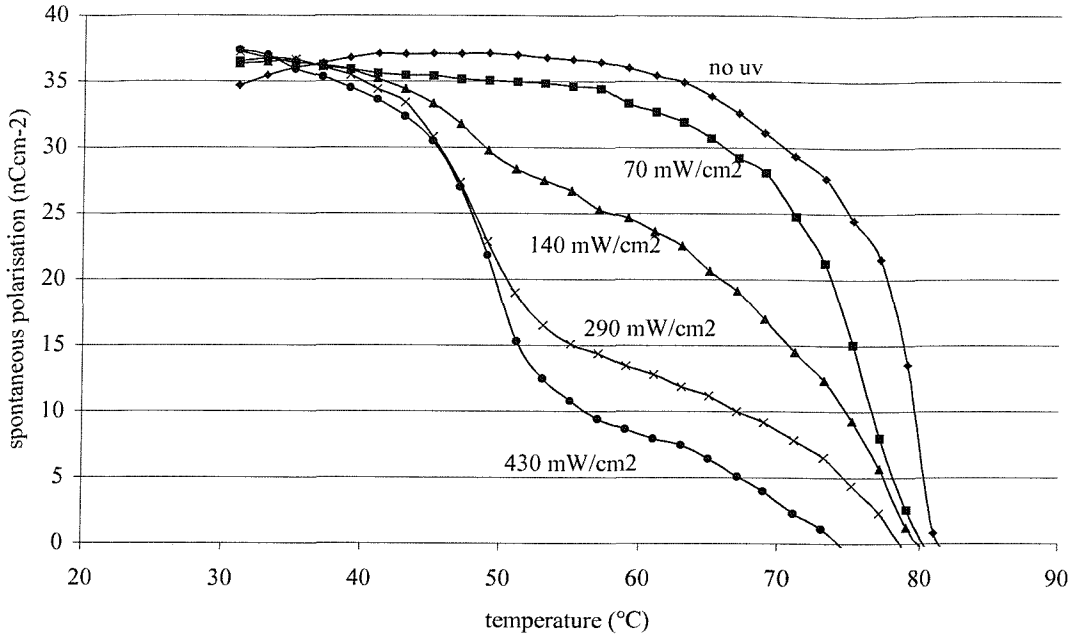

Figure 6.9 Spontaneous polarisation against temperature for the 50% mixture for a range of ultra violet intensities.

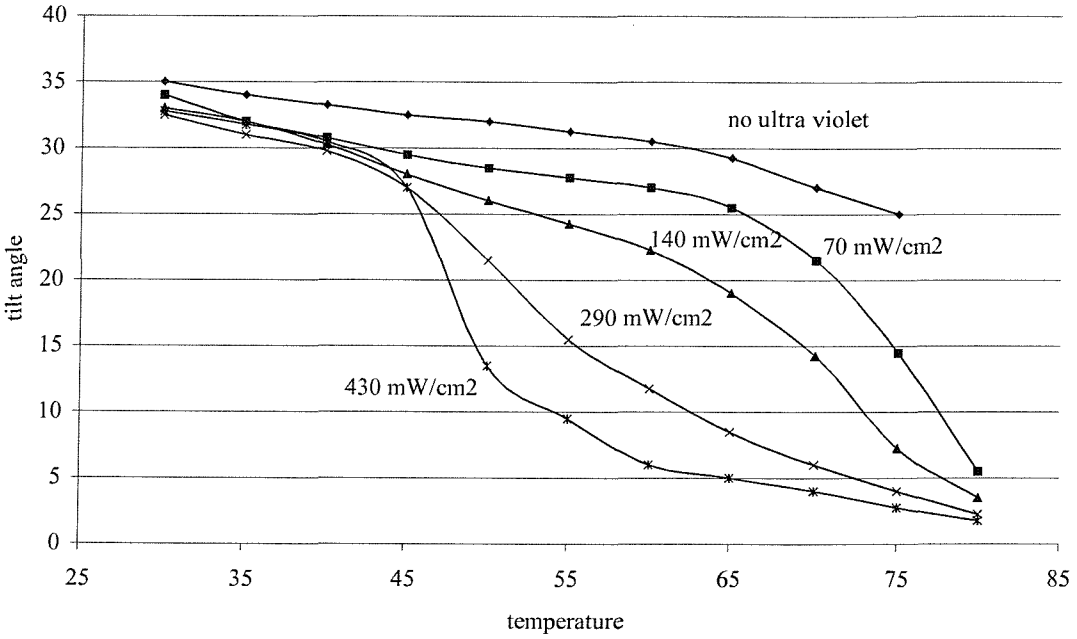

Figure 6.10 Tilt angle against temperature for the 50% mixture for the same range of ultra violet intensities.

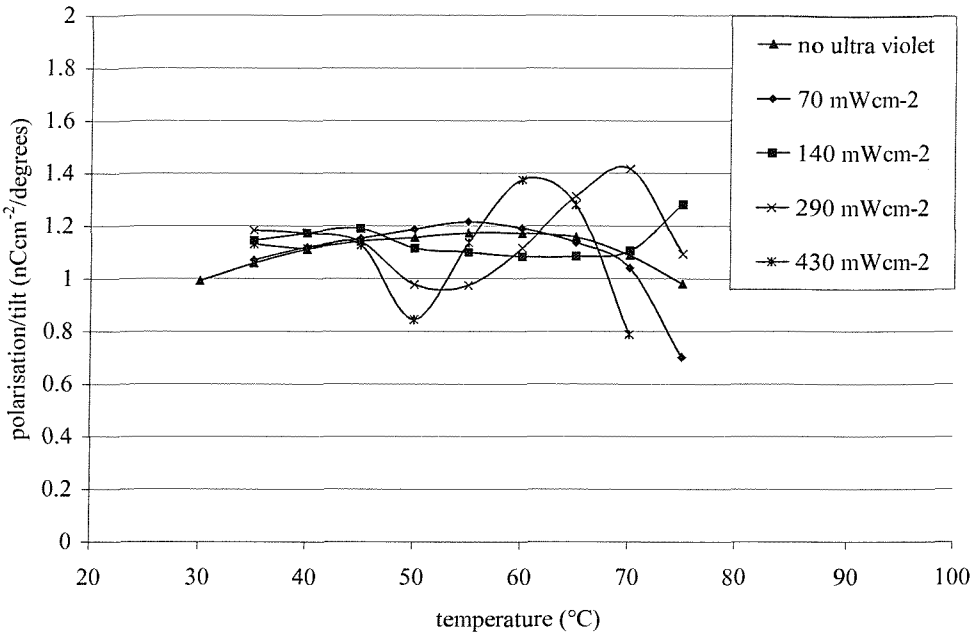

Figure 6.11 Ratio of polarisation to tilt against temperature for a range of ultra violet intensities.

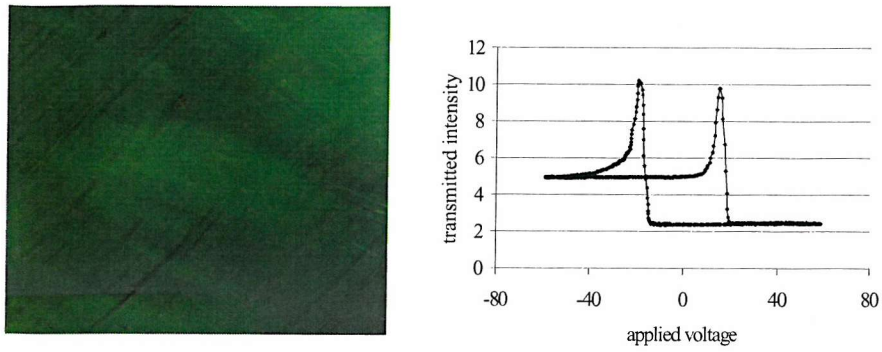

Figure 6.12 (a) Optical texture and hysteresis loop for no illumination at 35°C

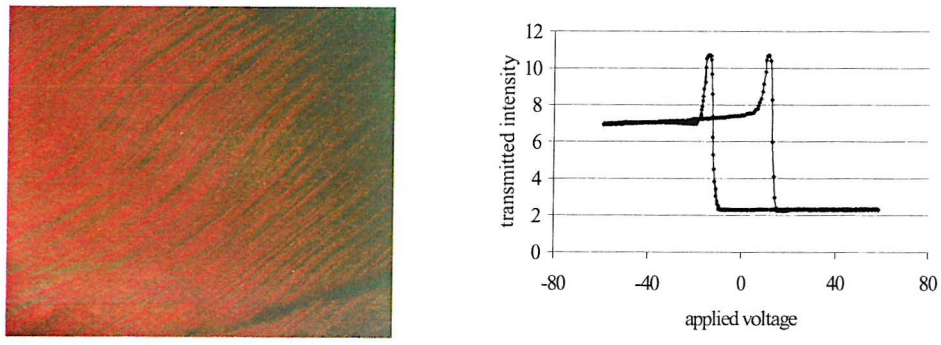

Figure 6.12 (b) Optical texture and hysteresis loop for 70 mW/cm^2 illumination at 45°C

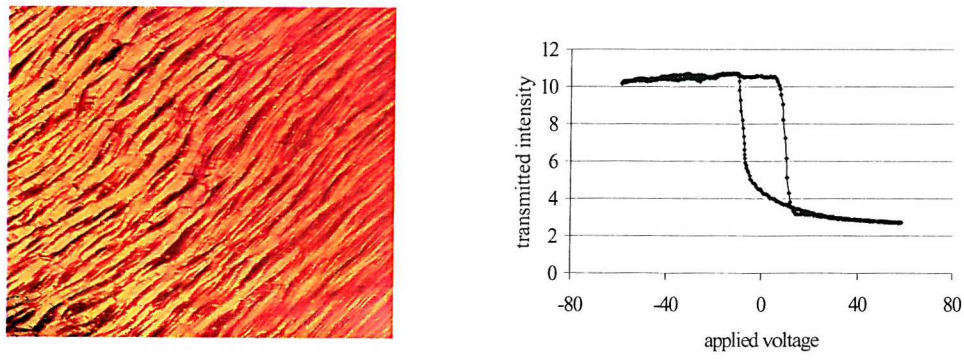

Figure 6.12 (c) Optical texture and hysteresis loop for 290 mW/cm^2 illumination at 50°C.

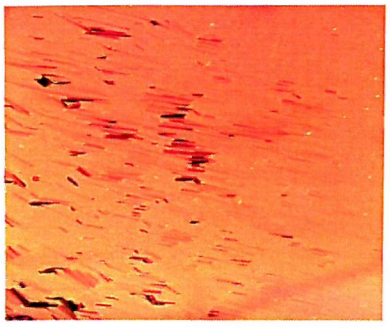

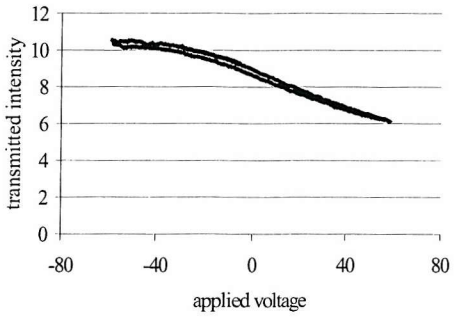

Figure 6.12 (d) Optical texture and hysteresis loop for 290 mW/cm^2 illumination at 70°C

6.3.4 Rate of response to ultra violet illumination

The change in the magnitude of the spontaneous polarisation was used to investigate the speed of the response of the mixtures to ultra violet illumination. Figure 6.13 shows that the change in spontaneous polarisation for the 25% mixture at 85°C and a range of ultra violet intensities is reversible. It was found for both mixtures that the rise and fall times of the polarisation were both close to 10 seconds at 85°C over a range of ultra violet intensities as shown in table 6.1, the rise time is slightly greater than the fall time

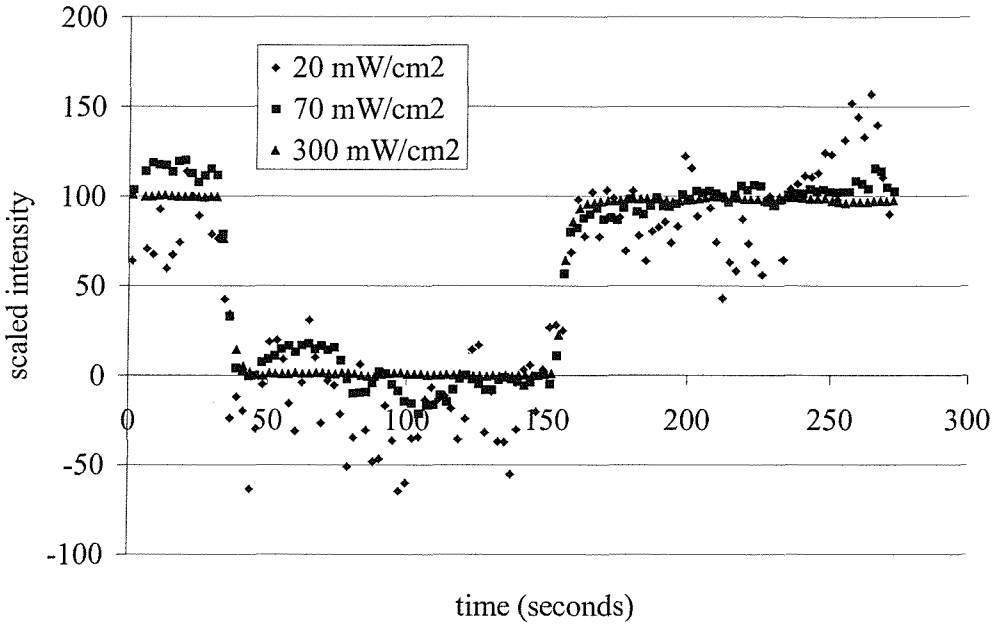

Figure 6.13 Scaled change in the spontaneous polarisation of Br11-Si3 and 25% NA11-Si3 due to ultra violet illumination.

NA11-Si3	Ultra violet	Intensity mW/cm^2	
Concentration	20	70	300
25% fall time (s)	5	7	12
25% rise time (s)	6	9	12
50% fall time (s)	2	12	10
50% rise time (s)	9	13	19

Table 6.1 The time taken for the spontaneous polarisation to fall to a steady value after illumination with ultra violet and rise back to the original value after ultra violet was removed.

6.4 Conclusion of Chapter Six

The complete miscibility of the dye and host materials including the same three-siloxane unit allowed a study to be made on a range of azo dye concentrations. The effect of ultra violet illumination on the transition temperatures, the spontaneous polarisation and tilt angle of both the samples was reversible but some degradation of the alignment was observed.

The 25% dye sample had a phase sequence isotropic-smectic C*-crystal. Illumination by ultra violet reduced the isotropic-smectic C* transition temperature linearly with ultra violet intensity. At a fixed temperature in the ferroelectric phase the spontaneous polarisation was reduced and the optical texture was modified. These changes indicate that the steric change in the dye molecules induces a change in the bulk host material.

The 50% dye mixture had the phase sequence isotropic-smectic A*-smectic C*-crystal with decreasing temperature. Both the isotropic-smectic A* and the smectic A*-smectic C* transition temperatures were reduced linearly with intensity of ultra violet illumination. The illumination of the sample by ultra violet reduced the magnitude of both the spontaneous polarisation and the tilt angle. The two variables are linked with respect to temperature. The microscopic textures and hysteresis loops show that illumination by ultra violet produces a phase maintaining the ferroelectric characteristics but with a change of birefringence. At higher ultra violet intensities the smectic C* phase was changed to the smectic A* phase with electroclinic rather than Goldstone switching. The reduction of the spontaneous polarisation and tilt angle and the isothermal phase change from the smectic C* to the isotropic are in good agreement with previous work[9,10,11,12]. These changes indicate that the change in shape of the dye molecules induces a change in the tilt, and subsequently the spontaneous polarisation and texture of the host material.

References for Chapter Six

[1] Photochromism, Ed. Brown, G.H., Wiley Interscience (1971)

[2] Sackman J. Am. Chem. Soc., **93**, 7088, (1971)

[3] Ikeda, T., Sasaki, T., Ichimura, K., Nature, **361,** 428-430 (1993)

[4] Walton, H.G., Coles, H.J., Guillon, D., Poeti, G., Liq. Cryst., **17(3)**, 333-349, (1994)

[5] Joly, G., Anakkar, A., Nguyen, H.T., Liq. Cryst., **26(8)**, 1251-1255, (1999)

[6] Shoosmith, D.E., Remnant, A., Perkins, S.P, , Coles, H.J., Ferroelectrics, **243(1-4),**75, (2000)

[7] Kloess, P., McComb, J., Coles, H.J., Ferroelectrics, **180**, 233, (1996)

[8] Robinson, W.K., Carboni, C., Kloess, P., Perkins, S.P., Coles, H.J., Liquid Crystals, **25(3)**, 301-307, (1998)

[9] Ikeda, T., Sasaki, T., Ichimura, K., Nature, **361,** 428-430 (1993)

[10] Walton, H.G., Coles, H.J., Guillon, D., Poeti, G., Liq. Cryst., **17(3)**, 333-349, (1994)

[11] Dinescu, L., Lemieux, R.P., Adv.Mater., **11(1)**, 42-45. (1999)

[12] Joly, G., Anakkar, A., Nguyen, H.T., Liq. Cryst., **26(8)**, 1251-1255, (1999)

Chapter 7

Effect of Photoisomerisation by Ultra Violet light on the Monomesogenic host and Bimesogenic Dye mixtures

Chapter 7

Effect of Photoisomerisation by Ultra Violet light on the Monomesogenic host and Bimesogenic Dye mixtures

7.1 Introduction

In this chapter the effect of ultra violet illumination on the mixtures of a ferroelectric host and a bimesogenic photoisomerising dye is examined and compared to that for the monomesogenic dye described in chapter six. It was shown in chapter five that the addition of the bimesogenic dye, NA11-Si3-11NA, to the organosiloxane ferroelectric host, Br11-Si3[1,2,3], produces both ferroelectric and antiferroelectric phases[4]. The miscibility of the organosiloxane host and dye allows a large range of dye concentrations to be examined. The effect of ultra violet illumination on both the ferroelectric and antiferroelectric phases has been investigated. A comparison has been made for the photoisomerisation of mixtures of the monomesogenic and bimesogenic dyes with similar transition temperatures and magnitudes of the spontaneous polarisation.

7.2 Photoisomerisation of pure dyes NA11-Si3 and NA11-Si3-11NA

Both the monomesogenic dye NA11-Si3 and the bimesogenic dye NA11-Si3-11NA have a smectic A phase. This smectic A phase exists at a much higher temperature for NA11-Si3-11NA. The transition temperatures, measured by optical microscopy, of the smectic A phase are reduced by ultra violet illumination for both mixtures. As shown in figure 7.1 there is a much smaller reduction for the bimesogenic NA11-Si3-11NA than for the monomesogenic dye.

Figure 7.2 shows the absorption spectra of a sample of NA11-Si3-11NA dissolved in DCM. The dye produced very similar spectra to that of NA11-Si3 shown in figure 6.1 and is shown to absorb ultra violet in the wavelength range of 350 to 450 nm at which the trans to cis isomerisation of azobenzene occurs[5].

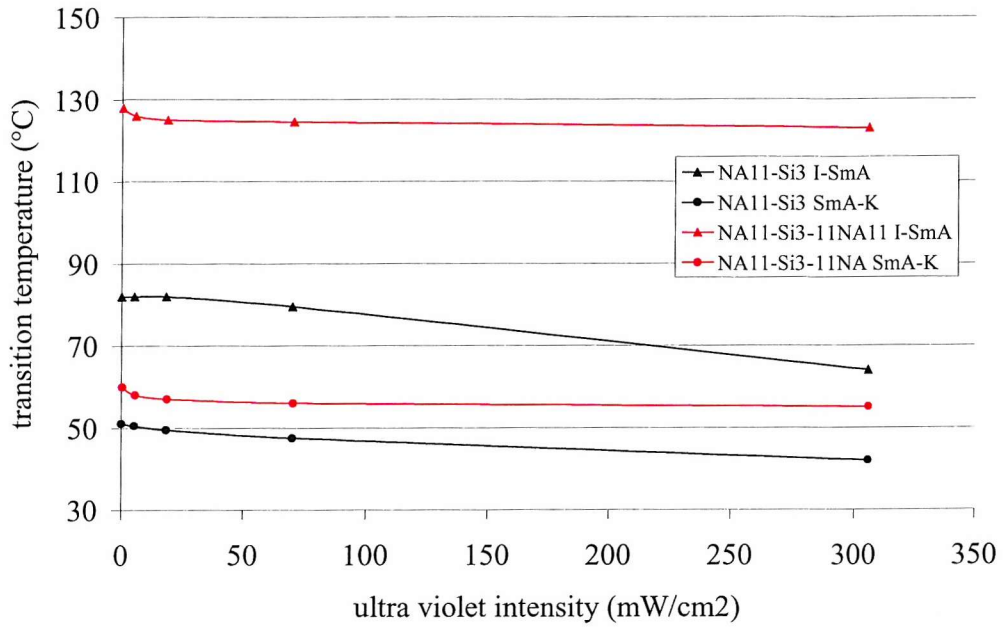

Figure 7.1 Reduction of isotropic to smectic A and smectic A to crystal transition temperatures for the monomesogenic NA11-Si3 and the bimesogenic NA11-Si3-11NA measured by optical microscopy.

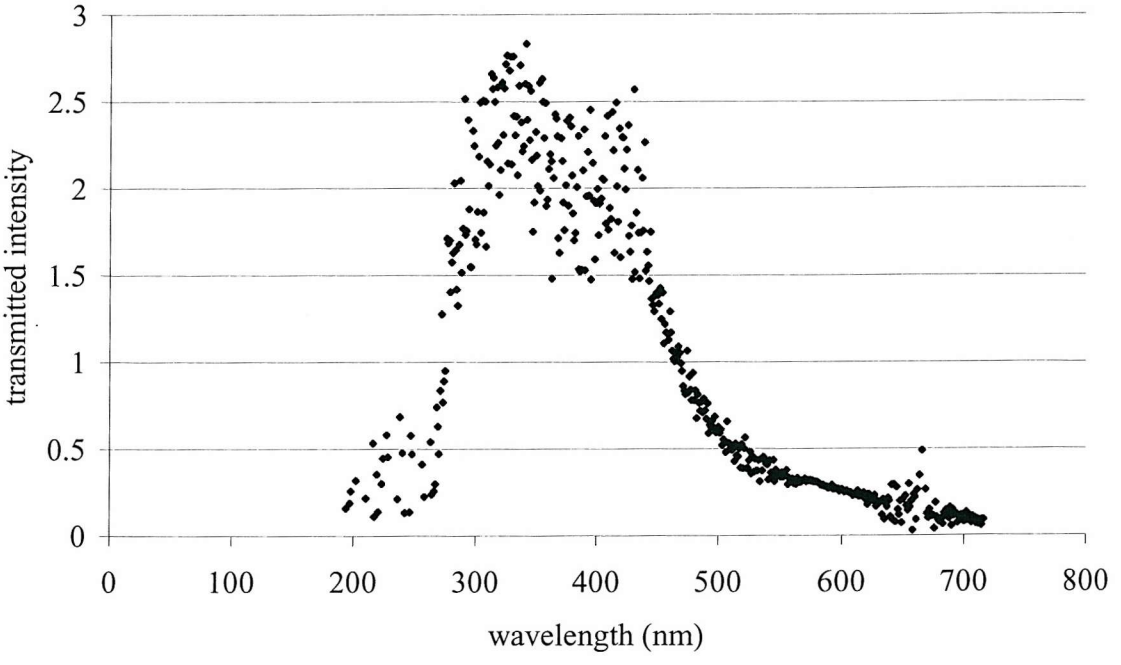

Figure 7.2 Absorption spectra of NA11-Si3 and NA11-Si3-11NA dissolved in DCM.

7.3 Effect of Ultra Violet illumination on Bimesogen Mixtures

The samples used for comparison were made by heating the weighed mixtures to above both component's isotopic transition temperatures for up to 12 hours. Cells of 5μm thickness with anti-parallel rubbed polyimide alignment layers were used for all the observations and measurements described in this chapter. The effect of ultra violet illumination on the Br11-Si3 and NA11-Si3-11NA mixtures was to reduce the isotropic to smectic C* transition temperatures as shown for the 4% and 8% mixtures in figures 7.6 and 7.7 respectively. The spontaneous polarisation, measured by the current pulse technique, was also reduced with ultra violet illumination while maintaining the temperature independence of the host as shown in figure 7.3 for 4% NA11-Si3-11NA.

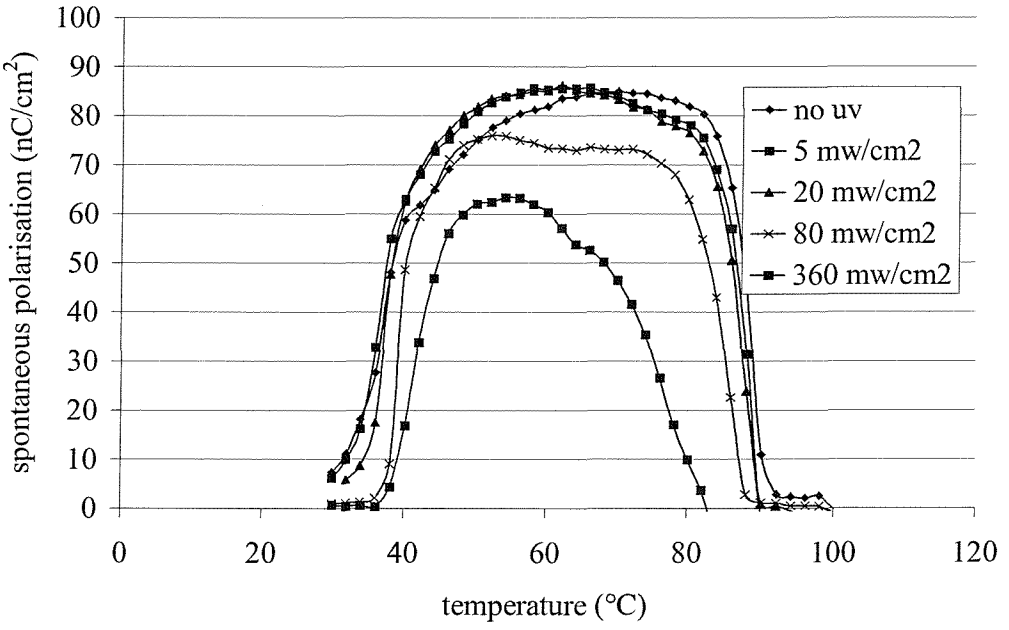

Figure 7.3 Spontaneous polarisation against temperature for the 4% NA11-Si3-11NA mixture with ultra violet illumination

7.4 Comparison of NA11-Si3-11NA with NA11-Si3 mixtures

7.4.1 Choice of mixtures

Figure 7.4 compares the phase diagrams of the monomesogenic and bimesogenic dyes. It can be seen that for dye concentrations up to about 25% the transition temperatures for the two dyes are of a similar magnitude. After the smectic A phase forms the transition temperatures rise more for the bimesogenic dye than the monomesogenic homologue. Consequently mixtures with concentrations below those where a smectic A phase appears will be considered for comparison. Figure 7.5 shows a comparison of the maximum value of the spontaneous polarisation for the two sets of mixtures. It was decided to make two sets of comparison between the mixtures having 7% NA11-Si3 and 4% NA11-Si3-11NA and 15% NA11-Si3 to 8% NA11-Si3-11NA. For each comparison the concentration of monomesogenic dye is approximately double that of the bimesogenic dye. This results in an equivalent number of NA11 mesogens.

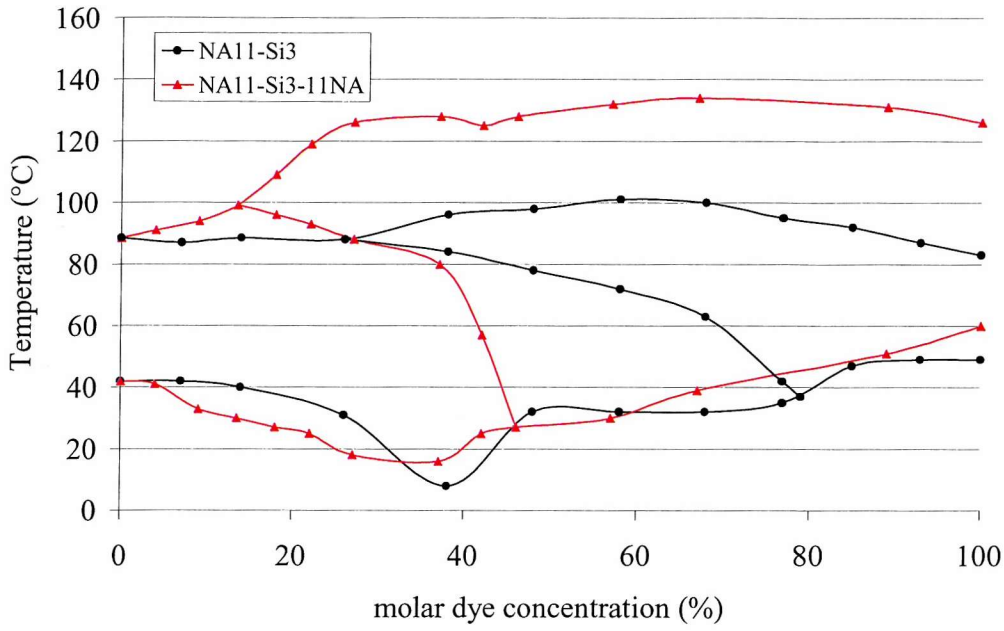

Figure 7.4 Comparison of phase diagrams against temperature of NA11-Si3 and NA11-Si3-11NA, transition temperatures measured by optical microscopy.

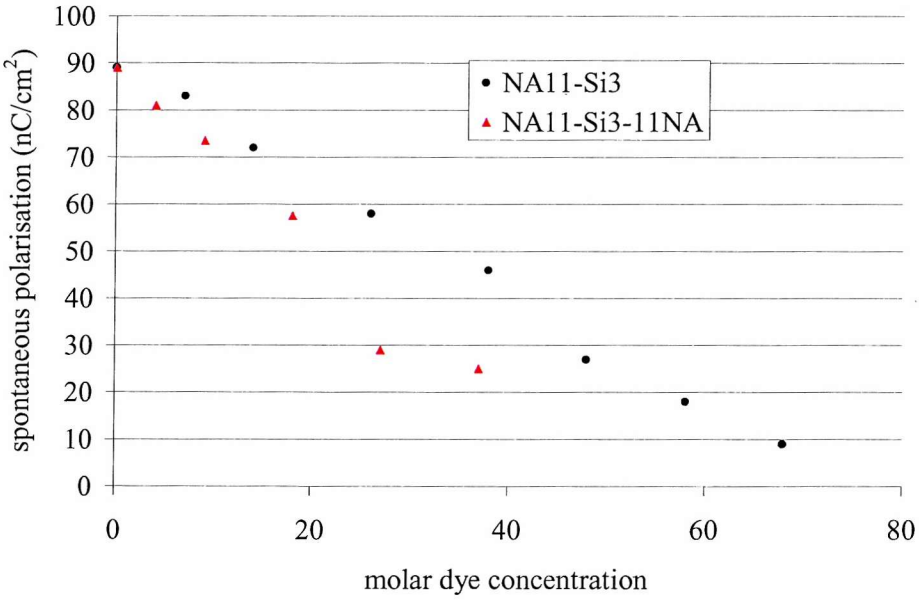

Figure 7.5 Comparison of the maximum value of the spontaneous polarisation against molar dye concentration for NA11-Si3-11NA

7.4.2 Change in Transition temperatures

The isotropic to smectic C* transition temperatures were measured against ultra violet intensity for both the NA11-Si3 and NA11-Si3-11NA mixtures. As shown in figure 7.6 the reduction in the transition temperatures was very similar for both the 4% mixtures of NA11-Si3 and 7% mixture of NA11-Si3-11NA. However the reduction for the 8 % NA11-Si3-11NA was much greater than the 15% NA11-Si3 mixture as shown in figure 7.7.

7.4.3 Change in Spontaneous Polarisation

The reduction in the spontaneous polarisation was measured for both the NA11-Si3 and the NA11-Si3-11NA mixtures and is shown in figures 7.8 and 7.9. The changes were measured 10°C below the isotropic to Smectic C* transition without ultra violet illumination. The reduction of the 7% NA11-Si3 and 4% NA11-Si3-11NA is very similar. However this does not hold for the comparison between 8% NA11-Si3-11NA and 15% NA11-Si3, the reduction for the bimesogenic dye is much greater.

7.4.4 Change in Rate of Change

The rate of change of the spontaneous polarisation was used to measure the effect of ultra violet illumination on the dyed mixtures. Table 7.1 lists the times for the fall of the spontaneous polarisation to a stable value after ultra violet illumination, and the rise time back to the original value after illumination was removed. Both the rise and fall times of the spontaneous polarisation are short, of the order of ten seconds. For all mixtures the time taken for the spontaneous polarisation to relax back to the original value was slightly longer than the fall time due to ultra violet illumination.

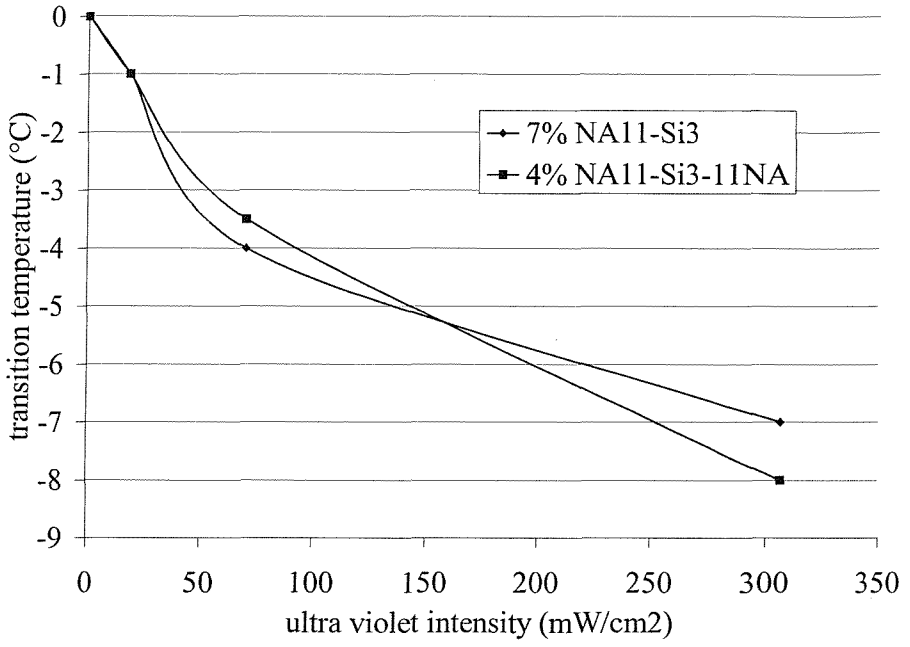

Figure 7.6 Reduction of the Isotropic to Smectic C* transition temperature against ultra violet intensity for 7% NA11-Si3 and 4% NA11-Si3-11NA.

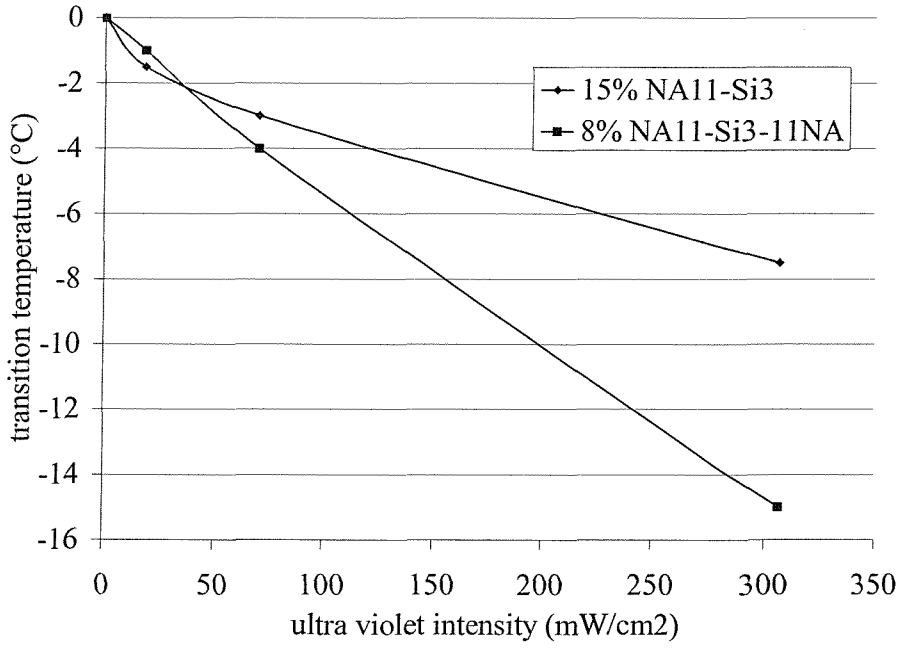

Figure 7.7 Reduction of the Isotropic to Smectic C* transition temperature against ultra violet intensity for 15% NA11-Si3 and 8% NA11-Si3-11NA.

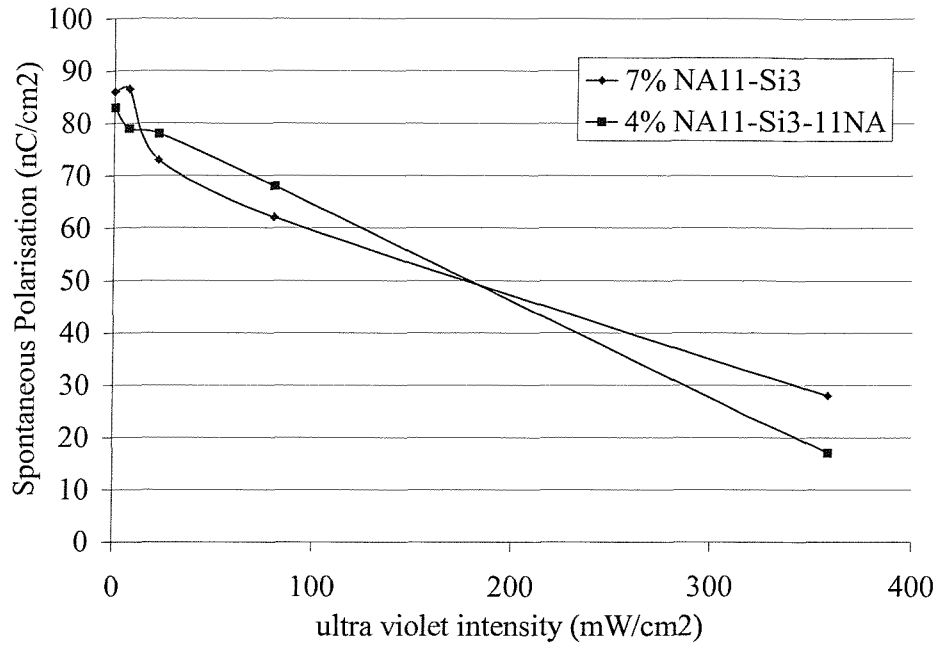

Figure 7.8 Change in the spontaneous polarisation for ultra violet illumination for 7% NA11-Si3 and 4% NA11-Si3-11.

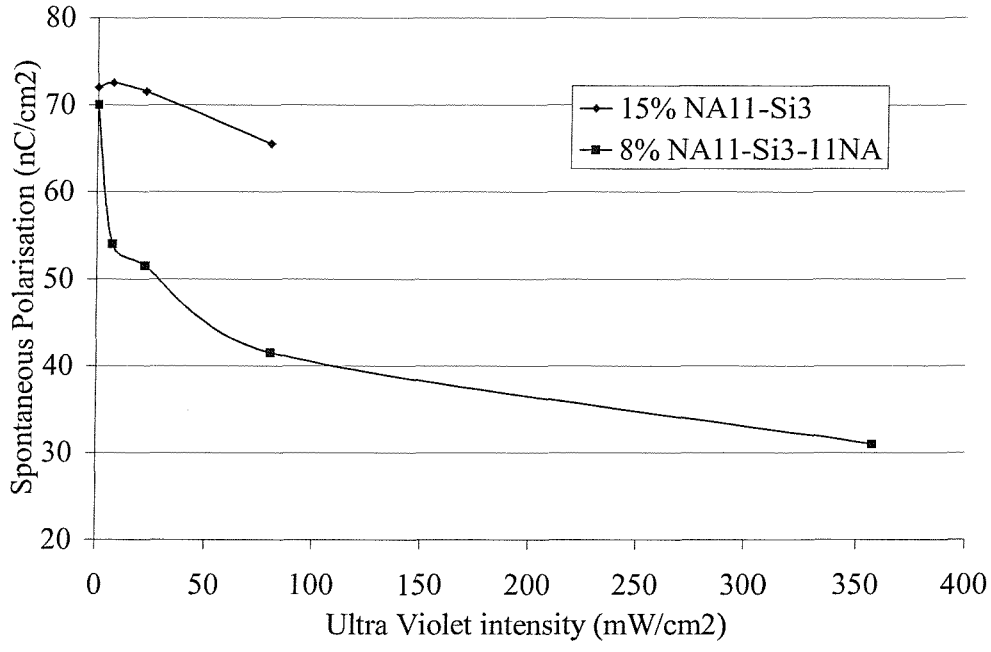

Figure 7.9 Change in the spontaneous polarisation for ultra violet illumination for 15% NA11-Si3 and 8% NA11-Si3-11.

Dye Concentration	Fall time (s)	Rise time (s)
5% NA11-Si3	5	10
5% NA11-Si3-11NA	8	12.5
10% NA11-Si3	10	12
10% NA11-Si3-11NA	8	10

Table 7.1 The time taken for the spontaneous polarisation to fall to a steady value after illumination with ultra violet and rise back to the original value after ultra violet was removed.

7.5 Effect of ultra violet on antiferroelectric phases

Figure 7.10 shows the hysteresis loops of transmitted intensity against applied voltage for the mixture of Br11-Si3 and 37% NA11-Si3-11NA. The hysteresis loop before ultra violet illumination is clearly antiferroelectric with a double hysteresis. As the intensity is increased the antiferroelectric switching is reduced and becomes electroclinic in nature showing that increased illumination transforms the antiferroelectric smectic C_A* phase to the electroclinic smectic A* phase.

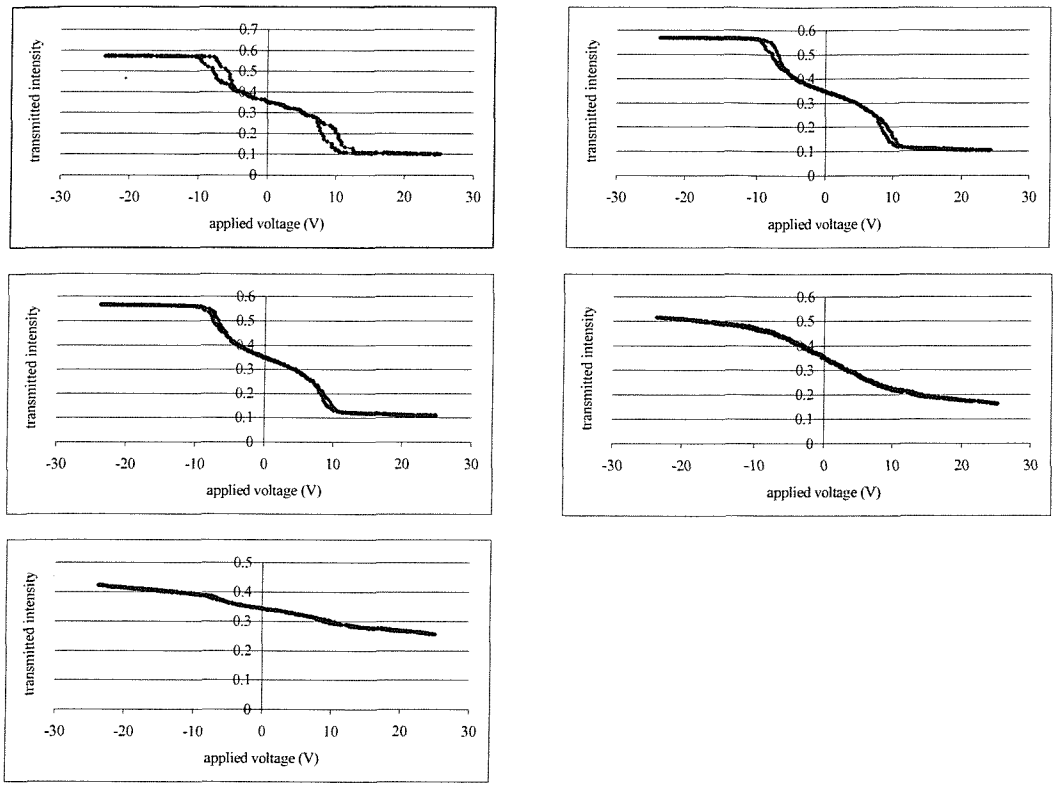

Figure 7.10 Hysteresis loops for the Br11-Si3 plus 37% NA11-Si3-11NA with (a) no ultra violet (b) 5 mW/cm^2 (c) 20 mW/cm^2 (d) 70 mW/cm^2 (e) 300 mW/cm^2 measured at 10 Vp-p/μm and 5Hz

7.6 Conclusion of Chapter Seven

The bimesogenic dye NA11-Si3-11NA has been shown to photoisomerise in the presence of ultra violet illumination by the reduction of the isotropic to smectic A and smectic A to crystal transition temperatures and by the absorption of ultra violet in the dark state. The effect of ultra violet illumination on the transition temperatures is smaller in magnitude than for the monomesogenic dye NA11-Si3. It can be hypothesised that the changes in transition temperatures are smaller because they occur at higher temperatures and the opposite thermal process[5] from bent cis to the straight trans isomer is increased because of the increased temperature.

It has been shown that the effect of illuminating the mixtures by ultra violet illumination is to isothermally reduce the order of the phase. The phase transition temperatures are reduced, the spontaneous polarisation and tilt angle are reduced. It has been shown that the tristable switching of the antiferroelectric phase is maintained until the illumination is large enough to induce a transition to the smectic A phase. The reductions in the spontaneous polarisation and tilt angle agree with previous experimental observations[6,7,8,9].

Mixtures of Br11-Si3 and the monomesogenic and bimesogenic nitro azo dyes have been compared with similar numbers of bimesogenic units. For the comparison between 7% NA11-Si3 and 4% NA11-Si3-11NA the reduction in spontaneous polarisation and the isotropic to smectic C* transition temperatures were of a similar order of magnitude against ultra violet illumination. However this relationship does not hold true for the larger dye concentrations of 15% NA11-Si3 and 8%NA11-Si3-11NA. The reduction of the isotropic to smectic C* transition temperatures and the spontaneous polarisation is larger for the bimesogenic than the monomesogenic dye. This shows that for smaller dye concentrations the photochromic changes were proportional to the number of nitroazo mesogens present. For the larger dye concentrations the properties of the bulkier bimesogen caused a greater reduction than the more miscible monomesogen.

References for Chapter 7

[1] Kloess, P., McComb, J., Coles, H.J., Ferroelectrics, **180**, 233, (1996)

[2] Robinson, W.K., Kloess, P.S., Carboni,C., Coles, H.J., Liquid Crystals, **23(2)**, 309-312, (1997)

[3] Robinson,W.K., Carboni, C., Kloess, P., Perkins, S.P., Coles, H.J., Liquid Crystals, **25(3)**, 301-307, (1998)

[4] Shoosmith, D.E., Remnant, A., Perkins, S.P, , Coles, H.J., Ferroelectrics, **243(1-4),**75, (2000)

[5] Photochromism, Ch 1, Ed. G.H.Brown, Wiley Interscience (1971)

[6] Ikeda, T., Sasaki, T., Ichimura, K., Nature, **361,** 428-430 (1993)

[7] Walton, H.G., Coles, H.J., Guillon, D., Poeti, G., Liq. Cryst., **17(3)**, 333-349, (1994)

[8] Dinescu, L., Lemieux, R.P., Adv.Mater., **11(1)**, 42-45. (1999)

[9] Joly, G., Anakkar, A., Nguyen, H.T., Liq. Cryst., **26(8)**, 1251-1255, (1999)

Chapter 8

A Photochromic dye added to a Bimesogen Chiral Nematic Flexoelectric Mixture

Chapter 8
A Photochromic dye added to a Bimesogen Chiral Nematic Flexoelectric Mixture

8.1 Introduction

In addition to the work on dye guest host organosiloxane materials and their photochromic properties, described in the preceding chapters, bimesogenic flexoelectric chiral nematic systems have been investigated. Bimesogen molecules for chiral nematic systems have been developed in house to optimise the flexoelectric coefficients and to investigate the relationship between the molecular structure and the flexoelectric properties[1,2]. Molecules have been designed to combine both a pear and a banana shape anisotropy, associated with the splay and bend deformations respectively as described in section 2.7. The miscibility of mixtures of bimesogen molecules and an azo dye with a similar structure will be investigated. The effect on the phase characteristics and flexoelectric properties of the mixtures due to a photoisomeric shape change of the dye caused by ultra violet illumination will also be studied.

8.2 Flexoelectric Chiral Nematic Bimesogen Mixtures

The bimesogen materials[1,2,3,4] that will be studied in this chapter have been developed in an attempt to combine pear and banana shapes to produce large flexoelectric coefficients. A pear shaped molecule contributes to the splay deformation, while a banana shaped molecule contributes to the bend deformation[5]. The chiral nematic molecules must have a strong electric dipole and an asymmetric shape to exhibit flexoelectric properties. To exhibit a large polarisation the material will ideally have a short pitch, a high elastic constant and a small but positive dielectric anisotropy[6,7]. Studies of the homologous series of these molecules have shown that small changes in the shape of the molecules can cause large changes in the flexoelectric properties. Hence the shape change of bimesogenic dyes caused by photoisomerisation will be investigated.

The bimesogens, α,ω-bis(2',4-difluorobiphenyl-4'-oxy)alkanes, to be used in this study were synthesised in house and are shown schematically in figure 8.1.[8] For this study a 50:50 by mass mixture of bimesogens with chain length 7 and 11 respectively was used. As the bimesogens are non-chiral the chiral agent BDH1281 has been added to produce a chiral nematic phase. Samples were made by heating the weighed mixtures, to above all the component's isotopic transition temperatures for up to 12 hours. Cells of 5μm thickness with anti-parallel rubbed polyimide alignment layers were used for all the observations and measurements described in this chapter.

The isotropic-chiral nematic transition temperature, measured by optical microscopy, of the mixture is 58°C. A chiral nematic to crystal transition has not been observed down to below –10°C. The uniformly lying helix texture can be easily produced by simple shearing of the sample just above the voltage required to stimulate the focal conic texture.

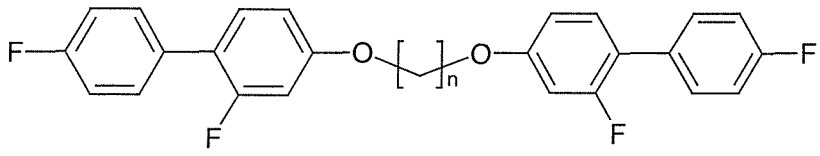

Figure 8.1 Schematic diagram of bi-mesogenic host molecule where n is the number of carbon atoms in the central chain

Figures 8.2 and 8.3 show that the optical tilt angle is linearly proportional to the applied electric field at a constant temperature and for a constant field the tilt angle is almost independent of temperature. There is a small increase in the tilt angle as the temperature is reduced. The pitch, measured as the maximum transmitted wavelength in the standing helix texture as explained in section 3.9, also increases slightly with decreasing temperature as shown in figure 8.4. The response time varies with temperature with an exponential Arrhenius relationship as shown in figures 8.5 and 8.6.

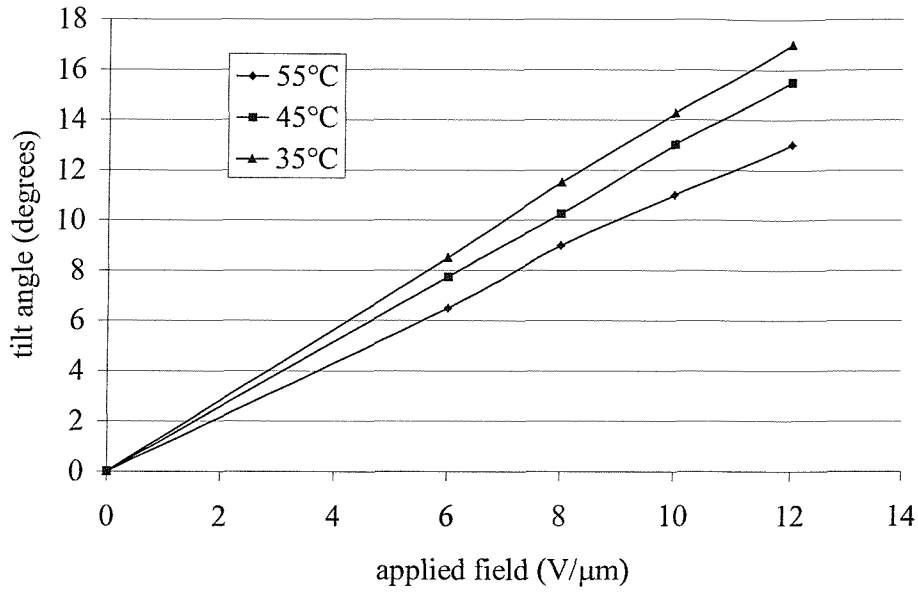

Figure 8.2 The linear relationship between the optical tilt angle and the applied field for the 7/11 bimesogen mixture measured at 20 Hz.

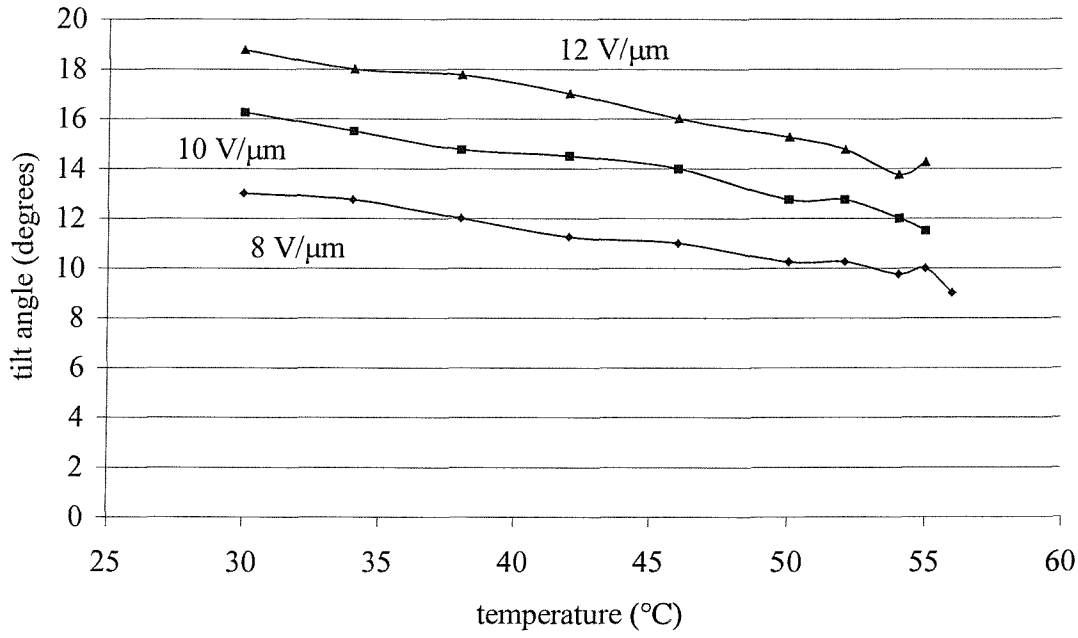

Figure 8.3 The relationship between the tilt angle of 7/11 bimesogen and the sample temperature

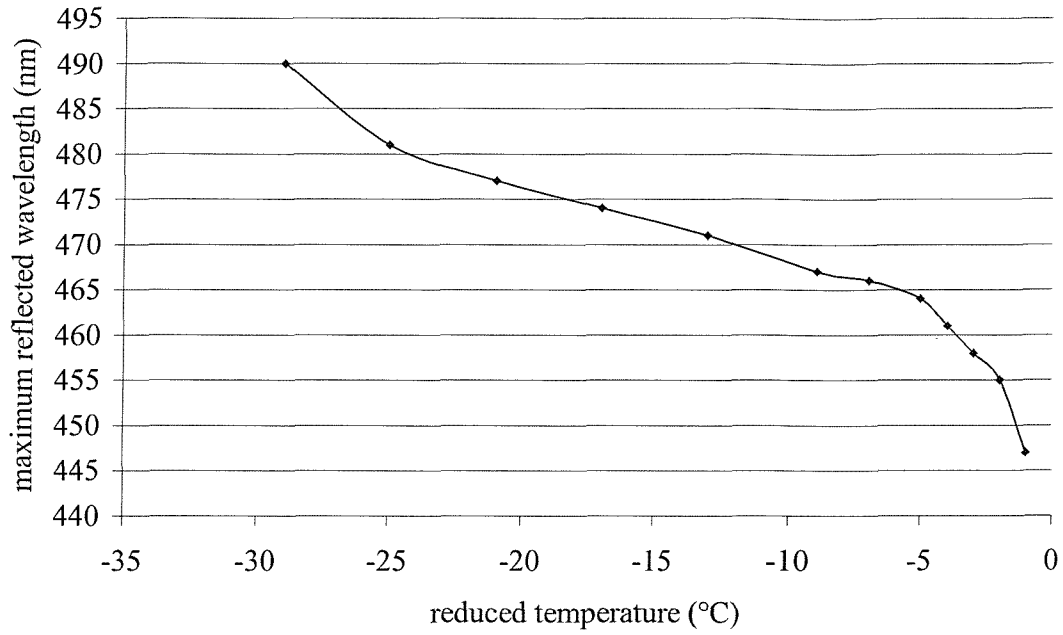

Figure 8.4 The pitch of the 7/11 bimesogen mixture plotted against sample temperature

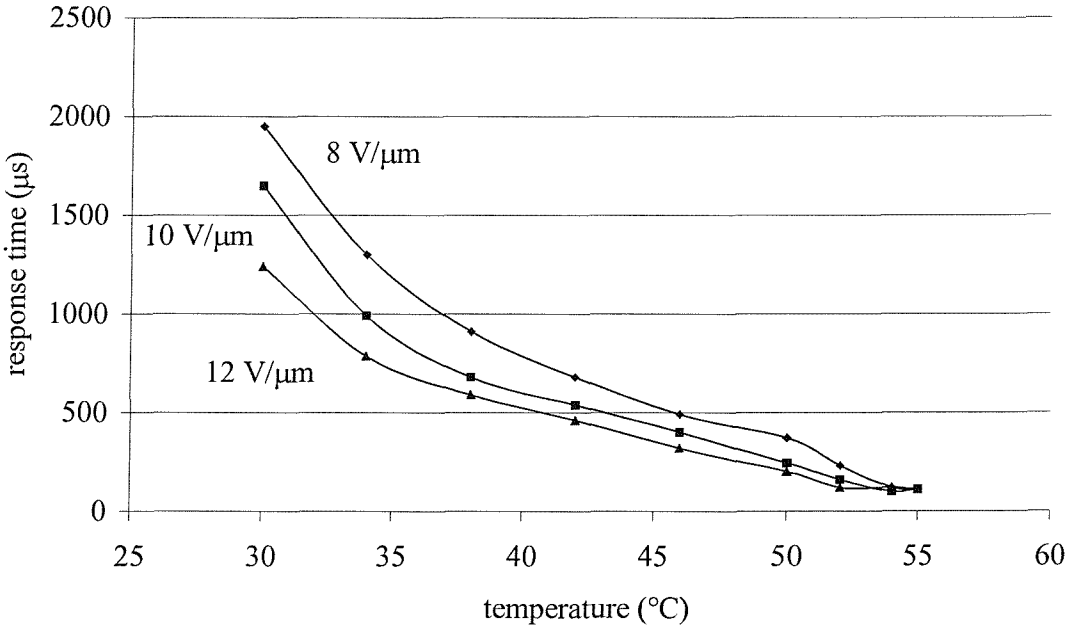

Figure 8.5 The relationship between the response time of the 7/11 bimesogen mixture and the sample temperature measured at a range of voltages and 20Hz.

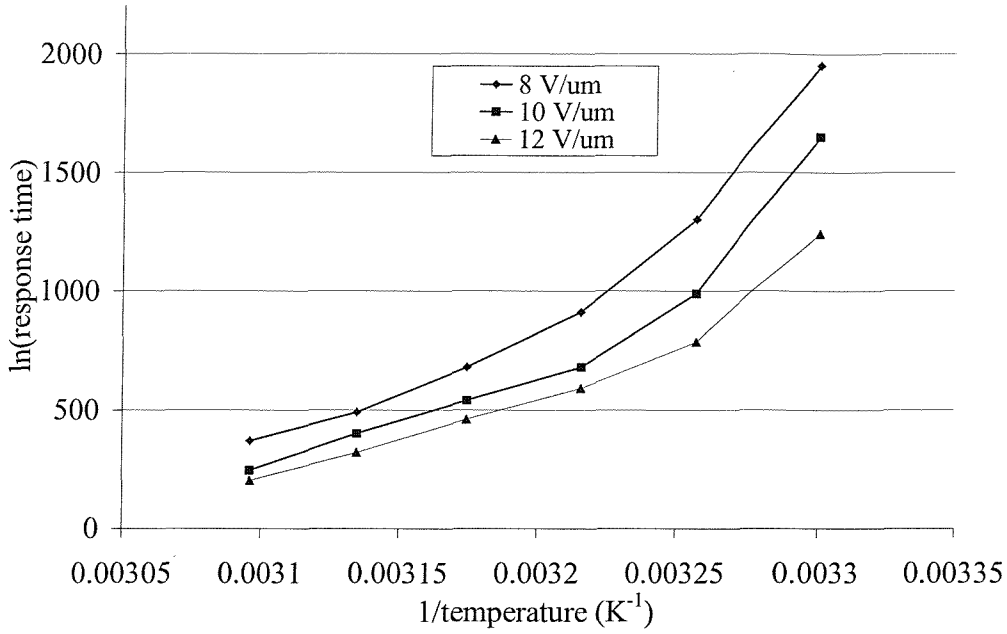

Figure 8.6 Linear relationship between the log of the response time and the inverse of the sample temperature measured at 20Hz.

8.3 Addition of Nitroazo bimesogenic dye to 7/11 mixture

A bimesogenic nitroazo dye has been designed and synthesised in house to have one mesogenic unit the same as the host material and the other unit containing a photoisomerising azo group. The dye, α-(2',4-difluorobiphenyl-4'-oxy)-α-(4-nitroazobenzene-4'-oxy)nonane, has a nematic phase and is denoted NA as shown in figure 8.8. The photoisomerising properties of this dye are illustrated by the reduction of phase transition temperatures measured by optical microscopy upon ultra violet illumination. The isotropic to nematic transition is reduced from 118 to 116°C and the nematic to crystal transition from 100 to 90°C for ultra violet illumination of 300 mW/cm^2. Figure 8.9 shows the absorption spectrum of the dye with a peak between 350 and 450 nm characteristic of the trans to cis isomerisation o f an azo molecule.

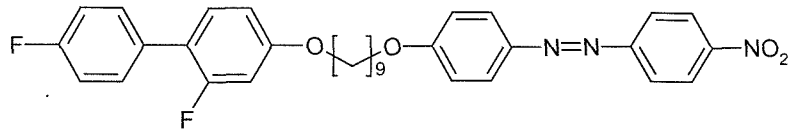

Isotropic – 118° - Nematic – 100° Crystal

Figure 8.8 Bimesogen dye, with one photoisomerising azo unit connected by a nine carbon chain to the same mesogen as the host material. Phase transition temperatures measured by optical microscopy.

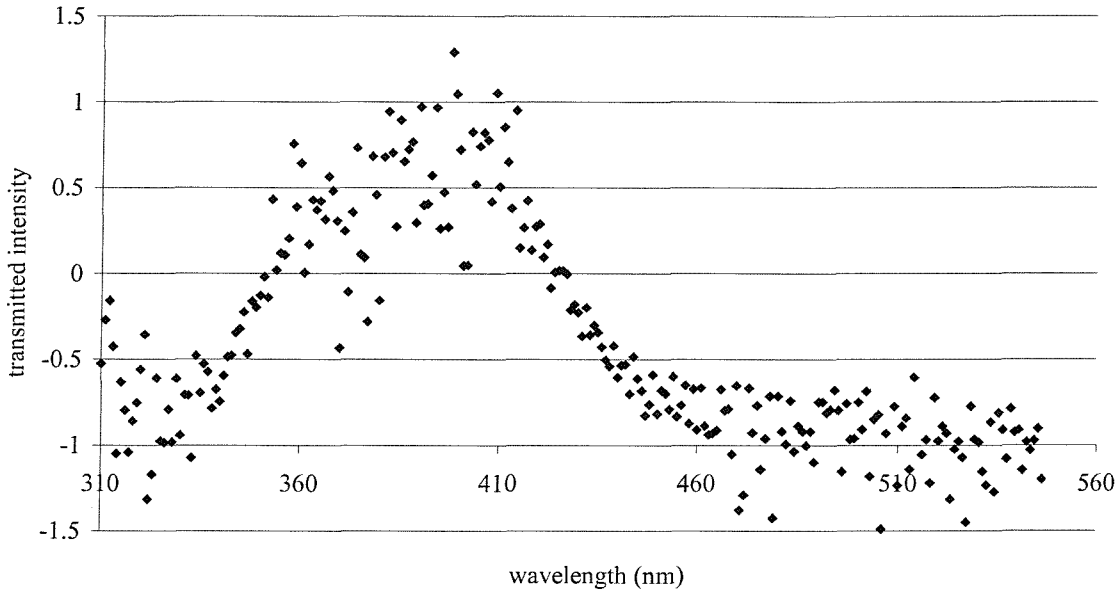

Figure 8.9 Absorption spectrum of NA bimesogen azo dye.

Mixtures have been made where this dye has been added in 5%, 10% and 20% concentrations by mass to the 7/11 bimesogen mixture. The addition of the dye has caused no significant changes to the flexoelectric properties of the mixtures. The isotropic to chiral nematic transition temperatures have not been significantly altered as shown in table 8.1. The pitch and tilt angles of the mixtures are slightly different, but that can be explained by the slightly different concentrations of the chiral agent.

Percentage dye concentration	I-N* transition temperature (°C)
0	58
5	59
10	61
20	61

Table 8.1 Transition temperatures of the mixtures of the 7/11 bimesogen host and NA bimesogen dye

8.4 Effect on mixtures of ultra violet illumination

As shown in figure 8.8 the isotropic to chiral nematic transition temperatures are reduced upon illumination with ultra violet. As the ultra violet intensity is increased the transition temperatures reach a threshold value. This threshold value decreases linearly with dye concentration as shown in figure 8.9.

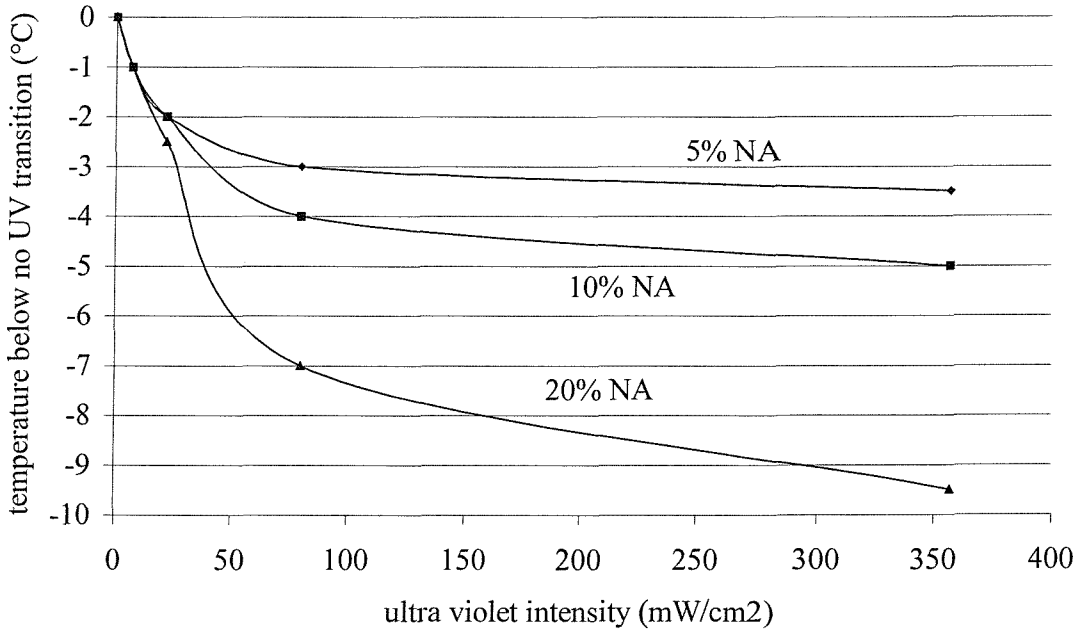

Figure 8.8 The isotropic to chiral nematic transition temperature for the three dye concentrations measured by optical microscopy plotted against the intensity of ultra violet illumination.

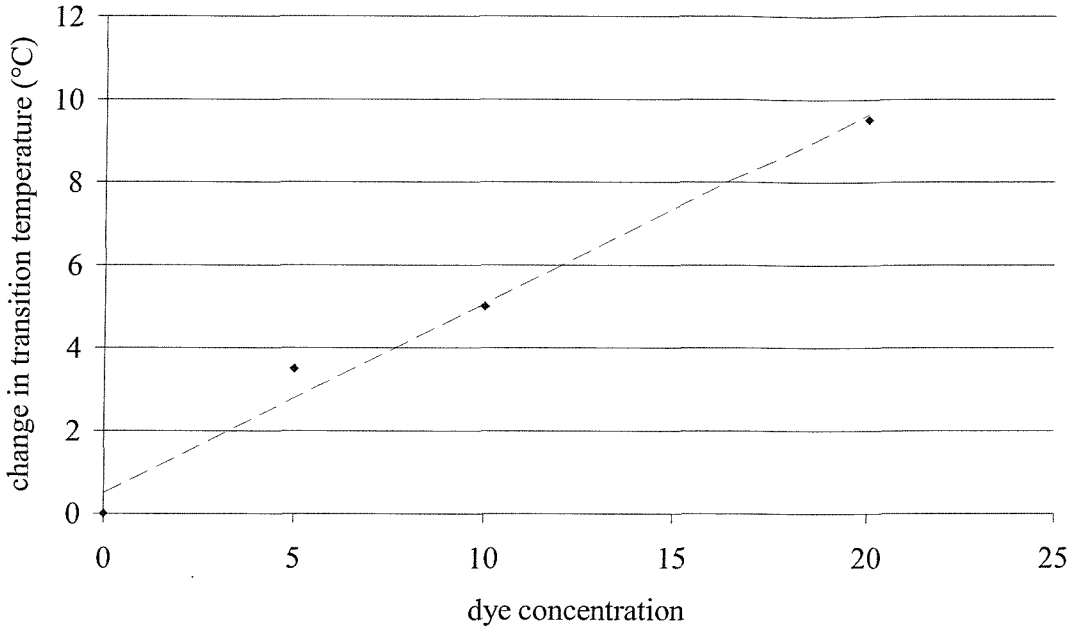

Figure 8.9 Reduction in transition temperature against the intensity of ultra violet illumination.

The tilt angle, the response time and the pitch of the 5%, 10% and 20% dye mixtures have been measured before and after ultra violet illumination. The measurements are plotted against sample temperature and against reduced temperature, which is dependent on the ultra violet intensity in figures 8.10 to 8.15.

For all three dye concentration no significant change in the tilt angle can be measured either at sample temperature, figure 8.10, or at reduced temperature, figure 8.11. The pitch is seen to decrease isothermally as shown in figure 8.12 plotted against sample temperature. When plotted against reduced temperature the pitch is unchanged, figure 8.13. The response time is unchanged at sample temperature as shown in figure 8.14. When plotted against reduced temperature, figure 8.15, the response time is seen to increase for increasing ultra violet intensity.

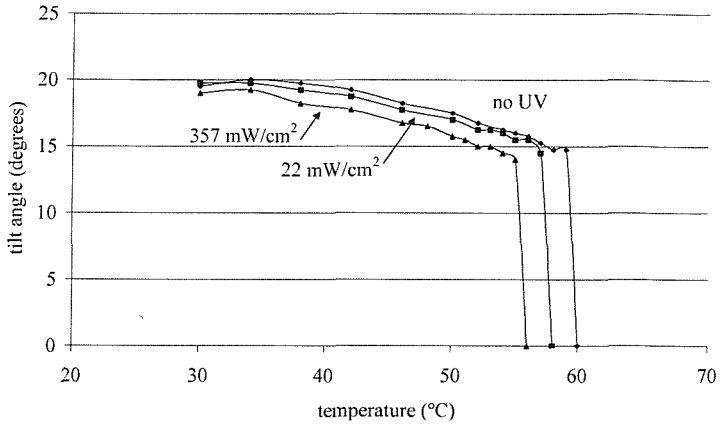

8.10(a)

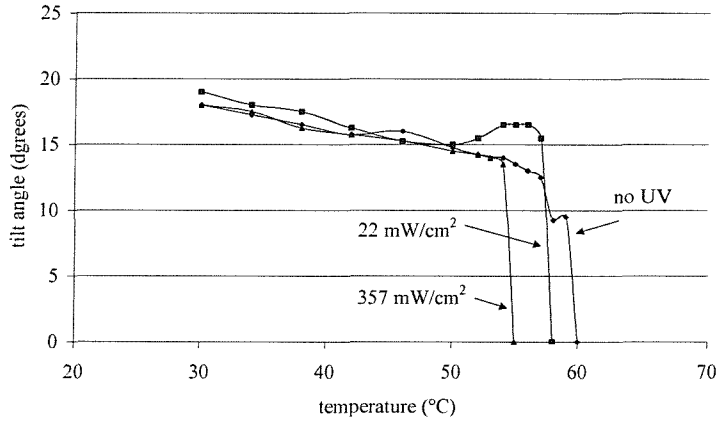

8.10(b)

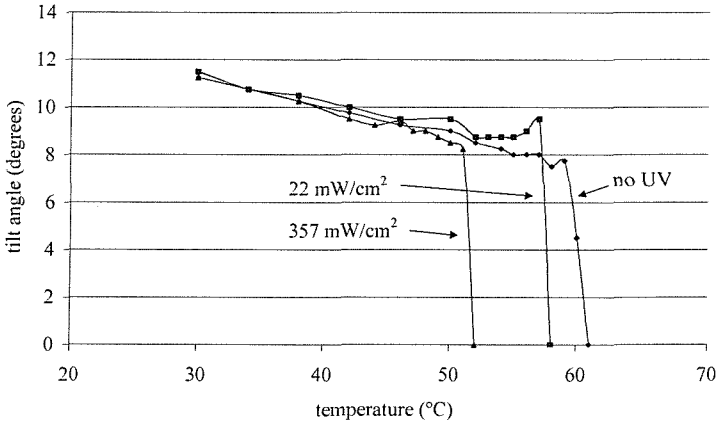

8.10(c)

Figure 8.10 Tilt angle against sample temperature(a)5%NA (b)10% NA (c) 20%NA measured at 20 Hz

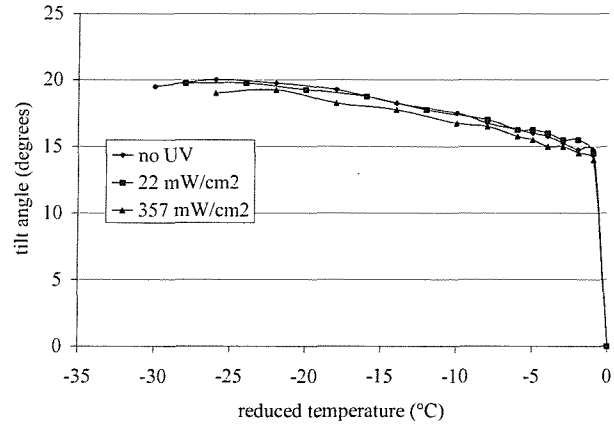

8.11(a) 5%

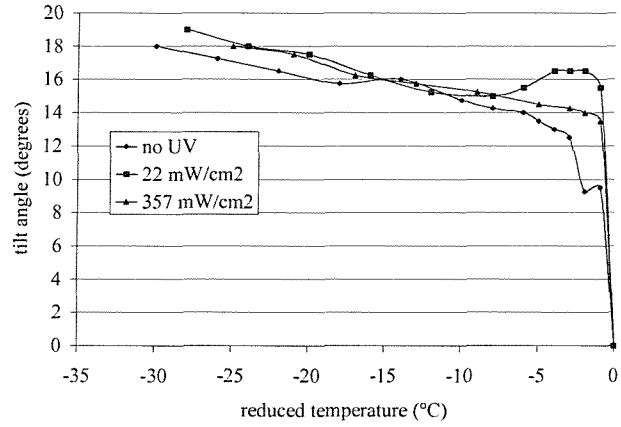

8.11(b) 10%

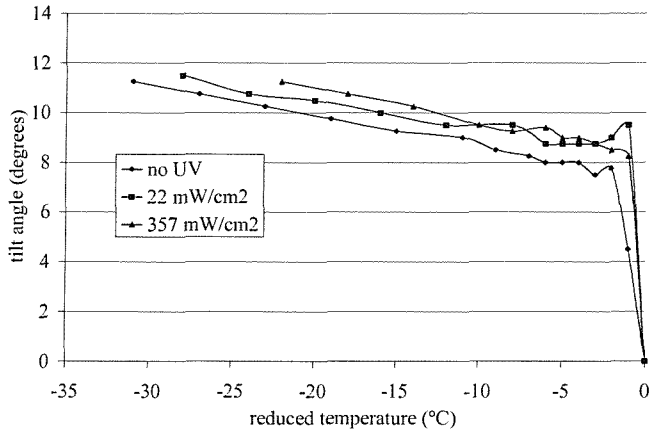

8.11 (c) 20%

Figure 8.11 Tilt angle against reduced temperature for (a) 5%NA (b)10% NA (c) 20%NA

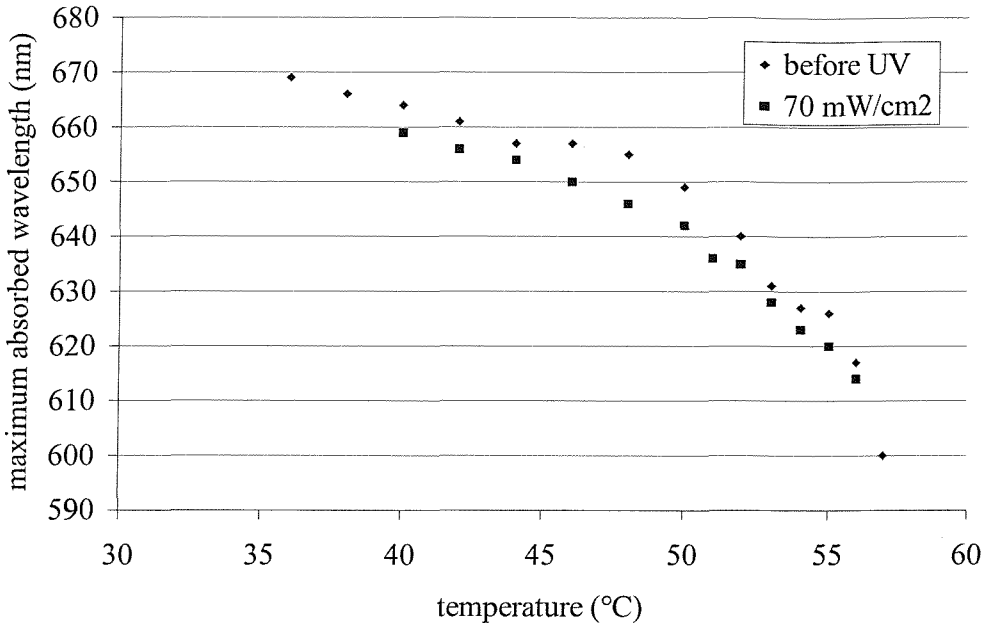

8.12 (a) 5%

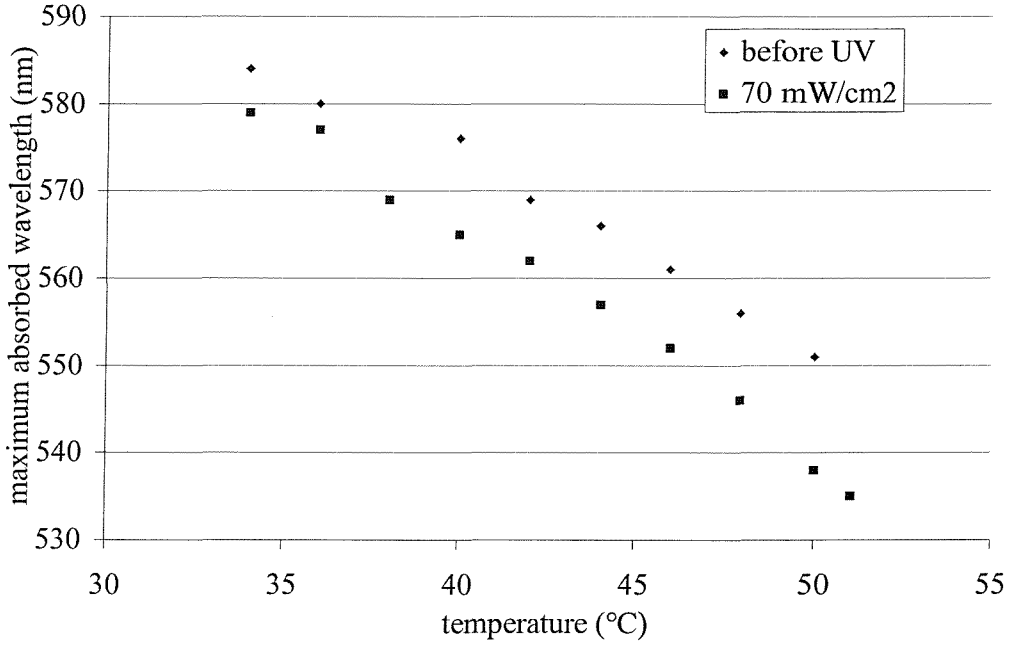

8.12 (b) 10%

Figure 8.12 Pitch measured as the maximum absorbed wavelength plotted against sample temperature for (a) 5%NA (b)10% NA

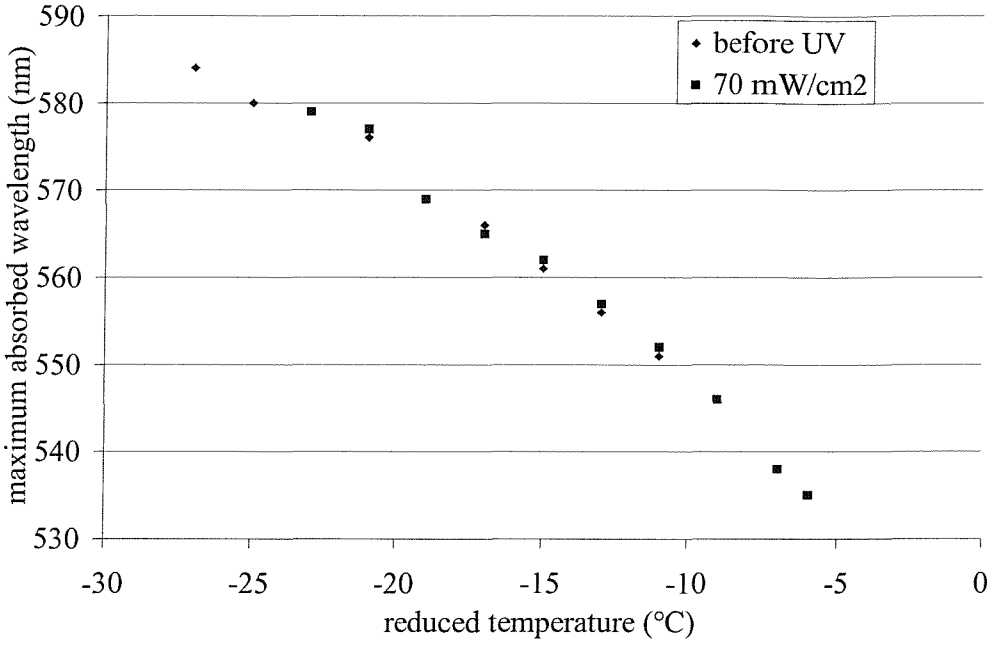

8.13 (a) 5%

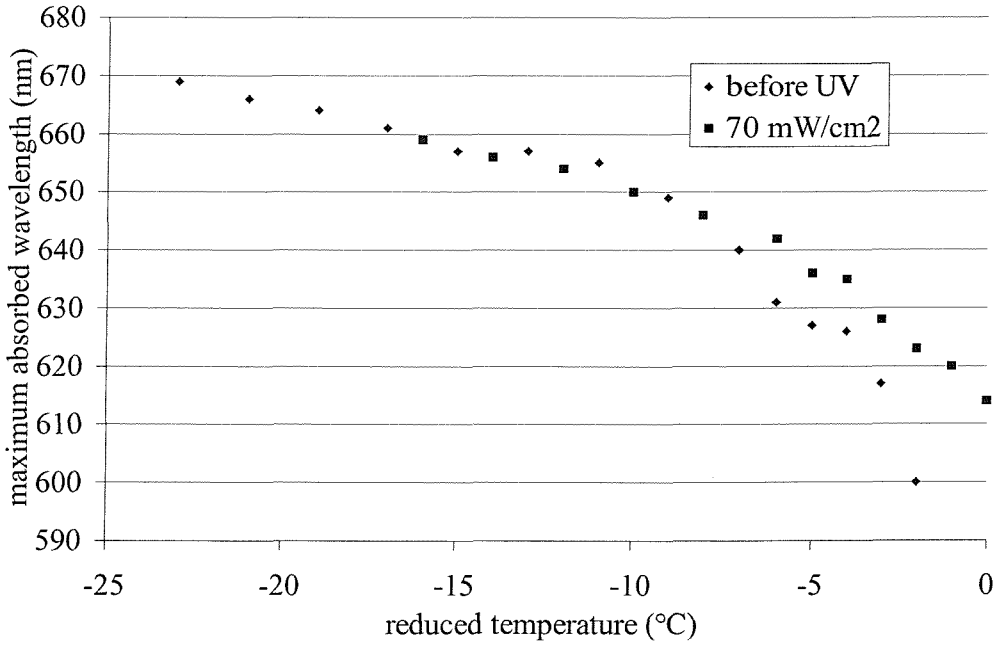

8.13 (b) 10%

Figure 8.13 Pitch measured as the maximum absorbed wavelength plotted against reduced temperature for (a) 5%NA (b)10% NA

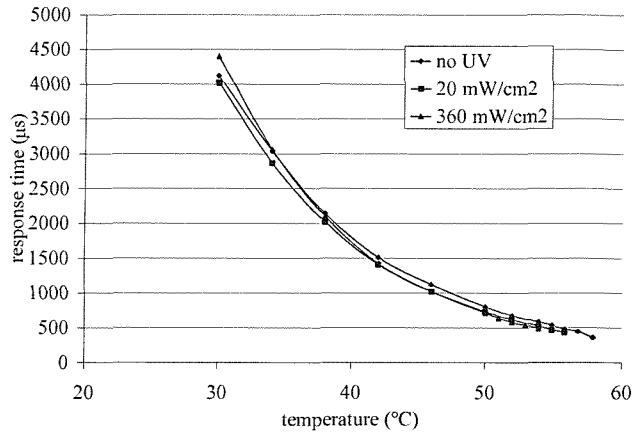

8.14 (a) 5%

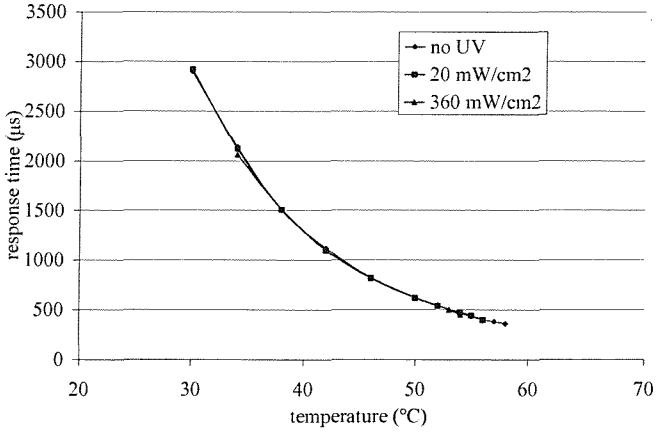

8.14 (b) 10%

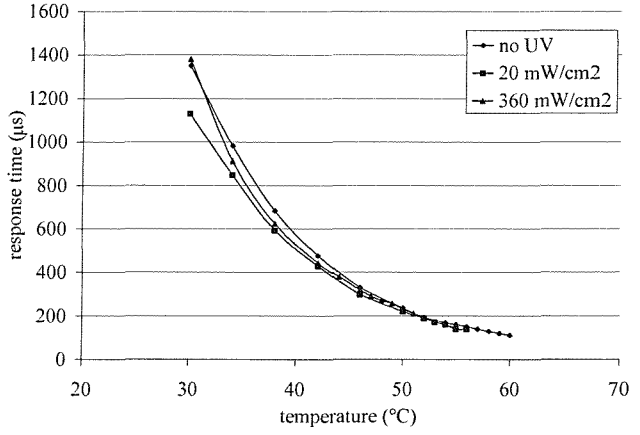

8.14 (c) 20%

Figure 8.14 Optical response time against sample temperature(a)5%NA (b)10% NA (c) 20%NA measured at 50 Hz.

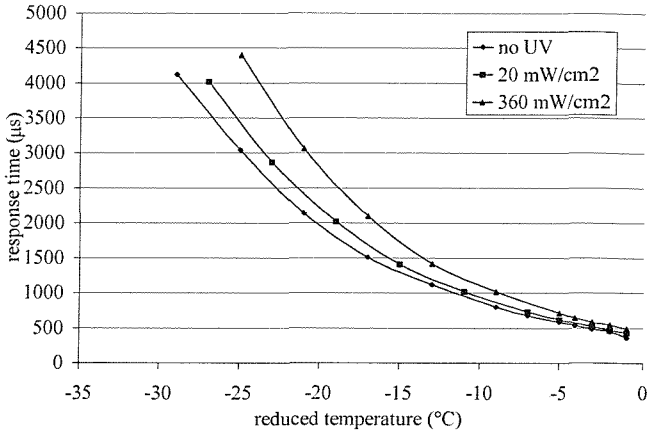

8.15 (a) 5%

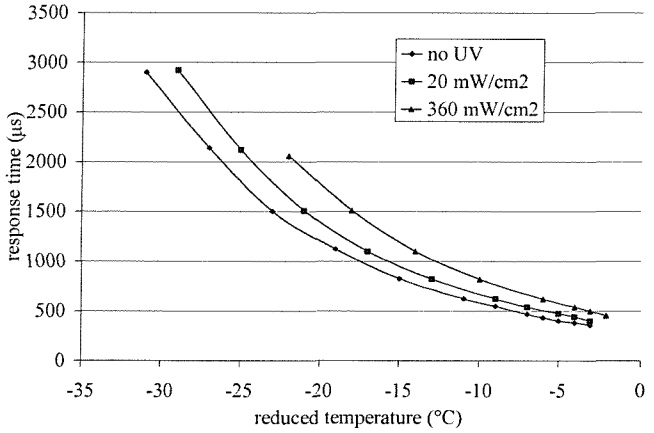

8.15 (b) 10%

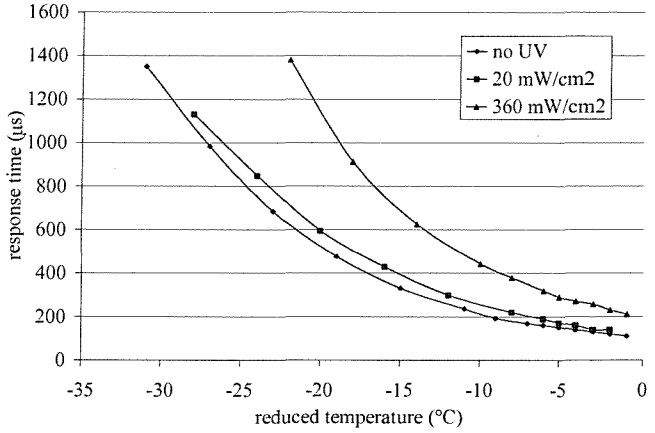

8.15 (c) 20%

Figure 8.15 Optical response time against reduced temperature for (a) 5%NA (b)10% NA (c) 20%NA

8.5 Conclusion on Chapter Eight

The 50:50 7/11 bimesogen mixture plus 5% by mass BDH1281 chiral agent has strong flexoelectric properties. The mixture is flexoelectric over a wide working temperature range from 60°C to below –10°C and a pitch and tilt angle that are almost temperature invariant. The uniformly lying helix texture can be easily induced by shearing and tilt angles close to 20° can be obtained for applied fields of less than 20 V/μm. The response times are short, of the order of ms. The addition of the photoisomerising nitro-azo dye in large concentrations of up to 20% by mass did not unduly alter these properties.

For all the concentrations of dye the effect of ultra violet illumination was to reduce the isotropic to chiral nematic transition temperature. For low illumination intensities the transition temperatures were reduced equally for all three dye concentrations. As the ultra violet intensity was increased the transition temperatures reached a minimum threshold. The magnitude of the reduction was directly proportional to the photoisomerising dye concentration.

The reduction in the transition temperature suggests that the system has become less ordered due to the shape change of the photoisomerising dye molecules. A phase transition will occur as the order parameter changes from zero to a positive value. If the order is reduced isothermally the phase transition temperatures will also be reduced. Low ultra violet intensities may only be sufficient to photoisomerise a proportion of the dye molecules and hence an increase in intensity will cause an incremental decrease of the transition temperature. Hence the threshold transition temperature occurs for ultra violet intensities that photoisomerise all available molecules.

In theory the tilt angle,[9] θ, depends upon the applied field, E, the flexoelectric coefficient, $\bar{e}$, the pitch, p, and the average elastic constant, K as described by equation 8.1. The elastic constant and flexoelectric coefficient both depend on the square of the order parameter so the tilt angle should be independent of changes to

the order parameter. However changes in the average flexoelectric coefficient should cause a change in the tilt angle.

$$\tan\theta = \frac{\bar{e}pE}{2\pi K} \qquad \text{equation 8.1}$$

The effect of ultra violet illumination on the tilt angle of any of the three mixtures was not significant enough to show a change in the flexoelectric coefficient of the material.

The helical pitch of the bimesogen mixtures has been shown to be dependant on the sample temperature. A reduction of the order parameter at a constant temperature would cause a small reduction in the pitch. The pitch of the mixtures is reduced by ultra violet illumination, at a constant sample temperature, for both the 5% and the 10% dye mixtures. When these pitches are plotted against reduced temperature there is no change caused by ultra violet illumination.

The reduction of the pitch with sample temperature indicates a reduction of the order parameter of the system. This reduction of the order parameter is commensurate with the reduction of the isotropic to chiral nematic transition temperatures shown by the invariance with ultra violet intensity when plotted against reduced temperature.

The effect of ultra violet illumination of the response times of the mixtures was also investigated. As shown by equation 8.2 the response time,[6]τ, is inversely proportional to the average elastic constant K, and hence the square of the order parameter and via the viscosity, γ, to the sample temperature, T.

$$\tau = \frac{p^2\gamma}{\pi^2 K} \qquad \text{equation 8.2} \qquad\qquad \gamma = \gamma_0 e^{\frac{E_A}{RT}}$$

Measured against the temperature of the sample the response times were unchanged. However at reduced temperatures, below the transition temperature for each ultra violet intensity, the response times were increased by ultra violet

illumination. This suggests that the response time of the chiral nematic materials is more strongly dependent on the sample temperature than on the order parameter. Small changes of the order parameter, as suggested by the reduced transition temperatures and the reduction of the helical pitch, may be masked by the strong dependence of the response time on the temperature.

As a comparison to the investigation shown here, work has been done by Komitov et al[10] on mixtures of short pitch cholesteric liquid crystals with azo dopants. The reduction in phase transition temperatures for these mixtures were much less than those shown in the bimesogen mixtures, indicating that the isothermal disorder caused by the photoisomerisation of the molecules was more significant in the bimesogen mixtures. A reduction in the pitch upon ultra violet illumination was also shown for the short pitch cholesteric materials but this could not be explained by the change in the order parameter as it could for the bimesogens. A change in the effective tilt angle of up to 5% was also observed which is much less than that observed for the bimesogen materials.

In conclusion the effect of the microscopic photoisomerisation of the azo dye by ultra violet illumination is to cause a macroscopic change of the chiral nematic flexoelectric system. This is shown by the reduction of the transition temperatures and helical pitch. However no significant change in the flexoelectric coefficient can be observed in these mixtures.

Further investigation of the effect of a photo-induced shape change of the dye molecules in a thermochromic chiral nematic system will be investigated in the next chapter. The variation with temperature of the tilt angle and pitch of such a system is greater and it is hoped that any change in the flexoelectric properties will be more easily observed.

References for Chapter 8

[1]Musgrave, B., Lehmann,P., Coles,H.J., Liquid Crystals, **26(8)**, 1235-1249, (1999)

[2]Musgrave, B., Lehmann, P., Coles, H.J., Mol.Crys.Liq.Cryst, **238**, 309-316(1999)

[3] B.Musgrave, M.J.Coles, S.P.Perkins, H.J.Coles, Mol.Cryst.Liq.Cryst. **Vol 364-8**, (2001)

[4] H.J.Coles, M.J.Coles, S.Perkins, B.Musgrave, D.Coates, E.U. Patent EP 99119114, (1999)

[5] Meyer, R.B., Phys.Rev.Lett., **22(18)**, 918-921, (1969)

[6] Patel, J.S., Meyer, R.B., Phys. Rev. Lett. **58(15)**, 1538-1540, (1987)

[7] Rudquist, P., Buivydas, M., Komitov, L., and Lagerwall, S.T., J. Appl. Phys., **76(12)** 7778-7783 (1994)

[8]Coles, H.J., Coles, M.J., Perkins, S., Musgrave, M., Coates, **D**., E.U. Patent, EP991191149, (1999)

[9] Patel, J. S., Lee, S. J. Appl. Phys., **66**, 1879, (1989)

[10] Komitov,L., Ruslim,C., Ichimura,K., Phys.Rev.E., **61(5)**, 5379-5384, (2000)

Chapter 9

A Photoisomerising dye added to a Thermochromic Flexoelectric Mixture

Chapter 9
A Photoisomerising dye added to a Thermochromic Flexoelectric Mixture

9.1 Introduction

The effects of ultra violet illumination on bimesogen flexoelectric mixtures containing a nitro azo dye were discussed in the previous chapter. The shape change of the dye did not produce significant changes in the flexoelectric properties of these bimesogen mixtures. The properties of a chiral system that has a pitch and tilt angle that change significantly across the nematic temperature range and shows flexoelectric switching will be discussed in this chapter. A material with such temperature dependence is called thermochromic and is commonly found in materials that have a smectic A phase at temperatures below the chiral nematic phase. The material to be investigated in this section is 8OCB to which the chiral agent BDH1281 and a nitro azo dye N3 were added to produce a chiral nematic photoisomerising system.

9.2 Properties of 8OCB and BDH1281 mixture

9.2.1 The Thermochromic Nematic 8OCB

8OCB is a member of a series of 4'-n-4alkoxy-4-cyanobyphenyl materials first synthesised by G.W.Gray[1] all having a positive dielectric anisotropy. The molecular structure of the series is shown schematically in figure 9.1. Molecules with a value of n between 5 and 7 only have a nematic phase while 8OCB has a smectic A phase present below the nematic phase.

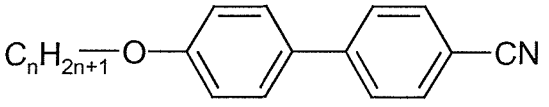

Figure 9.1 Schematic diagram of the molecular structure of the nOCB series.

Experiments have shown a pre-transitional divergence of the bend and twist elastic constants of 8OCB just above the nematic to smectic A transition. In the nematic phase the splay, twist and bend deformations all exist while in the smectic A phase only the splay deformation is present. As the nematic is cooled to the smectic A phase, short range smectic like ordering appears causing a sharp divergence of the twist and bend elastic constants[2].

The twist and splay visco-elastic constants of the nOCB series have been measured by M Sefton[3] using electric field dynamic light scattering. A sharp increase in the twist elastic constant was observed just above the nematic to smectic A transition. The bend and splay Frank constants of the nOCB series have been measured by Bradshaw[4]. A divergence of the bend elastic constant occurred in 8OCB.

By equations 9.1 and 9.2 a sharp increase in the elastic constant, K, would cause an inverse decrease in the tilt angle and response time. However the exponential dependence of the viscosity, γ, on the temperature will cause the response time to increase at lower temperatures.

$$\tan\theta = \frac{epE}{2\pi K} \qquad \text{equation 9.1} \qquad K = \frac{K_{11} + K_{33}}{2}$$

$$\tau = \frac{p^2\gamma}{\pi^2 K} \qquad \text{equation 9.2} \qquad \gamma = \gamma_0 e^{\frac{E_A}{RT}}$$

9.2.2 The effect of a chiral additive, BDH128, to the nematic 8OCB.

After the addition of 5% by mass of BDH128, a chiral additive, the mixture has the phase sequence Isotropic – 79°C – Chiral Nematic – 49°C – smectic A and exhibits a small flexoelectric switching. The characteristics of these flexoelectric properties will be shown with special interest in the area close to the nematic to smectic A transition.

The dependence of the optical tilt angle on the sample temperature can be seen in figure 9.2. For much of the chiral nematic phase the tilt angle is independent of the

sample temperature while it is reduced to zero in a 10° C temperature range above the smectic A phase. The tilt angle depends linearly upon the applied field as shown in figure 9.3 for a range of sample temperatures.

The response time is independent of the sample temperature across most of the chiral nematic phase increasing rapidly close to the cholesteric to smectic A transition. The response time increases slightly with the applied field.

The pitch of 8OCB increases slowly as the temperature decreases across the phase, increasing more rapidly close to the smectic A transition as shown in figure 9.5.

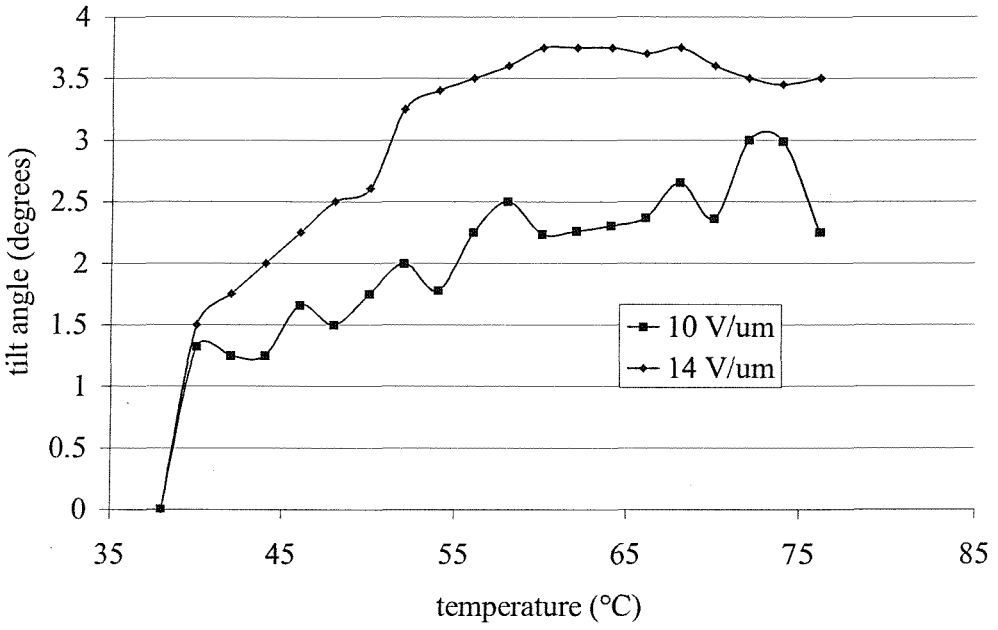

Figure 9.2 The variation with temperature of the tilt angle of 8OCB + 5% BDH1281 across the nematic phase measured at 25 Hz.

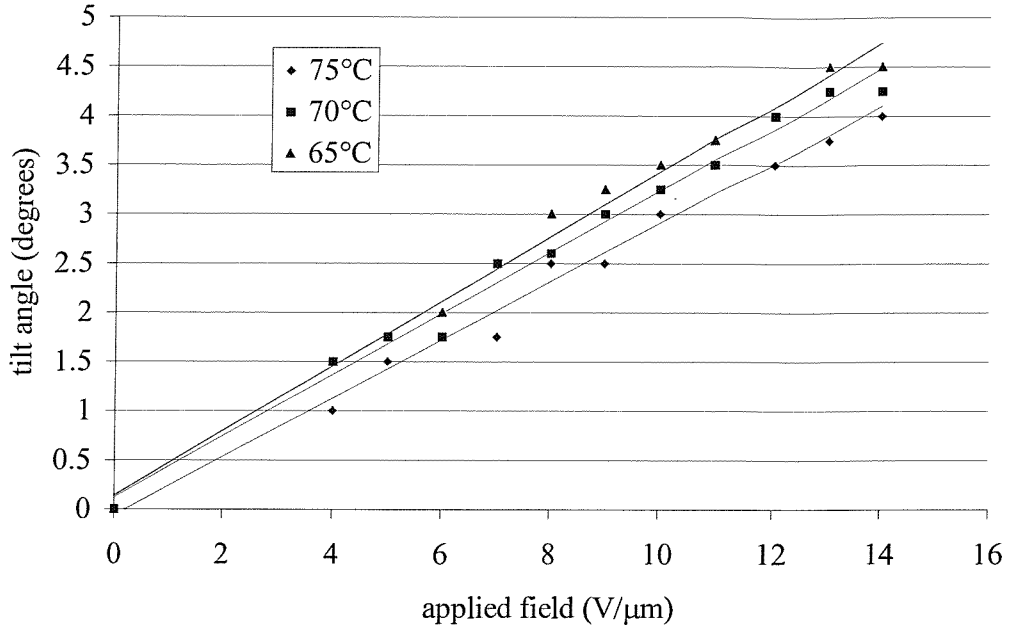

Figure 9.3 The linear dependence of the tilt angle on the field applied to 8OCB + 5% BDH1281 measured at 25 Hz.

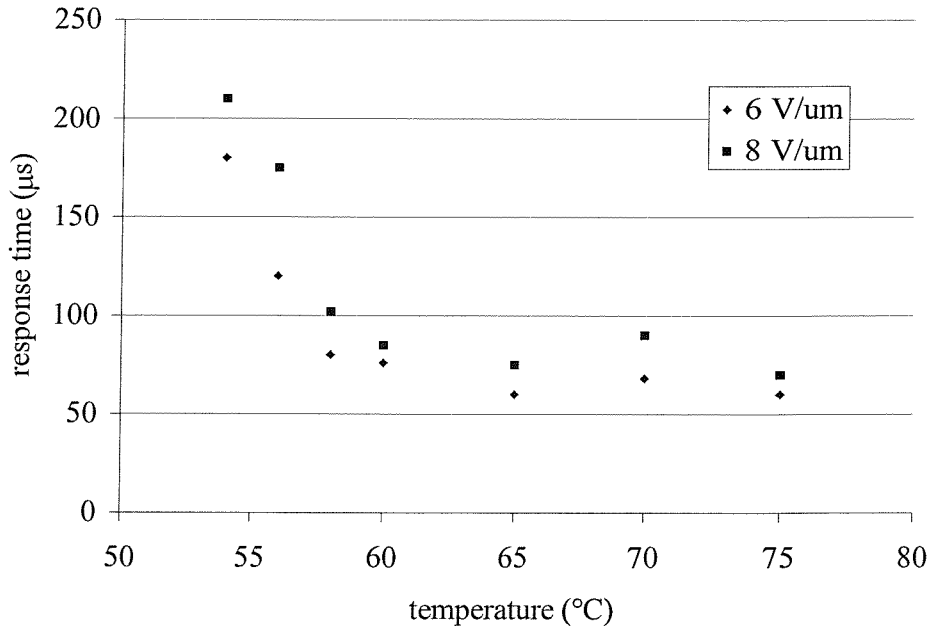

Figure 9.4 The variation of the response time with the sample temperature across the nematic phase measured at 6 Vp-p/μm and 20 Hz for to 8OCB + 5% BDH1281.

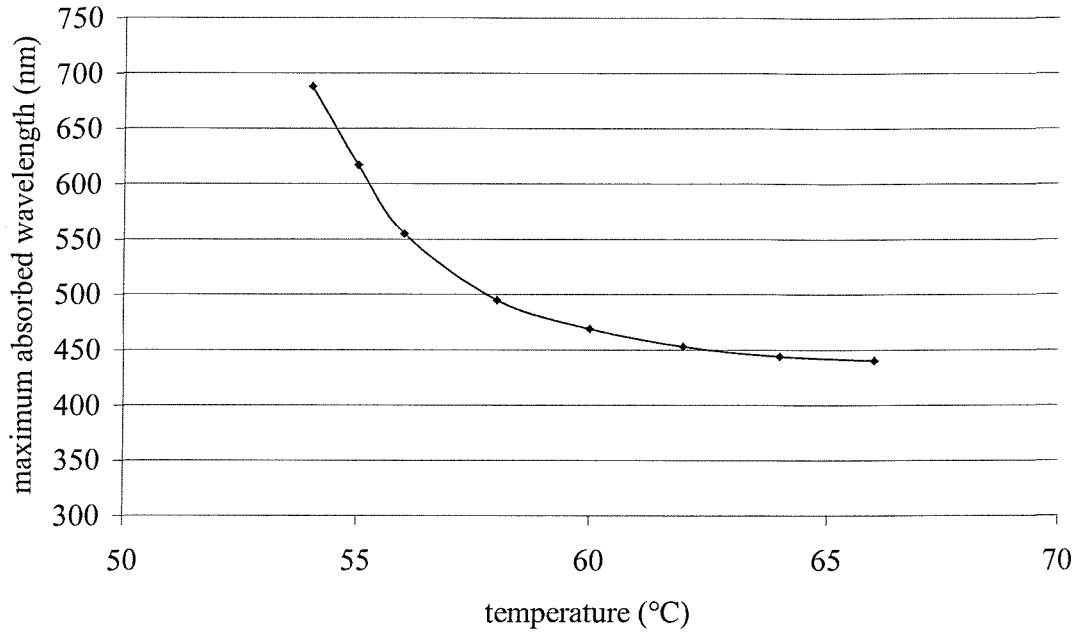

Figure 9.5 Pitch plotted against sample temperature as the maximum absorbed wavelength for 8OCB + 5% BDH1281.

9.3 Addition of N3 to 8OCB mixture

A small nitro-azo molecule was chosen, 3-Methylpentanoic acid 4'-pentanoylazobenzene-4-yl ester, to be introduced as a dye into the 8OCB and BDH1281 mixture. The molecular structure is shown in figure 9.6. This molecule has been shown previously to have photoisomerising effects[5] and will be denoted N3. The dye, N3, has an isotropic to chiral nematic to smectic A to crystal phase sequence so should be miscible with a liquid crystal system. The effect of 5 mW/cm^2 of ultra violet illumination is to reduce the phase transition temperatures by 2-3°C. Figure 9.7 shows the absorption spectrum of the dye with a peak at 500 nm characteristic of the cis trans isomerisation of and azo unit. As shown in table 9.1 the effect of dye addition up to 20% only had a small effect on the transition temperatures of the 8OCB mixture.

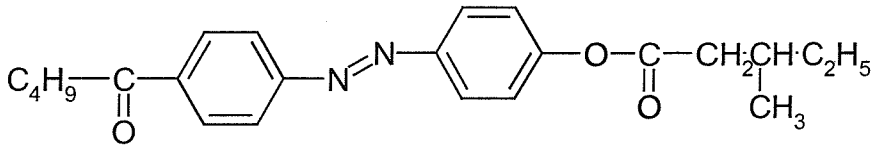

Isotropic – 101°C – Nematic* - 95°C – Smectic A* - 78°C – Crystal

Figure 9.6 Schematic diagram and phase transition temperatures of the N3 molecule measured by optical microscopy.

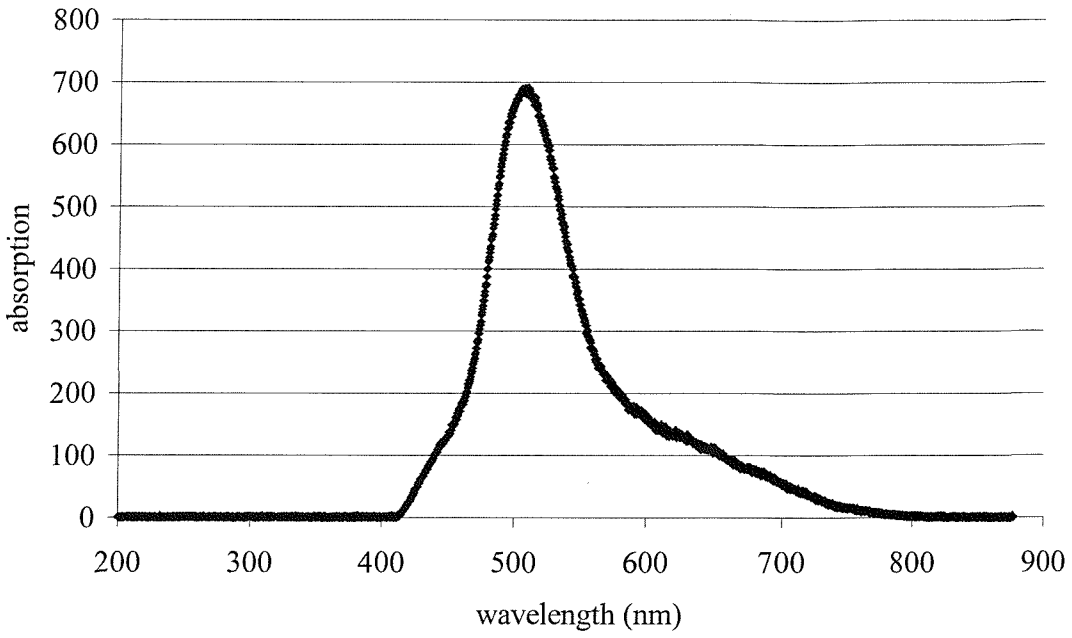

Figure 9.7 Absorption spectrum of NA bimesogen azo dye.

Percentage dye concentration	I-N* transition temperature (°C)	N*-SmA Transition temperature (°C)
0	79	49
5	82	57
10	79	44
20	81	57

Table 9.1 Transition temperatures of 8OCB + BDH1281 and N3 mixtures.

9.4 Effect of ultra violet illumination on the mixtures

As discussed more fully in chapter eight the photoisomerisation of the azo dye can cause a macroscopic change in the flexoelectric chiral nematic system. This effect may be a change in the order parameter or in the flexoelectric coefficient. Changes in the phase transition temperatures, the tilt angle, the helical pitch and the response time will be measured to investigate the macroscopic changes of the system.

Figure 9.7 shows that both the isotropic to nematic and nematic to smectic A transition temperatures are reduced by ultra violet illumination. At large illumination intensity the transition temperature reaches an equilibrium minimum. A plot of the reduction in transition temperature against the dye concentration as shown in figure 9.8 shows that this reduction is proportional to the dye concentration.

The effect of ultra violet illumination on the properties of tilt angle, response time and pitch will be investigated further for the 8OCB plus BDH1281 plus 5% N3 mixture. The measurements are plotted against sample temperature and against reduced temperature which is dependent on the ultra violet intensity in figure 9.9 to 9.14.

As shown in figures 9.9 and 9.10 no measurable change in the tilt angle can be determined either plotted against sample temperature or reduced temperature. The pitch is seen to decrease isothermally, shown in figure 9.11, plotted against sample temperature. When plotted against reduced temperature the pitch is unchanged, figure 9.12. The response time is unchanged when measured against sample temperature as shown in figure 9.13. An increase is observed if the response time is plotted against reduced temperature as shown in figure 9.14.

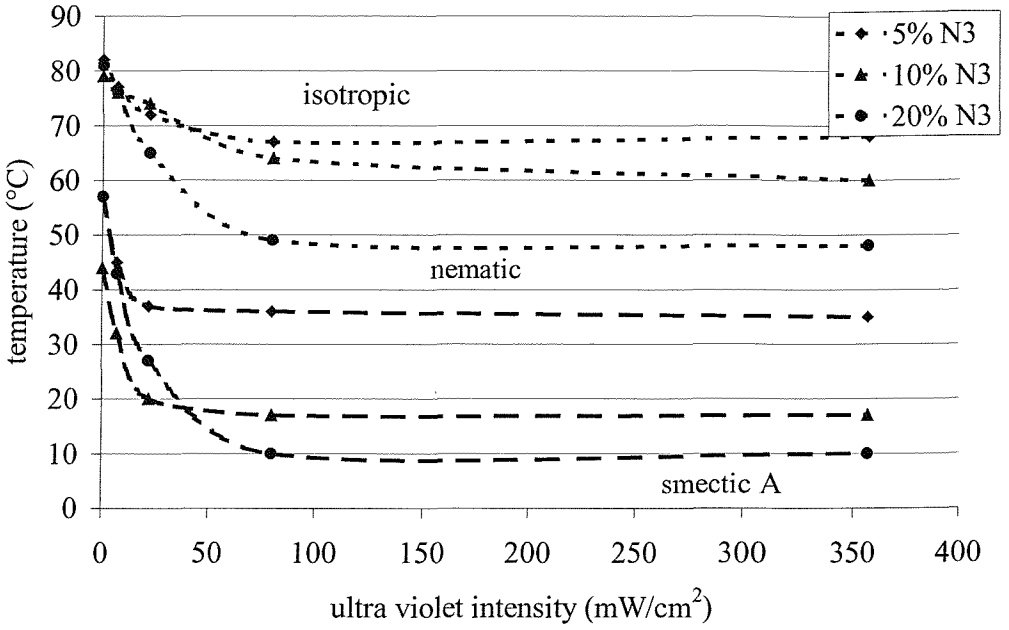

Figure 9.7 Isotropic to nematic and nematic to smectic A transition temperatures for the 5%, 10% and 20% N3 mixtures illuminated by ultra violet measured by optical microscopy.

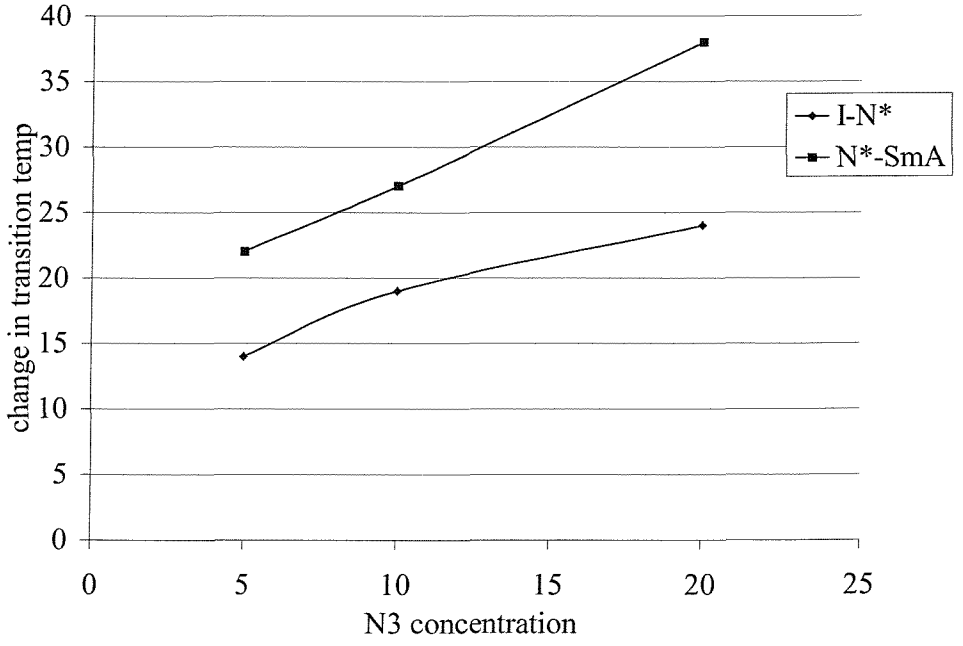

Figure 9.8 Maximum change in transition temperature plotted against dye concentration.

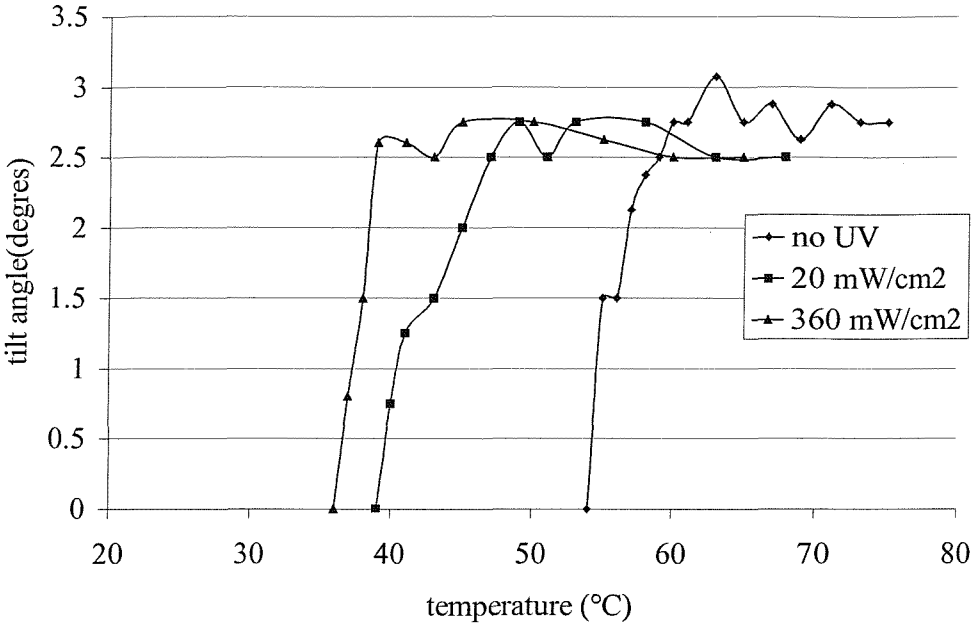

Figure 9.9 Tilt angle of the 5% N3 mixture plotted against sample temperature for ultra violet illumination.

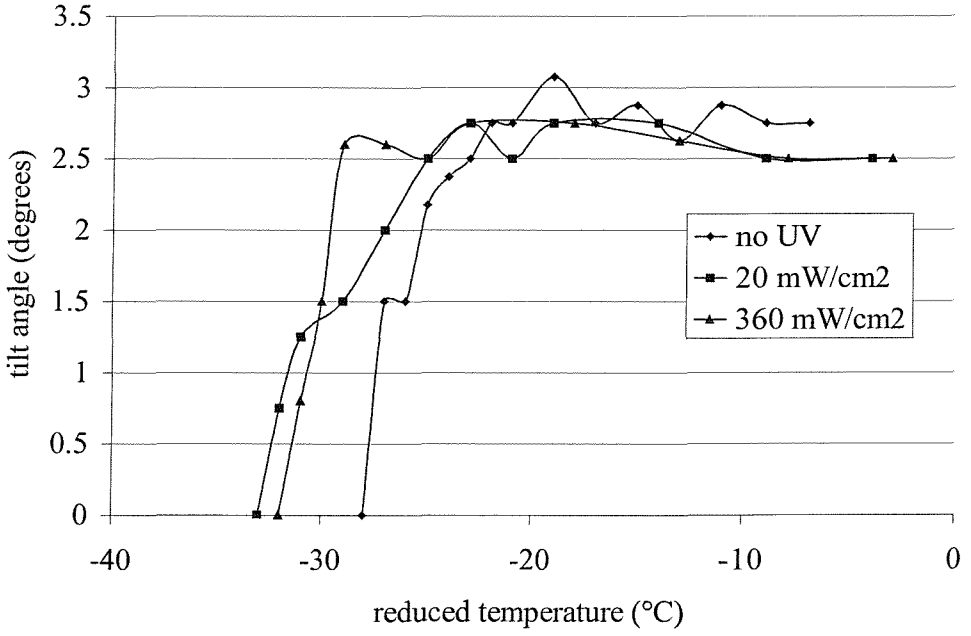

Figure 9.10 Tilt angle of the 5% N3 mixture plotted against reduced temperature for ultra violet illumination.

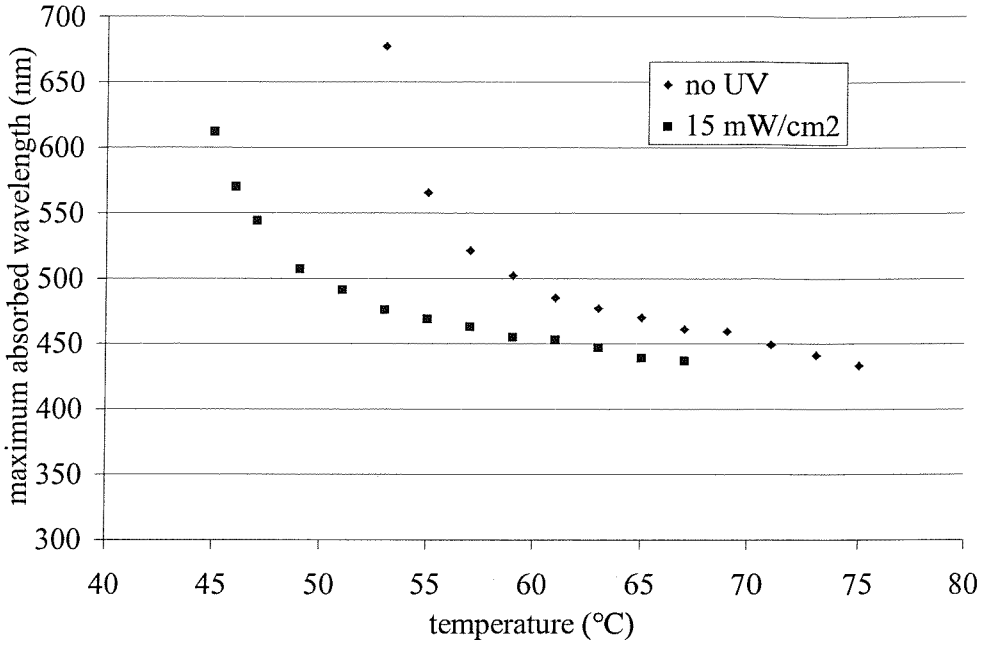

Figure 9.11 Maximum absorbed wavelength for the 5% N3 mixture plotted against sample temperature for ultra violet illumination.

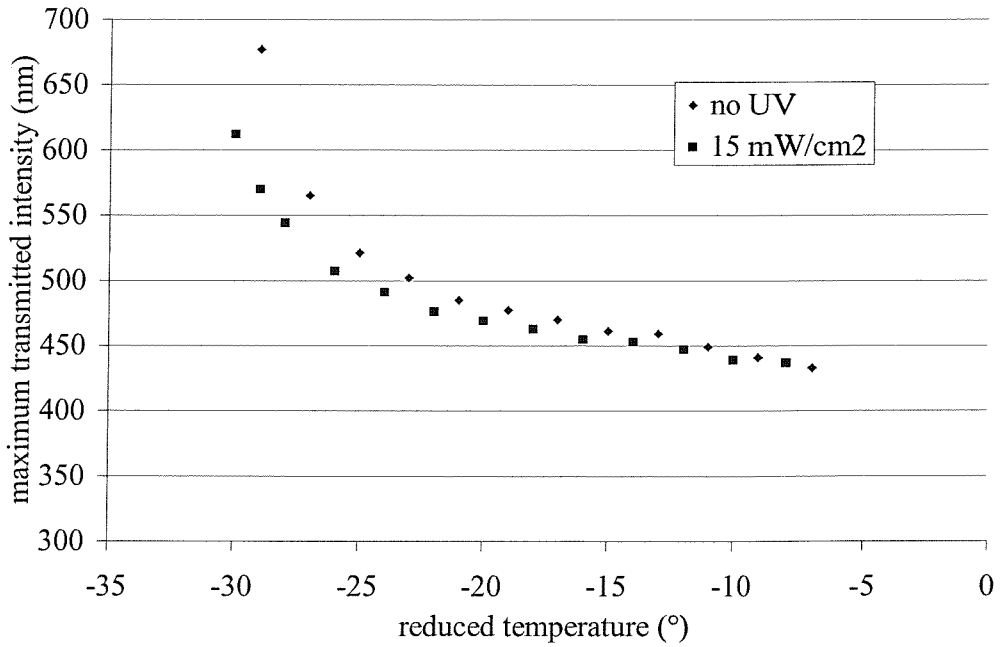

Figure 9.12 Maximum absorbed wavelength for the 5% N3 mixture plotted against reduced temperature for ultra violet illumination.

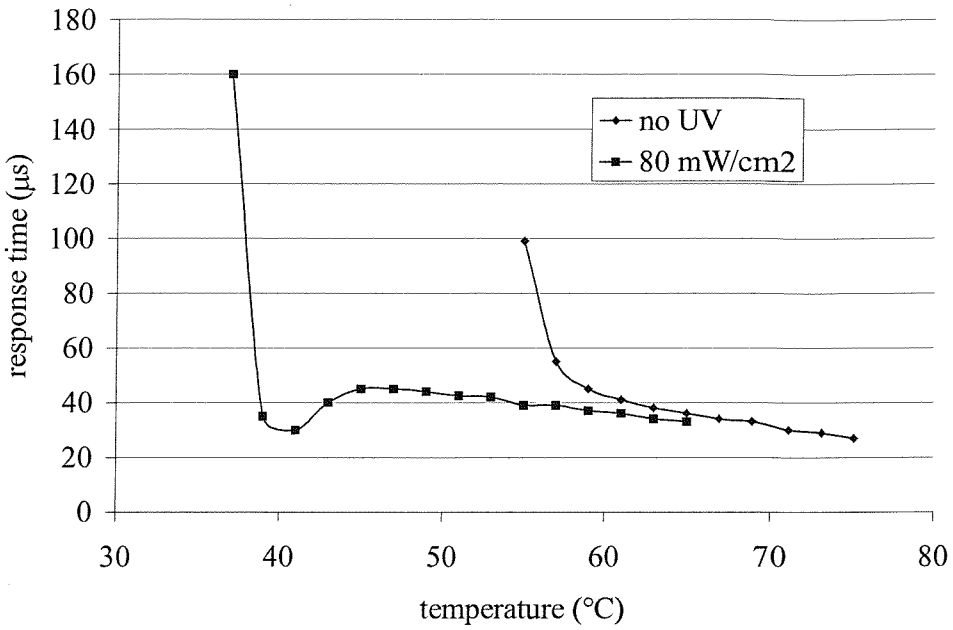

Figure 9.13 Response time of the 5% N3 mixture plotted against sample temperature for ultra violet illumination.

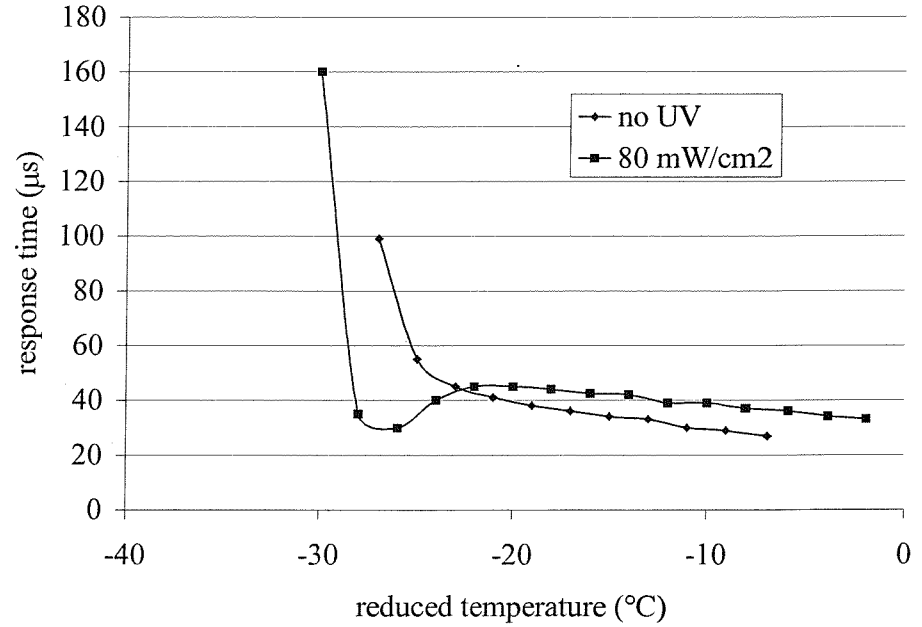

Figure 9.14 Response time of the 5% N3 mixture plotted against reduced temperature for ultra violet illumination.

9.5 Conclusion of Chapter Nine

The mixture of 8OCB and BDH1281 shows a small flexoelectric switch compared to the bimesogens studied in chapter 8. However the flexoelectric pitch and tilt angle change over a significant temperature range (~10°C) above the chiral nematic to smectic A phase transition as suggested by the pretransitional elastic coefficient changes. The N3 photoisomerising dye dissolves into the host in concentrations of up to 20% without adverse effect to the switching properties so useful measurements of the photoisomerising effect could be made.

For all the concentrations of dye the effect of ultra violet illumination was to reduce the isotropic to chiral nematic, and the nematic to smectic A transition temperatures. The changes in the transition temperature were much larger than for the bimesogen mixtures, up to 40°C. For low illumination intensities the transition temperatures were reduced equally for all three dye concentrations. As the ultra violet intensity was increased the transition temperatures reached a minimum threshold. The magnitude of the reduction was directly proportional to the photoisomerising dye concentration.

The reduction in the transition temperature suggests that the system has become less ordered due to the shape change of the photoisomerising dye molecules. Low ultra violet intensities may only be sufficient to photoisomerise a proportion of the dye molecules, so the threshold transition temperature occurs when all the molecules have the bent conformation. The large reduction of the transition temperatures, due to ultra violet illumination, can be used to isothermally induce switching well below the transition to the smectic A phase.

The tilt angle was not significantly changed by ultra violet illumination at temperatures well above the chiral nematic to smectic A transition. However in the temperature range close to the smectic A transition an isothermal increase in the tilt angle could be observed. The tilt angle, θ, depends[6] upon the applied field, E, the flexoelectric coefficient, $\bar{e}$, the pitch, p, and the average elastic constant, K as described by equation 9.3. The elastic constant and flexoelectric coefficient both

depend on the square of the order parameter so the tilt angle should be independent of changes to the order parameter. However changes in the average flexoelectric coefficient should cause a change in the tilt angle. Hence the increase of the tilt angle suggests a small increase in the flexoelectric coefficient.

$$\tan\theta = \frac{\bar{e}pE}{2\pi K} \qquad \text{equation 9.3}$$

The pitch of the mixture is reduced by ultra violet illumination, at a fixed sample temperature. When the pitch is plotted against reduced temperature there is no change caused by ultra violet illumination. The helical pitch of the bimesogen mixtures has been shown to depend on the sample temperature. A reduction of the order parameter at a constant temperature would cause a small reduction in the pitch. This reduction of the order parameter is commensurate with the reduction of the isotropic to chiral nematic transition temperatures shown by the invariance with ultra violet intensity when plotted against reduced temperature.

The relationship between the response time of the mixture plotted against sample temperature was unchanged by ultra violet illumination. However at reduced temperature below the transition temperature for each ultra violet intensity the response times were increased by ultra violet illumination. As shown by equation 9.4 the response time, τ, is inversely proportional[7] to the average elastic constant K, and hence the square of the order parameter and via the viscosity, γ, to the sample temperature, T.

$$\tau = \frac{p^2\gamma}{\pi^2 K} \qquad \text{equation 9.4} \qquad\qquad \gamma = \gamma_0 e^{\frac{E_A}{RT}}$$

The results suggest that the response time of the chiral nematic materials is more strongly dependent on the sample temperature than on the order parameter.

The effect of the microscopic photoisomerisation of the azo dye by ultra violet illumination is to cause a macroscopic change of the chiral nematic flexoelectric system. The reduction of the order parameter is shown by the lowered transition

temps and helix pitch. The increase in the tilt angle close to the smectic A transition may show an increase in the flexoelectric coefficient but this cannot be observed into the bulk of the phase.

References for Chapter 9

[1] Gray. G.W., J.Physique, 36, C1-337-347 (1975)

[2] de Gennes, P.G., The Physics of Liquid Crystals, Clarendon Press (1974)

[3] M Sefton Thesis

[4] Bradshaw, M.J., Raynes, E.P., J.Physique, 46, 1513-1520, (1985)

[5] Harry Walton Thesis University of Manchester 1994

[6] Patel, J. S., Lee, S. J. Appl. Phys., **66**, 1879, (1989)

[7] Patel, J.S., Meyer, R.B., Phys. Rev. Lett. **58(15)**, 1538-1540, (1987)

Chapter 10

Concluding Chapter

Chapter 10 Concluding Chapter

The purpose of the work presented in this thesis is to describe the effect of the addition of photoisomerising azo dyes to liquid crystalline systems. The dyes have been designed to have similar structures to the host materials to ensure good miscibility and contain a photoisomerising azo unit. The first part of the work describes the significant transformations of the host liquid crystal systems due to the addition of the dyes. The effect of a photoisomerising shape change of the dye, caused by ultra violet illumination, on the macroscopic properties of the liquid crystalline mixtures makes up the second part of the work.

Liquid crystalline materials exhibit phases with a degree of ordering greater than that of a liquid but less than that of a solid. This ordering can be described in terms of positional or orientational order as explained more fully in chapter 2. The materials discussed in this thesis fall into two categories. Smectic liquid crystals that have a layered position order and chiral nematic liquid crystals that have a spiral orientational order. The application of electrical fields to samples causes an orientational change that can be detected optically.

The effect of the photoisomerisation of a molecule is to cause small conformational changes to its structure. In the case of the azobenzene molecules studied in this thesis this change is caused by excitation of the molecules by ultra violet illumination. The change from the straight trans to the bent cis isomer coverts a molecule that is very compatible with the liquid crystalline phase to one that is much less compatible. The conformational changes of the dye molecules will alter the order of the liquid crystalline host altering its electro-optic properties.

Liquid crystalline materials are ideal for the measurement of these small changes because they posses a molecular ordering that can be measured with a high accuracy and depends greatly on the molecular conformation of the constituents.

The photoisomerising effects of dyes in two types of liquid crystal systems are investigated. First the ferroelectric, antiferroelectric and electroclinic switching of smectic organosiloxane materials are investigated. Secondly the linear switching

properties of bimesogen molecules specially designed to maximise the flexoelectric effect have been studied. Finally thermochromic chiral nematic materials which exhibit divergent properties close to the smectic A transition are also investigated. The properties of these phases and the switching that occurs within them are described theoretically in chapter two. The methods, based about a microscope, used to investigate these liquid crystalline phases are described in chapter three.

Chapter four describes the mixtures made between a ferroelectric organosiloxane host Br11-Si3 and a dye with a similar structure, NA11-Si3. The organosiloxane material forms a stable ferroelectric smectic C* phases with a high tilt angle, close to 45° and high spontaneous polarisation ~100 nC/cm^2. The combination of a high spontaneous polarisation and tilt angle close to 45° makes this material particularly attractive for use in single polariser devices. The dye NA11-Si3 is designed to have a three siloxane core, the same as that of the host, and a photoisomerising nitro azo mesogen. The compatibility of the molecules gives exceptional miscibility of up to 100%. This is much greater than that used in current dye guest host technology.

For low dye concentrations, up to 20 %, the addition of the dye has only a small effect on the phase transition temperatures, the spontaneous polarisation, the tilt angle and the response times of the mixtures. For greater dye concentrations a smectic A* phase is produced at temperatures above the smectic C* phase. This phase exhibits a significant electroclinic effect and aids the alignment of the smectic C* phase. It is possible to add dye in concentration of up to 80% maintaining a ferroelectric smectic C* phase. The spontaneous polarisation and tilt angles of the mixtures maintain the temperature invariance of the host material. This invariance is useful for display applications where a constant temperature is not guaranteed. Both the polarisation and tilt scale with dye concentration, although the tilt angle is held close to 45° for all the mixtures without a smectic A phase.

Chapter five shows the effect of the addition of a bimesogenic dye. This dye comprises of two mesogens the same as those of the monomesogenic dye attached at either end of a three siloxane core unit. Again complete miscibility was achieved by the compatibility of the siloxane units of the dye and host materials. In the same way as for the monomesogenic dye the phase sequence, and transition temperatures

were hardly changed for low dye concentrations. As the bimesogenic dye concentration was increased a smectic A phase appeared above the smectic C* phase, again improving the ease of alignment of the smectic C* phase and exhibiting a substantial electroclinic effect. However at dye concentrations where the smectic A* phase appeared the smectic C* phase showed antiferroelectric switching. This switching is characteristic of the bimesogenic dye rather than of the ferroelectric monomesogenic host.

It has been shown that the bimesogenic analogue of the ferroelectric host material, with two mesogens attached either end of the three siloxane core exhibits an antiferroelectric phase. The mesogens themselves do not produce the anticlinic ordering required for antiferroelectricity so the conformation caused by the three siloxane unit must be responsible. A templating effect of the bimesogen molecules inducing an anticlinic arrangement for the ferroelectric host materials can be proposed.

Chapters six and seven describe the effect of ultra violet illumination on the mixtures of Br11-Si3 and NA11-Si3 and NA11-Si3-11NA. For both dyes the transition temperatures, tilt angle and spontaneous polarisation are reversibly decreased by ultra violet illumination. The reduction of the tilt angle can be measured electro-optically and a change in the birefringence is observed. No microseparation of the dye and host was observed. The spontaneous polarisation could be seen to couple linearly with the tilt angle in mixtures where a smectic A phase was present indicative of a second order transition. These changes indicate that the modification of the dye molecules causes a reduction in the ordering of the phase and hence a decrease in the tilt angle and polarisation.

Chapter eight introduces the bimesogen chiral nematic mixtures which show a substantial flexoelectric switching with tilt angles of up to 15° for 10 V/μm. A photochromic dye incorporating both the mesogen from the bimesogen molecule and a nitroazo mesogen was added to the bimesogen mixtures in large concentrations of up to 20% without unduly effecting the flexoelectric properties.

The effect of ultra violet illumination was to reduce the isotropic to chiral nematic transition temperatures. The magnitude of the reduction was directly proportional to the concentration of the photoisomerising dye. The effect of ultra violet illumination on the tilt angle of any of the mixtures was not significant enough to show any change in the flexoelectric coefficient of the material. The pitch of the mixtures was reduced by ultra violet illumination, at a constant sample temperature. When these pitches are plotted against reduced temperature, below the transition temperature at each ultra violet intensity, it is found that the ultra violet illumination causes no change in the pitch. Measured against the temperature of the sample the response times were unchanged. However at reduced temperatures the response times were increased by ultra violet illumination.

The reduction of the transition temperatures after ultra violet illumination indicates a reduction in the order of the system. The reduction of the helical pitch with sample temperature also indicates a reduction of the order parameter of the system. This reduction of the order parameter is commensurate with the reduction of the isotropic to chiral nematic transition temperatures shown by the invariance of the pitch with ultra violet intensity when plotted against reduced temperature.

The invariance of the response time with sample temperature suggests that the response time of the bimesogen materials is more strongly dependent on the sample temperature than on the order parameter. Small changes of the order parameter, as suggested by the reduced transition temperatures and the reduction of the helical pitch, may be masked by the strong dependence of the response time on the sample temperature.

Another chiral nematic flexoelectric system is investigated in chapter nine. The 8OCB mixtures differ from the bimesogens by having a smectic A phase below the chiral nematic phase. The presence of the smectic A phase produces pretransitional effects in the tilt angle and pitch close to the chiral nematic smectic A transition. The changes in the phase transition temperatures were much greater for the 8OCB mixtures than the bimesogen mixtures. However similar small changes to those of the bimesogen mixtures were observed in the tilt angle, helix pitch and response

time. These again indicated a small reduction in the order but no observable change in the flexoelectric coefficient.

Komitov et al have also made measurements of the effect of ultra violet illumination on flexoelectric systems containing azo dyes. The tilt angles of these dyes were very small (less than 3°) and although the percentage changes shown by ultra violet illumination were significant (from 5 to 18%) the actual changes were less than 0.3°. If changes of this magnitude were to occur in the bimesogen flexoelectric materials where tilt angles of up to 15° for 10 V/μm can be observed they should be readily observable.

Liquid crystalline materials are conventionally used to regulate light, stimulated by an external electric field. In the case of the photoisomerising mixtures, the incident light effects the state of the liquid crystal. This effect could be used as a detector of ultra violet illumination. The change in the tilt angle or spontaneous polarisation of the ferroelectric materials depends upon the intensity of the illumination. The materials could also be used as a medium to control light with light. Existent photomodulating technologies combine a photodiode with a liquid crystalline pixel. The change in the birefringence from the ferroelectric or chiral nematic state to the isotropic state caused by photoisomerisation could be used to modulate the light passing through the detector rather than using the signal from a photodiode as the stimulus.

Further work may be done to confirm the effect that photoisomerisation of the molecules can cause in liquid crystalline systems. For the smectic organosiloxane compounds the reduction of the tilt angle caused by ultra violet illumination as observed optically could be confirmed by x-ray measurement of the smectic layer spacing. The pitch, and its dependence on the order parameter, of the smectic C* materials could be evaluated in thick homogeneously aligned cells. Other methods of evaluating the order parameter of a smectic liquid crystal including birefringence measurements, time resolved Raman and nuclear magnetic resonance could be evaluated.

For the chiral nematic flexoelectric switching, photoisomerising dye molecules with terminal units other than the nitro azo or a different bimesogen system altogether could be used. A molecule or mixture could be synthesised that contained a photoisomerising group and exhibited flexoelectric switching.

The dye guest host properties of new smectic and chiral nematic mixtures have been shown. Very high dye concentrations have been shown to be possible without undue reduction of switching properties. The templating effect of a bimesogenic dye in a monomesogenic ferroelectric host has shown the change from ferroelectric switching in the pure host to antiferroelectric switching in a mixture. The photoisomerising effects of dye molecules have been shown to be useful in investigating the effect of molecular shape on the liquid crystalline order. The change from a linear arrangement to a bent conformation of the dye has shown a corresponding reduction in the phase transitions and switching properties of smectic C* mixtures. The reductions in the spontaneous polarisation and tilt angle have shown to be linked. A reduction in the order parameter of the chiral nematic flexoelectric mixtures has been shown, but more work is necessary to determine whether a shape change can alter the flexoelectric constants. These effects may also have possible commercial uses as detectors and optical modulators.

Journal Publications

Nitroazo and nitrostilbene dyes for low molar mass organosiloxane liquid crystal dye guest host ferroelectric displays
Shoosmith DE, Remnant A, Perkins SP, Coles HJ
Ferroelectrics, **243(1-4),**75, (2000)

Photoisomerising effects in nitroazo ferroelectric dye guest host systems
Remnant AM, Perkins SP, Coles HJ
Mol.Cryst.Liq.Cryst. **Vol 366**, 2603 ,(2001)

Photoisomerising effects in nitroazo flexoelectric dimeric nematic systems
Remnant AM, Perkins SP, Coles HJ
Mol.Cryst.Liq.Cryst. **Vol 366**, 2613-2621 ,(2001)

Photoisomerising effects in flexoelectric chiral nematic systems incorporating an azo dye
A.M. Remnant, Perkins SP, H.J. Coles
Ferroelectrics to be published

Conference Proceedings

Nitroazo and Nitrostilbene dyes for low molar mass organosiloxane liquid crystal dye guest host ferroelectric displays
D.E. Shoosmith, A. Remnant, S.P. Perkins and H.J. Coles
Poster Presentation Ferroelectric Liquid Crystal Conference 1999

Photoisomerising effects in nitroazo ferroelectric dye guest host systems
A.M. Remnant, S.P. Perkins, H.J. Coles
Poster Presentation British Liquid Crystal Society Conference 2000

Photoisomerising effects in nitroazo ferroelectric dye guest host systems
A.M. Remnant, S.P. Perkins, H.J. Coles
Poster Presentation International Liquid Crystal Society Conference 2000

Photoisomerising effects in nitroazo flexoelectric dimeric nematic systems
A.M. Remnant, S.P. Perkins, H.J. Coles
Poster Presentation International Liquid Crystal Society Conference 2000

Photoisomerising effects in flexoelectric chiral nematic systems incorporating an azo dye
A.M. Remnant H.J. Coles
Poster Presentation British Liquid Crystal Society Conference 2001

Photoisomerising effects in flexoelectric chiral nematic systems incorporating an azo dye
A.M. Remnant and H.J. Coles
Poster Presentation Ferroelectric Liquid Crystal Conference 2001